Supplemental material to this article can be found at:
http://molpharm.aspetjournals.org/content/suppl/2006/06/21/mol.106.023614.DC1

0026-895X/06/7003-909–924$20.00
MOLECULAR PHARMACOLOGY
Copyright © 2006 The American Society for Pharmacology and Experimental Therapeutics
Mol Pharmacol 70:909–924, 2006

Vol. 70, No. 3
23614/3136487
Printed in U.S.A.

MOLECULAR PHARMACOLOGY

Antitumor Activity of the Retinoid-Related Molecules (*E*)-3-(4′-Hydroxy-3′-adamantylbiphenyl-4-yl)acrylic Acid (ST1926) and 6-[3-(1-Adamantyl)-4-hydroxyphenyl]-2-naphthalene Carboxylic Acid (CD437) in F9 Teratocarcinoma: Role of Retinoic Acid Receptor γ and Retinoid-Independent Pathways[S]

Edoardo Parrella, Maurizio Giannì, Maddalena Fratelli, Maria Monica Barzago, Ivan Raska Jr, Luisa Diomede, Mami Kurosaki, Claudio Pisano, Paolo Carminati, Lucio Merlini, Sabrina Dallavalle, Michele Tavecchio, Cecile Rochette-Egly, Mineko Terao, and Enrico Garattini

Laboratory of Molecular Biology, Centro Catullo e Daniela Borgomainerio (M.G., M.F., M.M.B., I.R., L.D., M.K., M.Te., E.G.) and Department of Oncology (M.Ta.), Istituto di Ricerche Farmacologiche "Mario Negri", Milano, Italy; Sigma-Tau Industrie Farmaceutiche Riunite, Pomezia, Italy (C.P., P.C.); Dipartimento di Scienze Molecolari Agroalimentari, Università degli Studi di Milano, Milano, Italy (L.M., S.D.); and Institut de Genetique et Biologie Moleculaire, Illkirch, France (C.R.-E., E.P.)

Received February 23, 2006; accepted June 15, 2006

ABSTRACT

The retinoid-related molecules (RRMs) ST1926 [(*E*)-3-(4′-hydroxy-3′-adamantylbiphenyl-4-yl)acrylic acid] and CD437 (6-[3-(1-adamantyl)-4-hydroxyphenyl]-2-naphthalene carboxylic acid) are promising anticancer agents. We compared the retinoic acid receptor (RAR) trans-activating properties of the two RRMs and all-*trans*-retinoic acid (ATRA). ST1926 and CD437 are better RARγ agonists than ATRA. We used three teratocarcinoma cell lines to evaluate the significance of RARγ in the activity of RRMs: F9-wild type (WT); F9γ−/−, lacking the *RARγ* gene; F9γ51, a F9γ−/− derivative, complemented for the RARγ deficit. Similar to ATRA, ST1926 and CD437 activate cytodifferentiation only in F9-WT cells. Unlike ATRA, ST1926 and CD437 arrest cells in the G_2/M phase of the cell cycle and induce apoptosis in all F9 cell lines. Our data indicate that RARγ and the classic retinoid pathway are not relevant for the antiproliferative and apoptotic activities of RRMs in vitro. Increases in cytosolic calcium are fundamental for apoptosis, in that intracellular calcium chelators abrogate the process. Comparison of the gene expression profiles associated with ST1926 and ATRA in F9-WT and F9γ−/− indicates that the RRM activates a conspicuous nonretinoid response in addition to the classic and RAR-dependent pathway. The pattern of genes regulated by ST1926 selectively, in a RARγ-independent manner, provides novel insights into the possible molecular determinants underlying the activity of RRMs in vitro. Furthermore, it suggests that RARγ-dependent responses are relevant to the activity of RRMs in vivo. Indeed, the receptor hinders the antitumor activity in vivo, in that both syngeneic and immunosuppressed SCID mice bearing F9γ−/− tumors have increased life spans after treatment with ST1926 and CD437 relative to their F9-WT counterparts.

Downloaded from molpharm.aspetjournals.org at ASPET Journals on June 3, 2022

This work was made possible by the financial support of the Associazione Italiana per la Ricerca contro il Cancro (AIRC), the Istituto Superiore di Sanità, and the Fondo d'Investimento per la Ricerca di Base (FIRB). The financial support of the Weizmann-Negri Foundation is also acknowledged.

Article, publication date, and citation information can be found at http://molpharm.aspetjournals.org.

doi:10.1124/mol.106.023614.

[S] The online version of this article (available at http://molpharm.aspetjournals.org) contains supplemental material.

All-*trans*-retinoic acid (ATRA) and derivatives (retinoids) are promising antineoplastic agents (Garattini and Terao, 2004; Garattini et al., 2004b). The activity of classic retinoids is the consequence of selective antiproliferative and cytodifferentiating effects that are mediated predominantly by specific nuclear receptors of the RAR and RXR families (Altucci and Gronemeyer, 2001). In many cell types, classic retinoids

ABBREVIATIONS: ATRA, all-*trans*-retinoic acid; RAR, retinoic acid receptor; RXR, retinoid X receptor; RRM, retinoid-related molecule; CD437, (*E*)-3-(4′-hydroxy-3′-adamantylbiphenyl-4-yl)acrylic acid; ST1926, 6-[3-(1-adamantyl)-4-hydroxyphenyl]-2-naphthalene carboxylic acid; BAPTA, 1,2 bis (2-aminophenoxy)ethane-*N*,*N*,*N*′,*N*′-tetraacetic acid tetrakis (acetoxymethyl ester); FURA-2, Fura-2 acetoxymethyl ester; DEVD-amc, *N*-acetyl-Asp-Glu-Val-Asp-amino-4-methylcoumarin; PBS, phosphate-buffered saline; PI, propidium iodide; RT-PCR, reverse transcription-polymerase chain reaction; DMSO, dimethyl sulfoxide; ANOVA, analysis of variance; WT, wild-type; FACS, fluorescence-activated cell sorting; TNF, tumor necrosis factor; AV, annexin V.

exert unique actions of oncological interest, including growth inhibition, cytodifferentiation, and direct or indirect cytotoxicity. Because the molecular mechanisms of action of retinoids are generally different from those of other antineoplastic agents, there is growing interest in the synthesis of molecules with new properties (Rishi et al., 2003; Sabichi et al., 2003; Cao et al., 2004; Chun et al., 2005).

A novel series of synthetic retinoic acid derivatives [retinoid-related molecules (RRMs) or atypical retinoids], with activity in leukemia and cancer cells, has been described recently (Mologni et al., 1999; Ponzanelli et al., 2000; Sun et al., 2002; Zhang et al., 2002; Garattini et al., 2004a; Lopez-Hernandez et al., 2004; Zuco et al., 2004). In certain cellular contexts, these molecules do not show cross- resistance with ATRA (Marchetti et al., 1999) and other chemotherapeutics (Ponzanelli et al., 2000), suggesting novel features and mechanisms of action relative to classic retinoids and the available anticancer agents. The prototypes of RRMs are CD437 and ST1926 (Garattini et al., 2004). CD437 is a retinoid originally developed as a selective RARγ agonist (Delescluse et al., 1991). Although a preliminary report suggested that ST1926 is not an efficient RARγ agonist (Cincinelli et al., 2003), we have provided evidence that the compound does bind to and trans-activate the receptor (Garattini et al., 2004b). ST1926 is a more powerful antileukemic and anticancer agent (Cincinelli et al., 2003; Garattini et al., 2004a) with better toxicologic and pharmacokinetic profiles than CD437. ST1926 is under preclinical development in view of phase I clinical trials.

Various aspects of the molecular mechanisms of action of RRMs remain unclear. From a structural standpoint, RRMs are classified as synthetic retinoids. However, the contribution of nuclear retinoic acid receptors to the antineoplastic activity of ST1926 and CD437 is not completely defined. In particular, involvement of RARγ is debated (Hsu et al., 1997; Holmes et al., 2000; Sun et al., 2000a; Zhao et al., 2001). In certain cells, pharmacological inhibition of RARγ blocks the action of CD437 (Holmes et al., 2000), whereas in others, this is ineffective (Mologni et al., 1999). Synthesis of an active RRM with strong apoptotic properties and no RARγ binding activity (Dawson et al., 2001) adds to the controversy. Furthermore, although the activity of ST1926 and CD437 in myeloid leukemia is predominantly the result of an apoptotic process, RRMs also inhibit growth and induce cytodifferentiation in other tumor contexts. These two further actions may contribute to the overall antineoplastic activity of RRMs and have never been the object of a systematic study. Finally, the gene expression program set in motion by RRMs and its dependence on the activation of RARγ or other RAR isotypes is unknown.

F9 teratocarcinoma cells represent a useful cell-autonomous model to study the activity of retinoids (Boylan et al., 1993; Taneja et al., 1997; Faria et al., 1999; Rochette-Egly et al., 2000a,b; Rochette-Egly and Chambon, 2001; Zhuang et al., 2003; Bour et al., 2005). These cells undergo growth arrest and differentiation along the primitive endoderm in response to ATRA and other synthetic retinoids. Moreover, studies conducted with F9 sublines presenting genetic deletion of RARγ (Boylan et al., 1993) demonstrated that endodermal differentiation requires activation of the receptor. Thus, the F9 model is well suited to define the relative contribution of cytodifferentiation and growth inhibition to the overall antineoplastic activity of RRMs. Furthermore, the use of F9 teratocarcinoma cells is likely to provide information as to the relevance of the classic RAR/RXR and alternative or complementary pathways for the pharmacology of RRMs. Finally, the availability of F9 teratocarcinoma cell lines differing only in the expression of RARγ (Taneja et al., 1997) represents a unique tool to study the significance of the receptor for the antineoplastic activity of RRMs. The growth of F9 teratocarcinoma cells as solid tumors in syngenic strains of animals is a further advantage, permitting in vivo experiments.

In this study, three F9 teratocarcinoma cell lines with different expression of RARγ were used to investigate the cytodifferentiating, antiproliferative, and apoptotic effects of ST1926 and CD437 compared with ATRA. In the same system, using whole-genome microarrays, ST1926 specific responses and their RARγ-dependence were defined. Finally, the involvement of RARγ in the overall antitumor activity of RRMs was studied in normal and immunosuppressed mice transplanted with F9 cells.

Materials and Methods

Chemicals. ATRA and BAPTA were purchased from Sigma (St. Louis, MO). Fura-2 acetoxymethyl ester (FURA-2) was from Invitrogen (Carlsbad, CA). ST1926 and CD437 were synthesized by Sigma-Tau Industrie Farmaceutiche Riunite S.p.a. (Pomezia, Italy).

Cell Cultures and Transfections. COS-7 (American Type Culture Collection, Manassas, VA) and the F9 teratocarcinoma cell lines, F9-WT, F9$\gamma-/-$, and F9γ51 (Taneja et al., 1997), were grown in Dulbecco's modified Eagle's medium containing 10% fetal calf serum and were free from mycoplasma. COS-7 cells were transfected with human RARα, RARβ, RARγ, or RXRα pSG5-based plasmids along with the DR5-tk-CAT (RAR-dependent) or DR1-tk-CAT (RXR-dependent) reporter genes and the normalization plasmid pCH110 (β-galactosidase) (Garattini et al., 2004a). Transactivation assays on the various isoforms of RAR were performed using extracts of transfected COS-7 treated for 24 h with different concentrations of the test retinoid, as described previously (Garattini et al., 2004a)

Cellular Proliferation, Viability, and Apoptosis. Cell number and viability were determined after staining with erythrosin (Sigma). For the determination of the apoptotic index, adherent cells were detached, fixed in methanol, and stained with 4,6 diamidino-2-phenylindole (Giannì et al., 2000). The apoptotic index is the percentage of cells with features of nuclear fragmentation after counting a minimum of 300 nuclei/field under the fluorescence microscope. In some experiments, apoptosis was determined according to the Annexin-V assay by flow cytometry (Mebcyto Apoptosis Kit; MBL International, Woburn, MA) (Garattinì et al., 2004a), using the flow cytometer FACSCalibur (BD Biosciences, Palo Alto, CA). Caspase-3 activation was measured with the fluorogenic peptide substrate DEVD-amc (*N*-acetyl-Asp-Glu-Val-Asp-amino-4-methylcoumarin; Alexis, Laufelingen, Switzerland) (Mologni et al., 1999).

Flow Cytometric Cell Cycle Analysis. F9-WT and F9$\gamma-/-$ cells were counted using a Coulter counter (Beckman Coulter, Fullerton, CA) and fixed in 70% ethanol. Cells ($1–2 \times 10^6$) were washed with PBS and stained with 1 ml of a solution containing 10 μg/ml propidium iodide (PI) and 10,000 units of RNase overnight at 4°C in the dark. Flow cytometric analyses were performed using FACSCalibur, and the distribution of the cells in the different cell cycle phases calculated by the gaussian method (Ubezio, 1985).

RNA Preparation and RT-PCR. Total RNA was extracted according to the guanidinium-thiocyanate-cesium chloride method, reverse transcribed, and amplified by polymerase chain reaction (PCR) using synthetic amplimers (GeneAmp RNA-PCR core kit; Applied

Downloaded from molpharm.aspetjournals.org at ASPET Journals on June 3, 2022

Biosystems Inc., Branchburg, NJ). The amplimers used are shown in Table 1.

Real-time RT-PCR was performed using Taqman gene expression assays (Applied Biosystems, Foster City, CA) following the manufacturer's instructions, on a GeneAmp 5700 sequence detector (Applied Biosystems). The assays used were Mm00439359_m1, with primers located at the 1-2 exon boundary of the *HOXA1* gene; Mm00487803_m1, with primers located at the 1-2 exon boundary of the c-*myc* gene; Mm00445212_m1, located at the 7-8 exon boundary of the KIT oncogene; Mm01319677_m1, located at the 4-5 exon boundary of the *RARβ* gene; and Mm00435270, located at the 19-20 exon boundary of the Notch homolog 3 gene. The β-actin housekeeping gene (assay ID Mm00607939_s1) was used for the normalization of the results.

Measurement of Intracellular Calcium. Changes in intracellular calcium concentrations were measured at the single-cell level in a semiquantitative fashion. In brief, F9-WT or F9γ−/− cells were seeded (300,000/ml) on microscopic glass slides and allowed to adhere overnight. Cells were labeled with 4 μM Fluo3-AM (Invitrogen) at 37°C for 1 h. Slides were washed twice with PBS and incubated in PBS containing 1.26 mM CaCl2. After addition of vehicle (DMSO) or ST1926 (1 μM) the associated fluorescence was measured for a maximum of 1 h with an IX70 microscope (Olympus, Hamburg, Germany) equipped with an imaging system (Till Photonics GMBH, Gräfelfing, Germany). For each experiment, cells were scanned for at least 30 s to establish a baseline fluorescence reading before addition of the appropriate stimulus. All incubations were carried out while continuously scanning the cells every 200 ms.

For the quantitative determination of intracellular calcium in the entire cell population, a previously described protocol was used (Garattini et al., 2004a). For these experiments, the FURA-2-associated fluorescence was measured continuously at 37 ± 1°C with a spectrophotofluorometer (LS-50B; PerkinElmer Life and Analytical Sciences, Milano, Italy).

In Vivo Studies. F9-WT or F9γ−/− cells (3×10^6) were inoculated intraperitoneally in 129/Sv syngenic animals or in immunodeficient SCID mice (Charles River Italia, Calco, Italy). ST1926, CD437, or ATRA was dissolved in a diluent consisting of cremophor/ethanol (Garattini et al., 2004a). All the compounds were administered i.p. or orally once per day for up to 3 weeks. Body weight and lethality were recorded every day. All the experiments were approved by the Internal Animal Care Committee and conducted according to the pertinent International and Italian legislation.

Gene Microarrays. F9-WT and F9γ−/− were treated for 10 h with vehicle (DMSO), all-*trans*-retinoic acid (0.5 μM), or the synthetic retinoid ST1926 (0.5 μM). The polyadenylated RNA fraction was isolated from total RNA using magnetic oligo(dT) micro-spheres (DYNAL AS, Oslo, Norway). Polyadenylated RNA was amplified and labeled with the fluorochrome Cy3 or Cy5 using the Amino allyl MessageAMP II kit (Ambion Inc., Austin, TX). Each RNA preparation represents a pool of four flasks treated independently with the appropriate stimulus. Each experimental sample consists of 1) a replicate in which the control RNA is labeled with Cy3 and the treated RNA with Cy5 and 2) a swapped replicate in which the control RNA is labeled with Cy3 and the treated RNA with Cy5. An equal amount of Cy3- and Cy5-labeled cRNAs were mixed and hybridized to the oligonucleotide microarray (Agilent 60-mer microarray oligo processing protocol version 2.1; Agilent Technologies, Palo Alto, CA). After washing, microarray glass slides were scanned with the G2565AA dual laser scanner (Agilent Technologies). Images were analyzed with the Feature Extraction software version 7.1 (Agilent Technologies). Dye normalization was performed automatically, using the Rank Consistency filter and the LinearLOWESS normalization method. The raw data of the microarray experiments

TABLE 1
Amplimers

	Sequence	Nucleotides	GenBank Accession No.
Collagen type IV	5′-ATCAACAACGTCTGCAACTTCGCC-3′	4649–4672	J04694
Complementary	5′-TTCTTCTCATGCACACTTGGCAGC-3′	5113–5136	
Laminin B1 subunit 1	5′-AGAGCTGAGCTGTTGCTTGAGGAA-3′	4885–4908	NM_008482
Complementary	5′-TGCTGTTAGCTTGAGCCAAGAGTG-3′		
Notch Hom.3	5′-CTCAGCTTTGGTCTGCTCAATCCT-3′	6531–6554	NM_008716
Complementary	5′-CTGAGGGAGGGAGGGAACAGATAT-3′	7033–7056	
Apaf1	5′-GTGTGGAATGTCATTACCGGAA-3′	3756–3777	NM_009684
Complementary	5′-CGAGATTATCGACAGTCACATAGGTT-3′	4245–4270	
Ddit4	5′-CTGCTAAGTGATTTCGACTACTGGG-3′	283–307	NM_030143
Complementary	5′-GTCGTTCCAATCAGGGAGTACAG-3′	742–764	
Na Channel IIIβ	5′-AGATGCATCTCCTGCATGAAGAG-3′	361–383	NM_178227
Complementary	5′-ACCACAGAGTTCTCCTTGTTCTCTG-3′	839–863	
Caveolin 2	5′-AGAAGGCCGATGTGCAGCTCTTCA-3′	37–60	NM_016900
Complementary	5′-CAGTTGCATGCTGACCGATGAGAA-3′	474–497	
Kit oncogene	5′-ATCATGGAAGATGACGAGCTGGCT-3′	2288–2311	NM_021099
Complementary	5′-GCTGTCCGAGATCTGCTTCTCAAT-3′	2792–2815	
CYP26a1	5′-CTGCGACATCACTGATCACTTACC-3′	979–1002	NM_007811)
Complementary	5′-CTGGAAGTAGGTGAATCTTGCAGG-3′	1515–1538	
c-myc	5′-CAGCGACTCTGAAGAAGAGCAAGA-3′	1353–1376	NM_010849
Complementary	5′-TGAGCTTGTGCTCGTCTGCTTGAA-3′	1823–1846	
Homeobox B2	5′-CGAAAGGCAGGTCAAAGTCTGGTT-3′	307–330	NM_134032
Complementary	5′-GAAACTGCAAGTCGATGGCACAGA-3′	801–824	
RARα	5′-GAACATGGTGTATACGTGTCACCG-3′	758–781	NM_009024
Complementary	5′-TCAATGTCCAGGGAGACTCGTTGT-3′	1049–1072,	
RARβ	5′-AGAGAGCTATGAGATGACAGCGGA-3′	700–723	NM_011243
Complementary	5′-GAAAGTCATGGTGTCTTGCTCTGG-3′	1010–1033	
RARγ	5′-TGGAGACACAGAGCACCAGCTC-3′	440–461	NM_011244
Complementary	5′-TCCGAGAATGTCATAGTGTCCTGC-3′	1098–1121	
RXRα	5′-AAGGACTGCCTGATCGACAAGAGA-3′	705–738	NM_011305
Complementary	5′-TGAAGAGCTGCTTGTCTGCTGCTT-3′	1001–1024	
RXRβ	5′-ACCTGACCTACTCGTGTCGTGATA-3′	814–837	NM_011306
Complementary	5′-TTGTCAGCTGCCTGGCAGATGTTA-3′	1118–1141	
RXRγ	5′-AGATTGTCTCATCGACAAGCGCCA-3′	909–932	NM_009107
Complementary	5′-CCTCCAAGGTGAGATCTGAGAAGT-3′	1238–1261	

Downloaded from molpharm.aspetjournals.org at ASPET Journals on June 3, 2022

were deposited in the public database Miamexpress (http://www.ebi.ac.uk/miamexpress) with the accession number E-MEXP-361. Further Qspline normalization (Workman et al., 2002) of the intensity data was conducted using Gene Publisher (Knudsen et al., 2003). Two-way ANOVA based on F distribution (factor A: vehicle, ST1926, or ATRA; factor B: F9-WT or F9γ−/−) was performed with the T-MEV software (Saeed et al., 2003; http://www.tm4.org/mev.html). Significant genes ($p < 0.0001$) were classified based on Pavlidis template-matching algorithm and hierarchical clustering using Pearson correlation as the distance measure (Pavlidis and Noble, 2001; Kasturi et al., 2003).

Results

ST1926 and CD437 Were RARγ Activators. We compared the ability of ST1926, CD437, and ATRA to activate RARα, RARβ, and RARγ overexpressed in COS-7 cells (Table 2). The EC_{50} reflects the affinity of each retinoid for the three isoforms of RAR. For RARα and RARβ, the rank order of potency was ATRA = CD437 > ST1926, whereas for RARγ, it was CD437 > ATRA > ST1926. RAR selectivity was calculated as the inverse ratio of the EC_{50} values. The data obtained are consistent with previous results, indicating that ATRA was a nonselective (pan-RAR) agonist, whereas CD437 was a selective RARγ agonist. In addition, our results demonstrated that ST1926 bound and trans-activated the three receptors with similar affinity and, unlike CD437, lacked RARγ selectivity. Table 2 also shows the maximal activity of each compound at saturating concentrations. It is noteworthy that both ST1926 and CD437 activated RARγ more efficiently than ATRA. Cotransfection of RXRα did not change the EC_{50} values of ST1926, CD437, and ATRA for the various isoforms of RAR (data not shown). This is in line with the concept that COS-7 cells contain significant amounts of native RXRs that combine with overexpressed RARs to form transcriptionally active RXR/RAR heterodimers (Garattini et al., 2004b; Giannì et al., 2006).

ST1926 and CD437 are unlikely to possess significant RXR agonistic activity, as demonstrated by transfection of COS-7 cells with RXRα and an appropriate reporter gene activated by RXR/RXR homodimers. Under these experimental conditions, the RXR agonist 9-*cis* retinoic acid (1 μM) caused a 9.7 ± 0.8 (mean ± S.D., $n = 3$) induction of CAT reporter activity over the unliganded control sample. In contrast, the effects of ST1926 or CD437 were minimal, dose-independent, and did not exceed a 2-fold induction at all the concentrations investigated (0.01 μM-10 μM).

The F9 Teratocarcinoma Model. To define the relevance of nuclear retinoic acid receptors, and RARγ in particular, for the pharmacological activity of ST1926 and CD437, we chose the mouse F9 teratocarcinoma model. Experiments were performed on three clonal cell lines with different expression of RARγ. As shown in Fig. 1A, wild-type F9 cells (F9-WT) expressed RARα and RARγ constitutively. As expected, RARβ was not expressed under basal conditions. Ablation of the RARγ gene by homologous recombination results in an F9 subline (F9γ−/−), which maintains synthesis of RARα but has an absolute deficit of RARγ (Boylan et al., 1993). RARγ expression in the F9γ−/− cellular background is partially reconstituted by transgenesis in F9γ51 cells (Taneja et al., 1997).

Figure 1B demonstrates that the proliferation curves of F9-WT and F9γ−/− cell lines in standard culture conditions were very similar. Furthermore, the growth of the two cell types did not differ significantly from that determined for RARγ51. Finally, the morphology of the three lines growing in basal conditions is indistinguishable (data not shown). The similarities of F9-WT and F9γ−/− cells in vitro are recapitulated in vivo. Figure 1C illustrates the growth characteristics and the morphology of the tumors derived from the F9-WT and F9γ−/− cells in syngeneic 129/Sv mice. The two types of tumors grew as homogeneous solid masses in the peritoneal cavity and had similar and highly undifferentiated cell morphology. The growth kinetics of the two tumors were superimposable and resulted in masses of similar weight and volume. The median survival times of animals inoculated with F9-WT and F9γ−/− cells did not differ significantly and were 14.3 ± 3.2 and 13.0 ± 3.1 days (mean ± SD of three independent experiments), respectively. All together, our results indicate that RARγ expression had no influence on the in vitro or in vivo growth and morphology of

TABLE 2

Nuclear retinoic acid receptor specificity of RRMs

COS-7 cells (200,000/well) were transfected with expression vectors containing the indicated RAR isoforms (0.1 μg), a DR5-tk-reporter construct (1.0 μg) and pCH110 normalizing vector containing bacterial β-galactosidase (0.5 μg). Twenty-four hours after transfection, cells were treated for further 24 h with different concentrations of the retinoid (0.0001–10 μM), using logarithmic dilutions. CAT activity was measured in cell extracts and normalized for the level of transfection using β-galactosidase enzymatic activity. The Ec50 (the concentration giving 50% of the maximal transactivation effect) was obtained from appropriate dose-response curves run in duplicate and was calculated with the Prism version 4.0 software package (GraphPad Software, San Diego, CA). Receptor selectivity is calculated as the inverse ratio of the Ec50s determined for each couple of receptors. Each value is the mean + SD of 3 independent transfection replicates. The maximal activity is relative to ATRA, whose transactivation effect is taken as 100. This parameter is expressed as the % ratio of the CAT activity measured for each compound (1 mM) and ATRA (1 mM) after transfection of the indicated isoform. Each value is the mean + SD of 3 independent transfection replicates.

Compound		EC_{50}			Receptor Selectivity			Maximal Activity (1 μM)		
		RARα	RARβ	RARγ	RARγ/α	RARγ/β	RARα/β	RARα	RARβ	RARγ
		μM								
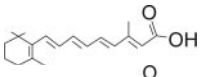	ATRA	0.02 (0.01–0.04)	0.05 (0.04–0.07)	0.03 (0.02–0.05)	0.9	1.7	2.1	100	100	100
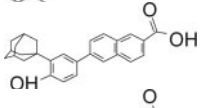	CD437	0.06 (0.05–0.55)	0.05 (0.04–0.08)	0.003 (0.002–0.004)	21.5	16.0	0.8	175 ± 8	176 ± 10	453 ± 30
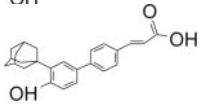	ST1926	0.16 (0.13–0.25)	0.14 (0.04–0.25)	0.14 (0.12–0.17)	1.2	1.0	0.9	201 ± 20	231 ± 9	412 ± 30

Downloaded from molpharm.aspetjournals.org at ASPET Journals on June 3, 2022

untreated F9 cells. These features support the relevance of the model for our comparative studies on RRMs and ATRA.

ST1926 and CD437, Like ATRA, Induce F9 Cytodifferentiation via RARγ. To study cytodifferentiation, we compared the ability of ATRA, ST1926, and CD437 to induce the expression of the mRNAs coding for two validated markers of the primitive endoderm, collagen IV and laminin B in F9-WT and F9γ−/− (Fig. 2A). As expected, the synthesis of the collagen IV and laminin B transcripts was induced in F9-WT cells treated with ATRA (0.1 μM) for 48 h but not in the F9γ−/− counterpart. Both ST1926 and CD437 (0.1 μM) were at least as effective as ATRA in inducing the two marker mRNAs; once again, this phenomenon was evident only in the F9-WT cell line. Hence, under the experimental conditions considered, the two RRMs acted as classic retinoids and induced primitive endodermal differentiation in a RARγ-dependent mode. Our results are consistent with the fact that RARγ expression is necessary for the retinoid-dependent differentiation of F9 into primitive endodermal cells (Boylan et al., 1993; Plassat et al., 2000). More importantly, they demonstrate that ST1926 and CD437 activated RARγ in a natural cellular context and behaved like classic retinoids at the concentration considered.

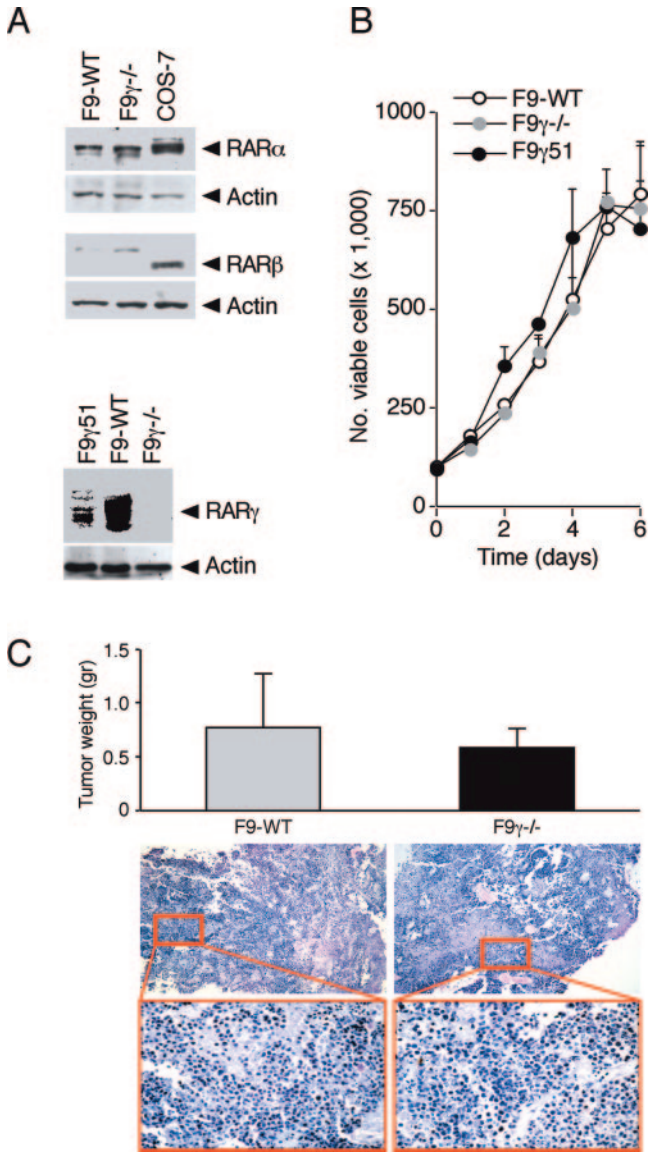

Fig. 1. RAR expression, proliferation, and differentiation of F9-WT, F9γ−/−, and F9γ51 cell lines. A, cell extracts were prepared from logarithmically growing F9-WT, F9γ−/−, and F9γ51 cells. Extracts of COS-7 cells transfected with RARα and RARβ cDNAs were used as positive controls. Western blot analyses were conducted with specific anti-RARα, RARβ, RARγ, and β-actin polyclonal antibodies. B, the proliferation curves of the indicated cell lines grown in complete medium are shown. The results are the mean ± S.D. of three replicate cell cultures. C, the bar graph shows the weight of the F9-WT and F9γ−/− tumors 10 days after i.p. transplantation of the corresponding cells (3×10^6/animal). The results are the mean ± S.D. of the tumor masses determined in 10 animals. The photographs illustrate the microscopic morphology of the F9-WT and F9γ−/− tumors after hematoxylin-eosin staining of representative tissue slices.

ST1926 and CD437 Induce Growth Arrest and Cell Death via a RARγ-Independent Mechanism. We evaluated whether the RARγ-dependent cytodifferentiation induced by the two RRMs was accompanied by growth inhibition. As documented by Fig. 2B, the action of ST1926 and CD437 could be divided in two phases. In fact, within the first 48 h, both compounds blocked the growth of F9-WT and F9γ−/− cells. At first, growth inhibition was not accompanied by a loss in cell viability, which was always above 80%, as observed in the case of control cultures (data not shown). After 2 days of treatment, a progressive and similar decrease in viability was evident in both cell lines. Contrary to what was observed in the case of the two RRMs, equimolar concentrations of ATRA induced only a delay in the growth of F9-WT and F9γ−/− cells and no significant cytotoxicity at any of the time points considered. As shown in Fig. 2C, increasing the concentration of ST1926 and CD437 to 2 μM caused a dose-dependent decrease in the number of viable cells already evident at 48 h. In these conditions, ST1926 and CD437 reduced the viability of F9-WT cells from 88 ± 1% (mean ± S.D., $n = 3$) to 66 ± 2 and 63 ± 6 at 0.5 μM, 29 ± 4% and 41 ± 10% at 1 μM, as well as 12 ± 4% and 6 ± 2% at 2 μM. Even at these relatively high concentrations, the cytotoxic effect of the two compounds did not correlate with RARγ expression. In fact, not only F9-WT and F9γ−/− cells but also F9γ51 cells showed very similar responses to the cytotoxic action of ST1926 and CD437. It is noteworthy that even the highest concentrations of ATRA (1 and 2 μM), though producing a growth inhibitory effect (Fig. 2C), continued to be devoid of significant cytotoxic activity on any of the cell lines considered. In fact in all cases, cell viability did not differ significantly from control conditions (data not shown). Overall, our results indicate that, in the case of both the RRMs and ATRA, growth inhibition was dissociated from the induced cytodifferentiating action. More importantly, they demonstrate that the observed growth inhibitory effects of ST1926 or CD437 and ATRA were intrinsically different. ATRA showed a pure antiproliferative action, whereas the activity of the other two compounds on F9 cell growth involved both an antiproliferative and a cytotoxic component.

ST1926 and CD437 Induce a G_2/M Arrest of the Cell Cycle. The cell cycle perturbations afforded by low concentrations (0.1 μM) of the two RRMs and ATRA were determined within the first 24 h of treatment. These experimental conditions were designed to avoid interferences caused by cytotoxicity. Figure 3 shows FACS profiles, along with the corresponding quantitative results, of F9-WT and F9γ−/− cells treated for 12 and 24 h with the three compounds. The overall picture of the cell cycle perturbations afforded by

Downloaded from molpharm.aspetjournals.org at ASPET Journals on June 3, 2022

ST1926 and CD437 was similar in both F9 lines. The two compounds caused a rapid depletion of the G_1 compartment that was already evident at 12 h. This was accompanied by an expansion of the S and/or G_2/M phase. The results obtained with ATRA were significantly different. Despite a slowed progression along the cell cycle, indicated by an increase in the S phase at 24 h, ATRA caused no accumulation in G_2/M in either F9-WT or F9γ−/− cells. The expected accumulation in G_1, as demonstrated in previous reports (Li et al., 2004), was observed at later time points (3–4 days, data not shown). It was clear that ST1926/CD437 and ATRA blocked the cells in two distinct phases of the cycle, demonstrating that the cellular mechanisms activated were different. Thus, our results support the concept that a classic retinoid dependent response was not at the basis of the early growth arrest afforded by RRMs.

ST1926 and CD437 Were Characterized by an Apoptotic Action That Did Not Require RARγ. As shown in Fig. 4A, treatment of F9-WT, F9γ−/−, and F9γ51 cells with ST1926 for 24 h induced morphological changes characteristic of apoptosis in a dose-dependent manner and regardless of RARγ expression. This was accompanied by the appearance of early apoptotic markers, such as annexin V binding to the plasma membrane (Fig. 4B) and caspase-3 activation (Fig. 4C). The fraction of viable (annexin V and PI negative, AV−/PI−), early apoptotic (AV+/PI−), late apoptotic (AV+/PI+), and necrotic (AV−/PI+) cells present in F9-WT and F9γ−/− cultures was evaluated by flow cytometry, after treatment with ST1926 or ATRA (0.5 μM) for 24 h. Fig. 4B, left, shows typical FACS scatter plots obtained upon challenge of F9 cells with vehicle or ST1926. A summary of the quantitative data is presented in bar graphs. In both F9-WT and F9γ−/− cultures, ST1926 caused a similar increase in the proportion of early and late apoptotic cells, leaving the number of necrotic cells basically unaltered. This was mirrored by a proportional decrease in the number of viable cells in ST1926 treated F9-WT and F9γ−/− cultures. Exposure of F9γ−/− and F9-WT cells to 0.5 μM ST1926 or CD437 for 24 h resulted in a similar activation of the early apoptotic marker, caspase-3, as measured by hydrolysis of the DEVD-amc substrate (Fig. 4C). Taken together, our re-

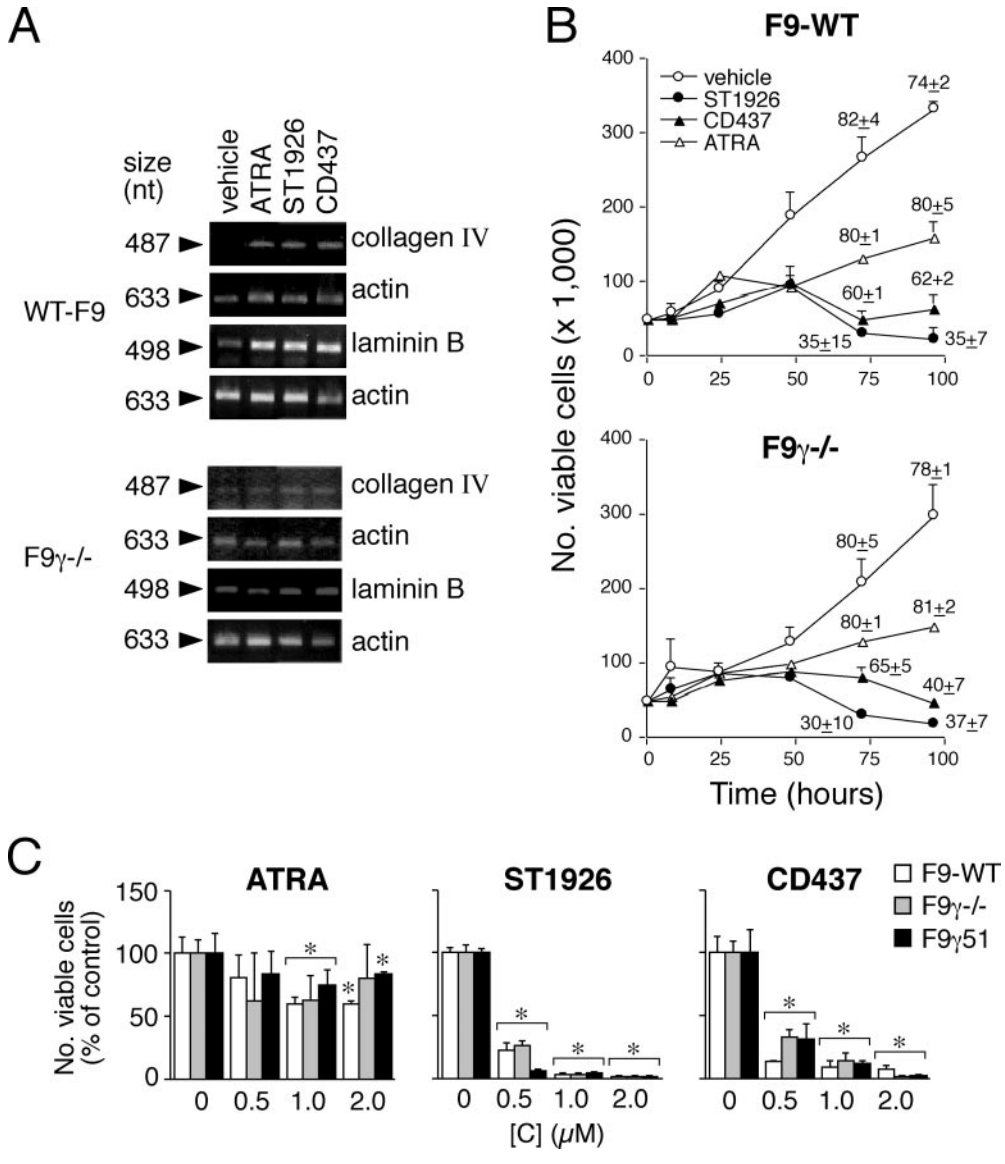

Fig. 2. Cytodifferentiating, antiproliferative, and cytotoxic activities of RRMs and ATRA in F9-WT, F9γ−/−, and F9γ51 cell lines. A, total RNA was extracted from the indicated cell lines after incubation for 48 h with vehicle, 0.1 μM ATRA, ST1926, and CD437. An equivalent amount of RNA (1 μg) was subjected to RT-PCR with couples of amplimers specific for collagen type IV, laminin B1 subunit 1, and actin. PCR-amplified bands were electrophoresed in 1% agarose gels and stained with ethidium bromide. The size of the amplified bands is indicated on the left. B, growth curves of F9 cells treated with low concentrations of RRMs and ATRA. F9-WT and F9γ−/− cells were treated with vehicle (DMSO) and the same concentration (0.1 μM) of ST1926, CD437, or ATRA for different lengths of time. The number of cells was determined after staining with erythrosine. During the first 48 h of treatment, the viability of cells is the same in all experimental groups (> 80%) and the corresponding values are not indicated. The viability observed for each experimental group is shown (mean ± S.D., $n = 3$) in correspondence, with each point of the graph starting from the 72-h time point. C, the indicated cell lines were treated with vehicle (DMSO), ATRA or the indicated RRMs for 48 h. At the end of the treatment, adhering cells were harvested and counted after staining with erythrosin. The values are the mean ± S.D. of three replicate cell cultures. *, significantly lower than the relative control value ($p < 0.01$ according to the Student's t test).

Downloaded from molpharm.aspetjournals.org at ASPET Journals on June 3, 2022

sults indicate that apoptosis was the main modality of the observed RRM-induced cytotoxic effect.

Equimolar concentrations of ATRA exerted no significant effect on the proportion of live or apoptotic cells relative to control conditions (Fig. 4B). The apoptosis markers considered were negative in all types of F9 cells treated with up to 1 μM ATRA and for up to 6 days. Indeed, F9γ−/− cell cultures exposed to 1 μM ATRA for 6 days contained 90 ± 1% live, 4 ± 1% early apoptotic, 1 ± 0.2% late apoptotic, and 4 ± 1% necrotic cells, compared with 92 ± 1% live, 5 ± 1% early apoptotic, 1 ± 0.1% late apoptotic and 3 ± 1% necrotic cells in the corresponding vehicle-treated cell cultures. Similar results were obtained in F9-WT cells (data not shown). Thus, in conditions of complete cell-kill by ST1926 and CD437, ATRA did not show apoptotic or cytotoxic activity. The data indicate that RARγ expression neither mediated nor modulated RRM-induced programmed cell death. In addition, they suggest that activation of the retinoic acid nuclear receptor pathway is unlikely to be significant for the apoptotic process activated by RRMs.

The Apoptotic Response of F9 Cells to RRMs Involved an Early Rise in Cytosolic Calcium. One of the earliest effects activated by RRMs in the NB4 leukemia cell line was is an increase in cytosolic calcium ions (Garattini et al., 2004a). We proposed that the phenomenon is at the basis of the apoptotic process activated in this cell line. To establish whether perturbations in the homeostasis of calcium are a general phenomenon, we performed a number of experiments in the F9 model.

In a first set of experiments (Fig. 5A), the amounts of intracellular calcium were determined semiquantitatively in single F9-WT cells grown as monolayers and preloaded with the calcium indicator Fluo3-AM. Treatment of F9-WT cells for up to one h with ST1926, but not vehicle (data not shown), resulted in a significant and time-dependent increase of intracellular calcium. This effect is evident in the majority of ST1926 treated cells. Similar results were obtained in F9γ−/− cells (data not shown). To get quantitative information on the phenomenon, FURA-2 was measured continuously on suspensions of F9-WT and F9γ−/− cells after addition of ST1926 or CD437 (Fig. 5B). Treatment with the two RRMs leads to an immediate increase in the cytosolic levels of calcium with very similar time courses. The time dependence values for the elevation of FURA-2 fluorescence induced by ST1926 and CD437 in the two cell lines are very similar. At equimolar concentrations, ATRA (Fig. 5B, right) and inactive ST1926 congeners (data not shown) exerted no significant action on calcium homeostasis. Our data demonstrate that RRMs induced a rapid and long-lasting elevation of cytosolic calcium that is independent of the adherence to an extracellular substratum. Furthermore, they suggest that calcium mobilization represents an upstream event in the biochemical cascade activated by ST1926 and CD437 in F9 cells. In particular, RRM-dependent increases in cytosolic calcium preceded the appearance of any sign of apoptosis. As documented by Fig. 5C, the intracellular calcium chelator BAPTA (10 and 50 μM) suppressed the elevation of calcium afforded by ST1926 or CD437 in both cell lines. Figure 5D demonstrates that BAPTA (10 μM) blocked the RRM-dependent caspase-3 activation observed in F9γ−/− and F9-WT cells. These results indicate a central role for calcium, even in the case of a transcription and protein synthesis-dependent process of apoptosis like the one activated by RRMs in F9 cells.

Comparison of the Expression Profiles Associated with ST1926 and ATRA in F9-WT and F9γ−/− Cells Indicates Activation of Retinoid-Dependent and -Independent Pathways by RRMs. F9-WT and F9γ−/− cells were used to compare perturbations of the transcriptome induced by equimolar concentrations of ST1926 and ATRA. With this type of experiment, we aimed at gathering information on the molecular mechanisms underlying the action of ST1926. In particular, we intended to identify the gene profiles associated with the retinoid-dependent and -independent components of the RRM action. Furthermore, we wanted to establish the fraction of genes whose expression is controlled or modulated by RARγ activation.

As shown in Fig. 6A, treatment of F9-WT and F9γ−/− cells with ST1926 or ATRA (0.5 μM) for 10 h results in a significant up- or down-regulation of 2523 probes (2296 genes) ($p < 0.0001$ after two-way ANOVA for any of the two factors, cell line or treatment). A total of 903 probes (847 genes) has regulation patterns relevant to the study and can be classified in nine groups after Pavlidis template matching (Pavlidis and Noble, 2001) and hierarchical clustering (Fig. 6 and Fig. 7). A complete list of these genes and

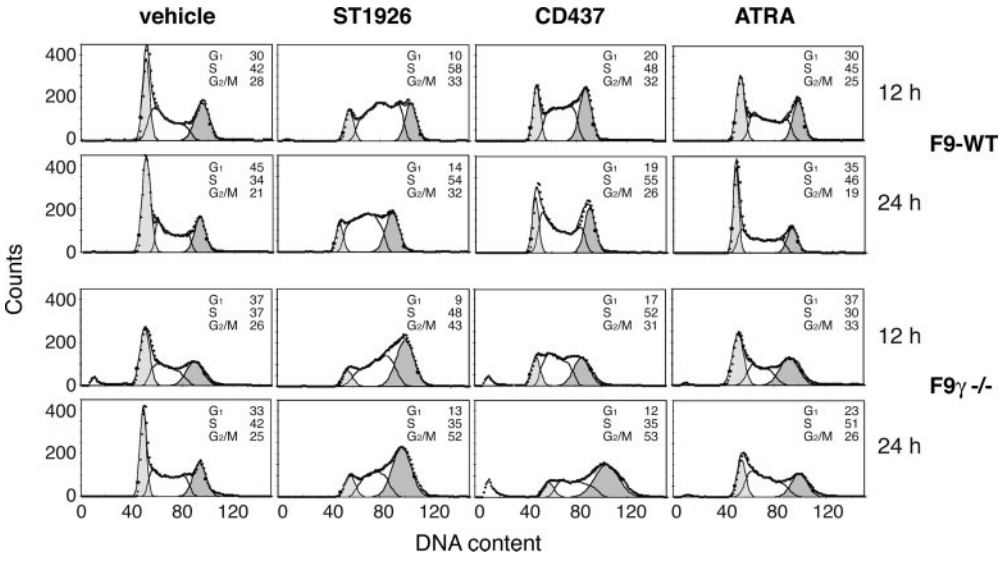

Fig. 3. Effects of RRMs and ATRA on the cell cycle phases of F9-WT and F9γ−/− cells. Representative FACS profiles of cells treated with 0.1 μM ST1926, CD437, and ATRA for 12 and 24 h. FACS analysis was performed after DNA staining with propidium iodide. The graphs show the experimental profile (dotted line) and the gaussian fitting (G_1 phase, light gray peaks; S phase, "empty" curves; G_2/M phase dark gray peaks; sum of the fitted curves, solid line). The percentage of cells present in the G_1, S, and G_2/M phases of the cycle is indicated. The data shown are representative of three experiments giving similar results.

Downloaded from molpharm.aspetjournals.org at ASPET Journals on June 3, 2022

their functional classification (using Ease; http://david.niaid.nih.gov/david/ease1.html) is presented in Supplementary Table 2. The diagram illustrates the number of genes falling in the various classes defined. Of the 178 probes under the control of ATRA (Fig. 6B, groups 1–6), 101 (57%) were regulated in a similar manner by ST1926 (groups 1–3). This supports the concept that the RRM is a bona fide retinoid and activates a substantial fraction of the same genetic program controlled by ATRA. However, our results also demonstrated that ST1926 regulated a much larger set of genes than ATRA in both F9-WT and F9γ−/− cells (826 versus 178; Fig. 6A). This indicates a major contribution of retinoid-inde-

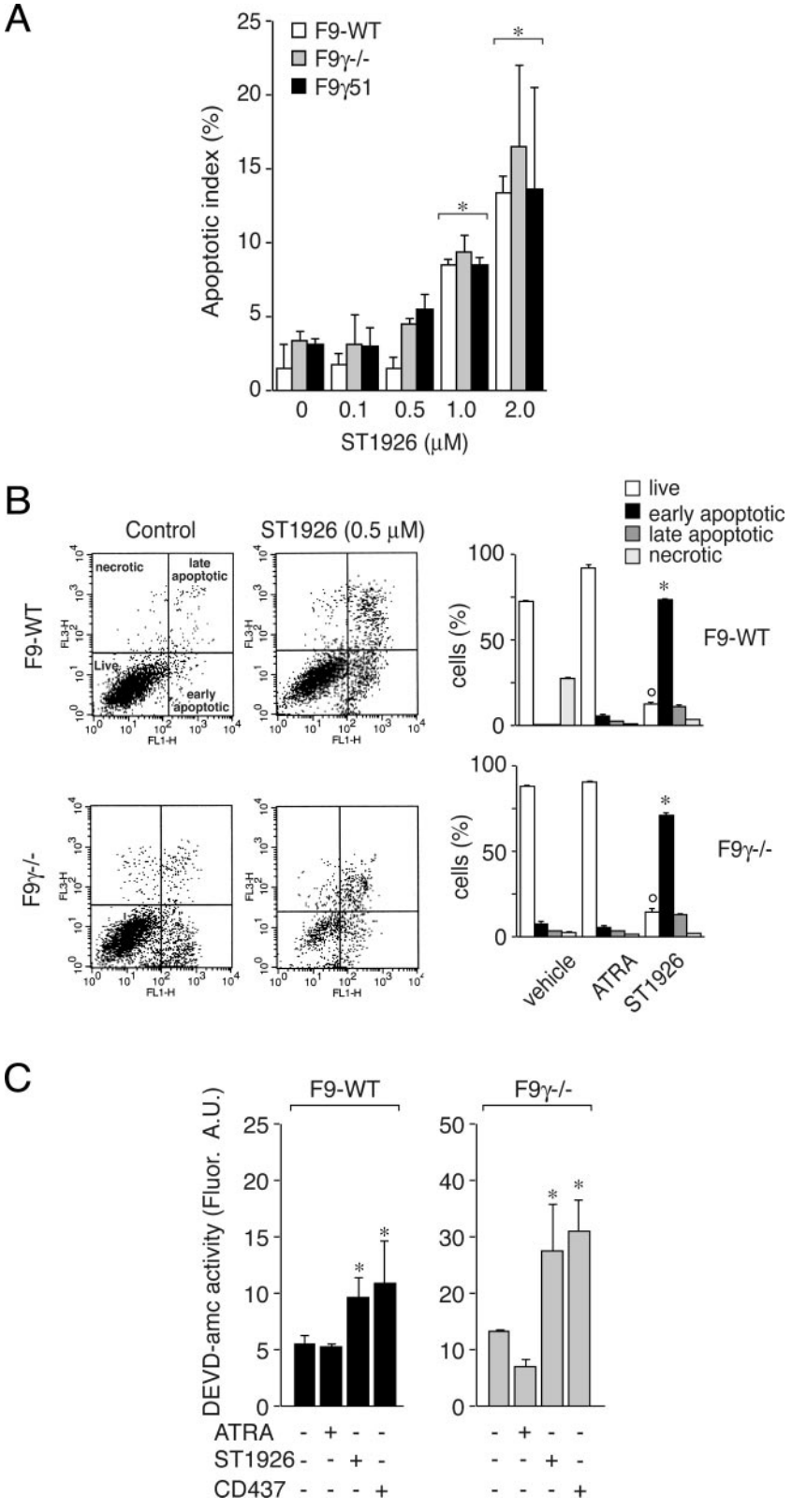

Fig. 4. Apoptosis and caspase activation of RRMs and ATRA in F9-WT and F9γ−/− cell lines. A, F9-WT and F9γ−/− cell lines were treated for 24 h with the indicated concentrations of ST1926. At the end of the treatment, adhering cells were scored for the number of fragmented nuclei (apoptotic index) after staining with 4,6 diamidino-2-phenylindole. Each value is the mean ± S.D. of three replicate cell cultures. *, significantly higher than the relative control value ($p < 0.01$ according to the Student's t test). B, left, shows representative FACS analyses of substrate adhering F9-WT and F9γ−/− cells treated for 24 h with vehicle (DMSO) or ST1926 (0.5 μM). Cells were stained with PI (vertical axis) and a fluorescein-conjugated antibody directed against annexin V (AV) (horizontal axis). AV−/PI− (lower left quadrant), AV−/PI+ (upper left quadrant), AV+/PI− (lower right quadrant), and AV+/PI+ (upper right quadrant) cells indicate live, necrotic, early apoptotic, and late apoptotic cells, respectively. Bar graphs of the quantitative results obtained on F9-WT and F9γ−/− cells treated for the indicated amounts of time with 0.5 μM ST1926 or ATRA are shown on the right. The results are the mean ± S.D. of three replicate cell cultures and were obtained after quantitation of the results shown by FACS analyses similar to those presented. Significantly higher (*) or lower (°) than the relative control value ($p < 0.01$ according to the Student's t test). C, F9-WT and F9γ−/− cells were treated with 0.5 μM ATRA, ST1926, and CD437 for 24 h. At the end of the treatment, DEVD-amc hydrolytic activity was measured on cell extracts and expressed in fluorescence arbitrary units (A.U.). Each value is the mean ± S.D. of three replicate cell cultures. *, significantly higher than the relative control value ($p < 0.01$ according to the Student's t test).

Downloaded from molpharm.aspetjournals.org at ASPET Journals on June 3, 2022

pendent pathways to the early action exerted by ST1926 on the F9 transcriptome.

Genes Regulated Concomitantly by ST1926 and ATRA Defined Classic Retinoid Responses. Group 1 includes target genes up- or down-regulated concomitantly by ST1926 and ATRA in both F9-WT and F9γ−/− cells (Fig. 6B). This group consisted of genes possibly modulated by ligand-induced activation of RARα/RARβ. Among the genes whose expression was diminished, Myc and the DNA methyltransferase 3B stand out. Myc is a gene down-regulated by retinoids in different cellular contexts and is known to control progression from the G_1 to the S phase of the cycle. Myc down-regulation may play a role in the cell cycle arrest triggered by ATRA in G_1 but is unlikely to be a major determinant of the G_2/M arrest observed in the case of ST1926. DNA methyl transferases are associated with gene silencing, and their inhibition has been implicated in the gene activation effects triggered by classic retinoids (Fazi et al., 2005).

The cluster of genes up- or down-regulated by ST1926 and ATRA in F9-WT cells preferentially (Fig. 6B, group 2) was likely to be under the control of ligand-activated RARγ. Homeobox A5 and iroquois-related-homeobox 2 belong to this group, suggesting a particular significance for the process of primitive endodermal maturation induced by ST1926 and ATRA. Indeed, homeotic genes are well known retinoic acid targets and are implicated in morphogenesis and organogenesis (Deschamps and van Nes, 2005). Several other members of this family were noticeably induced preferentially by ATRA in a RARγ-dependent fashion (Fig. 6B, group 5). Homeobox gene A1 (*HOXA1*) was the only HOX gene induced specifically by ATRA not only in F9-WT but also in F9γ−/− cells (Fig. 6B, group 4). However, the basal levels of HOXA1 expression were much higher in the former than in the latter cell line (Miamexpress; accession number E-MEXP-361), suggesting RARγ independence in the case of induced expression and possible RARγ dependence in the case of basal expression.

The molecular signature associated with ST1926 and ATRA in F9γ−/− cells (Fig. 6B, group 3) was of unknown significance and consisted of 11 genes. The sole gene up-

Downloaded from molpharm.aspetjournals.org at ASPET Journals on June 3, 2022

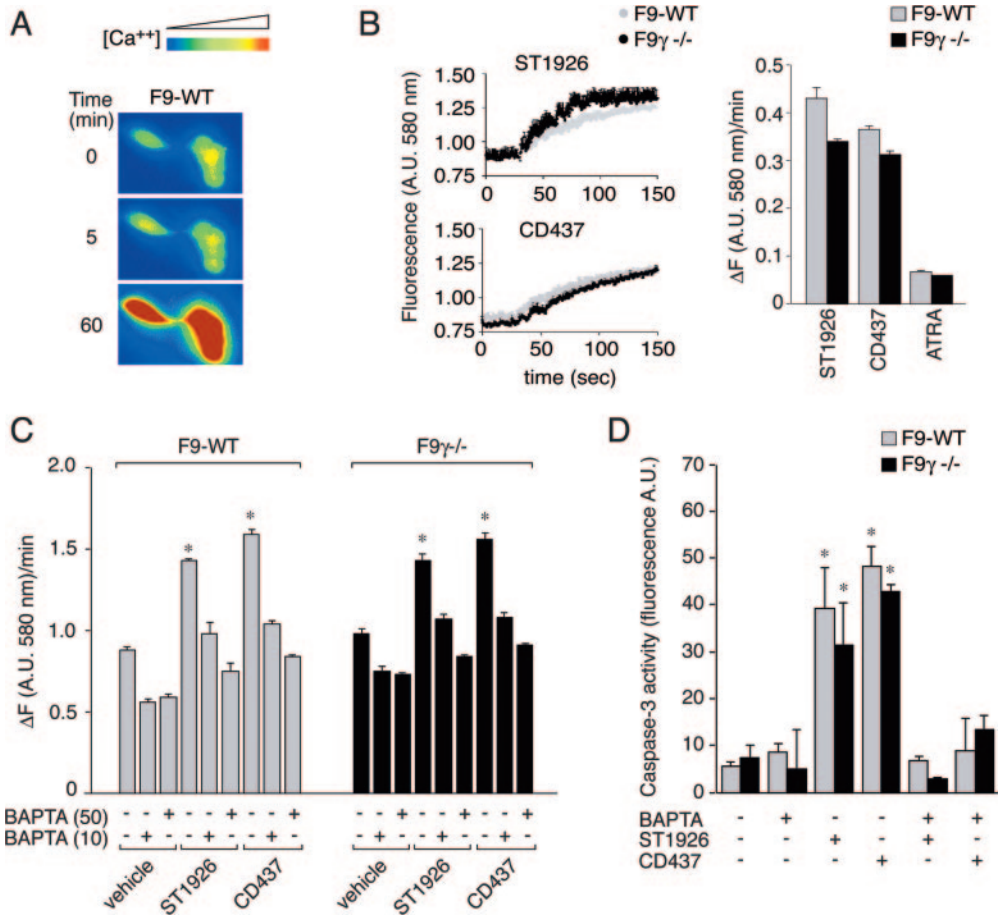

Fig. 5. Effect of ATRA, ST1926, and congeners on cytosolic calcium homeostasis. A, F9-WT and F9γ−/− cells were seeded on appropriately treated glass slides and loaded with the intracellular calcium indicator Fluo3-AM. Loaded cells were treated for up to 1 h with ST1926 (1 μM) and the amounts of Fluo3-AM derived fluorescence were measured continuously at the single cell level. The picture illustrates the levels of cytosolic calcium accumulation in two adjacent cells using pseudo-colors. B and C, FURA-2–loaded F9-WT and F9γ−/− cells were stimulated with the indicated compounds at a concentration of 1 μM and fluorescence measured continuously over the course of 2.5 min. B, left, shows continuous measurements, whereas C and B, right, show quantifications of the results, expressed as variation of fluorescence arbitrary units/time (ΔF/min) and calculated during the linear phase of calcium rise. In the case of the results shown in C, before addition of RRMs, cells were preincubated in the presence or absence of 10 and 50 μM BAPTA for 2 min. Each experimental value is the mean ± S.D. of three replicate cell cultures. ∗, significantly higher than the relative control value ($p < 0.01$ according to the Student's t test). D, DEVD-amc hydrolytic activity was measured in extracts of cells treated for 24 h with ST1926 (1 μM) or CD437 (1 μM) in the presence or absence of BAPTA (10 μM). The results are expressed in fluorescence arbitrary units (A.U.) and represent the mean ± S.D. of three replicate cell cultures. ∗, significantly higher than the relative control value ($p < 0.01$ according to the Student's t test).

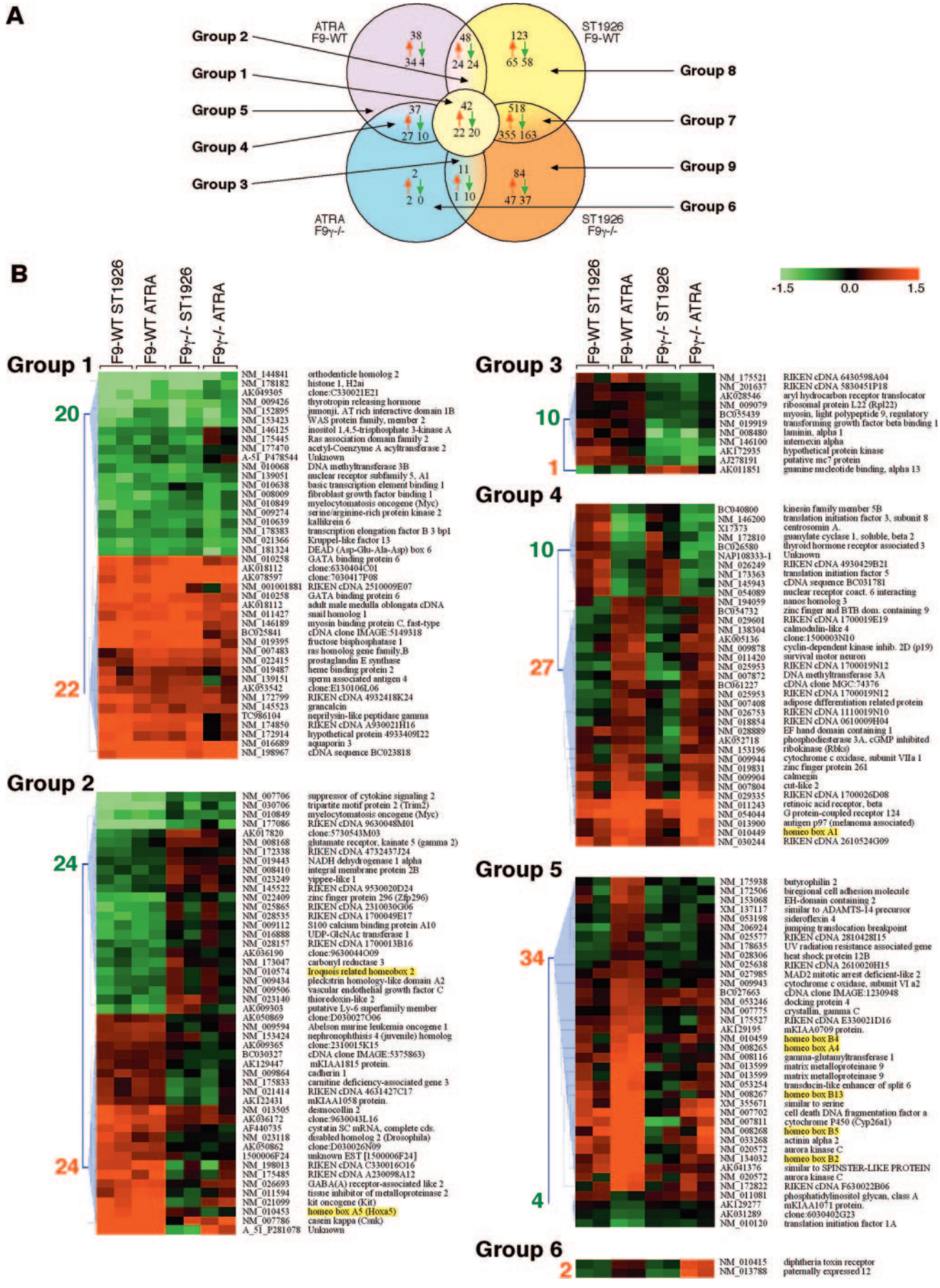

Downloaded from molpharm.aspetjournals.org at ASPET Journals on June 3, 2022

regulated in this group was the G protein α3, a polypeptide involved in G-protein signaling.

Genes Specifically Regulated by ST1926 Defined Nonretinoid-Associated Responses. The genes modulated by ST1926, and not by ATRA, in both F9-WT and F9γ−/− cells (Fig. 7, group 7) are likely to be relevant for the selective in vitro apoptotic action and G_2/M arrest triggered by the RRM. Consistent with this notion, 23 of the 355 up-regulated genes are proapoptotic or involved in the arrest of the cell cycle. For the same reason, 11 of the 163 down-regulated genes are positive modulators of cell growth. The list of proapoptotic genes includes elements of both the intrinsic and extrinsic pathways of programmed cell death, such as p73, caspase-3, members of the TNF receptor family, and TRAF4. As for TNF receptors, it is important to underscore that these proteins belong to the same family of the death receptors that plays a fundamental role in the extrinsic pathway of apoptosis. CD437 has been proposed to exert its apoptotic action through activation of autocrine or paracrine loops involving death receptors and corresponding ligands, such as the FAS and FAS-ligand couple (Sun et al., 2000b; Jin et al., 2005). In group 7, PERP, APAF1, and Bcl-2 binding component 3, are direct or indirect targets of p53. It is noteworthy that F9 teratocarcinoma cells are known to express wild-type p53 (Mayo and Berberich, 1996), which sensitizes other types of neoplastic cells to the action of RRMs (Sun et al., 1999). Given the importance of calcium in the process of apoptosis triggered by RRMs, the presence of 19 genes encoding polypeptides, such as protein phosphatase 1D and diacylglycerol kinase α, regulated by the cation, was of particular significance. The modulation of these genes might be the consequence of the early increase in calcium ions afforded by ST1926 and CD437. Group 7 contained a number of induced genes involved in DNA repair (four genes, six probes; Supplemental Table 1), suggesting that ST1926 may have DNA damaging activity (Garattini et al., 2004b).

Groups 8 and 9 consisted of genes modulated by ST1926, but not ATRA, in either F9-WT or F9γ−/− cells specifically. In F9γ−/− cells, treatment with ST1926 caused down-regulation of four genes involved in motility and angiogenesis and up-regulation of three genes responsible for cellular adhesion (Fig. 7, group 9). Conversely, the RRM induced the expression of two cell motility and angiogenesis genes (septin 2 and neuropilin) in F9-WT cells. Induction of group 8 gene products acting at the interface between the cell and the extracellular space, such as receptors of the platelet-derived growth factor or TNF family and BMP membrane bound inhibitor (Supplemental Table 1), are also of particular interest. These observations indicate that ST1926 has RARγ-dependent effects on cellular processes other than proliferation, differentiation, and apoptosis.

ST1926 and CD437 Modulated the Same Type of Genes. The results obtained with whole-genome microarrays were validated and extended to CD437 for a selected number of genes. A first validation was conducted by semi-quantitative agarose gel electrophoresis of the cDNA bands obtained by RT-PCR (Fig. 8A, left). For c-kit, c-myc, Notch Hom.3, and the homeo box A1 (*HOXA1*) gene, we also obtained quantitative results by Taqman real-time PCR (Fig. 8A, right). The experiments presented were totally independent of each other and of the ones used for the microarray analysis. The expression profile of all the genes considered was entirely consistent with what was observed with the microarray experiments. A small exception to this rule (1 of 10 genes, including *RARβ*; see below) is represented by c-kit, which shows induction by ST1926 (and CD437) also in F9γ−/− cells. This may be because the primers used for the RT-PCR and Taqman real-time PCR analyses are targeted against regions of the transcripts that are different from those represented by the corresponding microarray probes. Consistent with the primary microarray data, the Taqman data demonstrate that the constitutive levels of the HOXA1 transcript are lower in the F9γ−/− than in F9-WT cells. It is noteworthy that all these genes were regulated by CD437 in a fashion similar to that of ST1926, suggesting that the two compounds activate a very similar genetic program. This further supports the concept that ST1926 and CD437 belong to the same functional family of compounds (Garattini et al., 2004a).

RARβ belonged to the group of genes induced by ATRA more than ST1926 in both F9-WT and F9γ−/− cells (group 4). As a whole, the RT-PCR data (Fig. 8B) confirmed that the receptor was induced more efficiently by ATRA than by RRMs in F9γ−/− cells. However, this differential effect was not observed in F9-WT cells, also because of the lower basal levels of the transcript in this cell line. Although quantitative differences in the induction of RARβ by ATRA and ST1926 or CD437 were observed in F9-WT and F9γ−/− cells, the finding is in agreement with previous results indicating that RARβ2 can be up-regulated by multiple RAR isoforms in a redundant fashion (Rochette-Egly and Chambon, 2001). It is noteworthy that RARβ was the only retinoid receptor whose expression was modulated by RRMs or ATRA in F9 cells. In fact, ST1926, CD437, and ATRA did not affect the basal level

Fig. 6. Gene expression profiling: general results and classic retinoid responses. F9-WT and F9γ−/− cells were treated with vehicle (DMSO), ATRA (0.5 μM), or ST1926 (0.5 μM) for 10 h. Poly(A+) RNA was isolated from three separate culture flasks and pooled. In the first experimental replicate (leftmost lane of each experimental group), vehicle RNA was labeled with the fluorochrome Cy3, whereas ATRA- or ST1926-RNA was labeled with Cy5. In the second experimental replicate (rightmost lane of each experimental group), fluorochromes were swapped; i.e., vehicle-RNA was labeled with Cy5, whereas ATRA- or ST1926-RNA was labeled with Cy3. Cy3 and Cy5 RNAs were mixed in equimolar amounts and hybridized to oligonucleotide microarrays. After filtering the data for significant changes using two-way ANOVA ($p < 0.0001$), groups of genes with interesting regulation pattern were selected after hierarchical clustering (group 1) or Pavlidis template matching (all other groups). A, the scheme represents the number of probes up-regulated (red arrow) or down-regulated (green arrow) in the various experimental conditions. Probes are grouped according to the pattern of expression. B, the genes regulated by ST1926 and ATRA concordantly in both F9-WT and in F9γ−/− cells are presented in group 1. Group 2 contains genes controlled by ST1926 and ATRA in F9-WT cells preferentially. Group 3 consists of genes regulated by ST1926 and ATRA in F9γ−/− cells. Group 4 represents genes modulated by ST1926 alone in both F9-WT and in F9γ−/− cells. The genes whose expression is specifically modulated by ATRA in F9-WT and F9γ−/− exclusively are shown in groups 5 and 6, respectively. The values next to each node indicate the number of probes present in the corresponding cluster (green, down-regulated genes; red, up-regulated genes). Color scale refers to log2Ratios of treated samples versus corresponding control samples. Duplicates correspond to swapped samples. A shortened description of each gene and the relative GenBank accession number is indicated. The list of the genes in all clusters, with the gene ontology classification and the quantitative changes is reported in Supplemental Table 1.

Downloaded from molpharm.aspetjournals.org at ASPET Journals on June 3, 2022

of expression of RARα, RARγ, or the three RXR isoforms (Fig. 8B, left).

In Vivo, the Antitumor Activity of RRMs Was Hindered by RARγ Expression in the Neoplastic Cell. The microarray results provide information on the possible molecular determinants of the RARγ-independent processes (growth inhibition and apoptosis) triggered by RRMs in F9 cell cultures. However, they also point to a set of RARγ-dependent alterations in genes controlling processes of potential significance for the antitumor activity of RRMs in vivo, such as cell adhesion, motility, angiogenesis, proteolysis, and tumor/host interactions. Indeed, the microarray results suggest that RRM antitumor activity might be higher in the absence of RARγ.

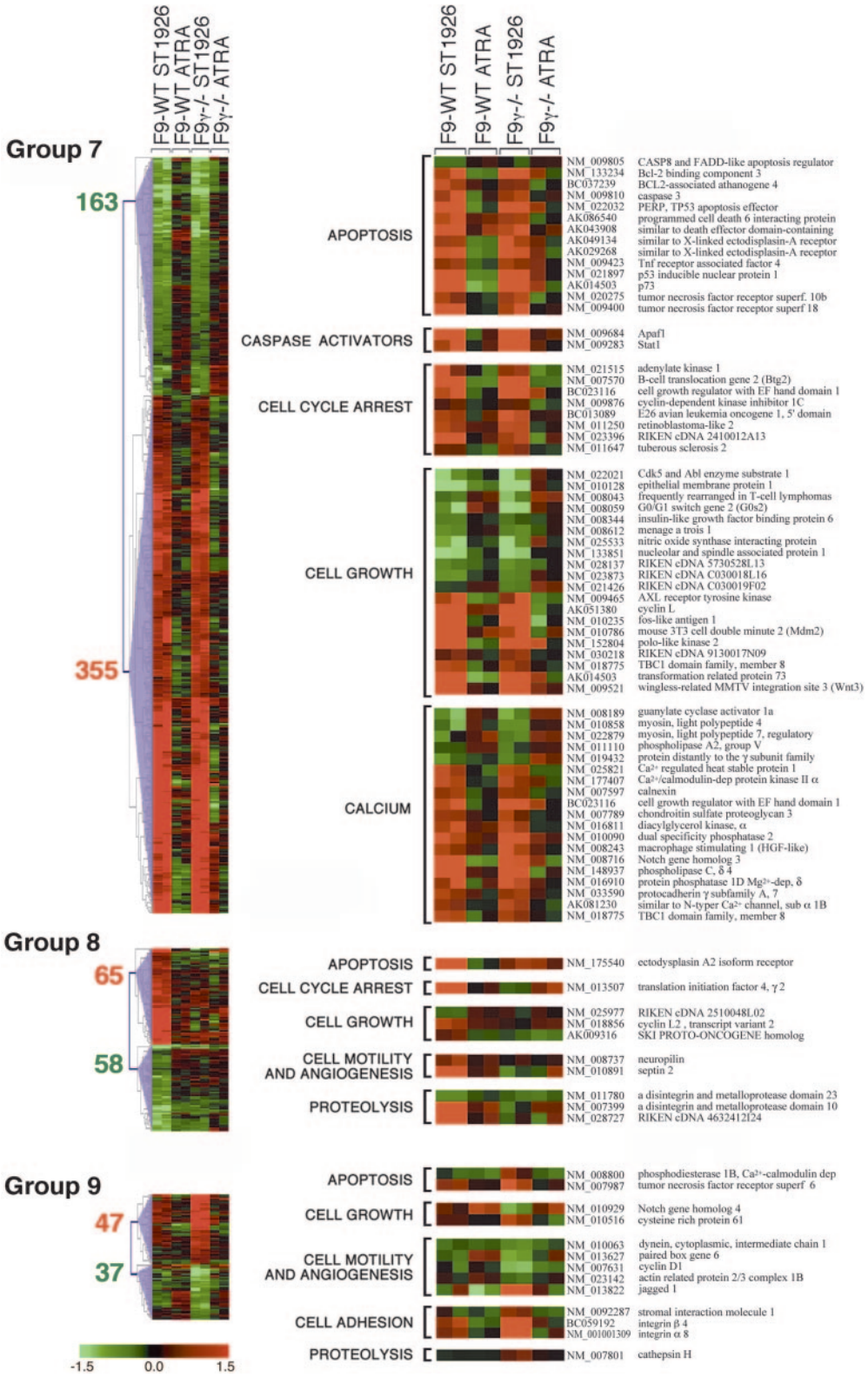

Fig. 7. Gene expression profiling: nonclassic retinoid responses. Left, hierarchical clustering of genes modulated preferentially by ST1926 in both F9-WT and F9γ−/− (group 7), F9-WT (group 8), or F9γ−/− (group 9) cells only. Data are organized and presented as in Fig. 8. The list of the genes in all clusters, with the gene ontology classification and the changes, is reported in Supplemental Table 1. Right, a selection of functionally interesting genes extracted from each group. Genes are classified according to the major area of functional interest.

Downloaded from molpharm.aspetjournals.org at ASPET Journals on June 3, 2022

The above hypothesis was tested directly in vivo, taking advantage of the fact that F9-WT and F9γ−/− grow as tumors in syngeneic mice (Fig. 1C). Figure 9A demonstrates that long-term intraperitoneal administration of ATRA at the maximal tolerated dose of 15 mg/kg did not alter the survival of either F9-WT or F9γ−/− tumor-bearing animals. The finding indicates that the ATRA-dependent antiproliferative and cytodifferentiation effects observed in cultures of F9 cells were not sufficient to translate into a therapeutic effect in vivo. In contrast, Fig. 9B demonstrates that oral administration of ST1926 (30 mg/kg) resulted in a significant increase in the median survival time of mice inoculated with both F9-WT and F9γ−/− cells. Consistent with our hypothesis, ST1926 was much more effective in F9γ−/− than in F9-WT tumor-bearing animals. Differential sensitivity of F9γ−/− and F9-WT tumors was independent of the administration route, in that a similar phenomenon was observed after i.p. treatment with ST1926 (Fig. 9C). Furthermore, the phenomenon was observed also in the case of the other RRM, CD437. Immunological responses do not seem to be at the basis of the observed differences in sensitivity between the F9γ−/− and F9-WT tumors. This is supported by the results obtained in the B- and T-cell–deficient SCID mouse (Fig. 9D). Even in this model, ST1926 and CD437 (i.p. administered) demonstrate a superior effect on mice bearing F9γ−/− tumors. Thus, our results demonstrate that RARγ expression hinders the response of F9 cells to the therapeutic activity of RRMs in vivo. More importantly, they suggest that the in vivo action of RRMs is not simply the result of a direct cytotoxic and growth inhibitory action on tumor cells and may involve effects on the processes of metastatization, angiogenesis, or interactions with the host environment.

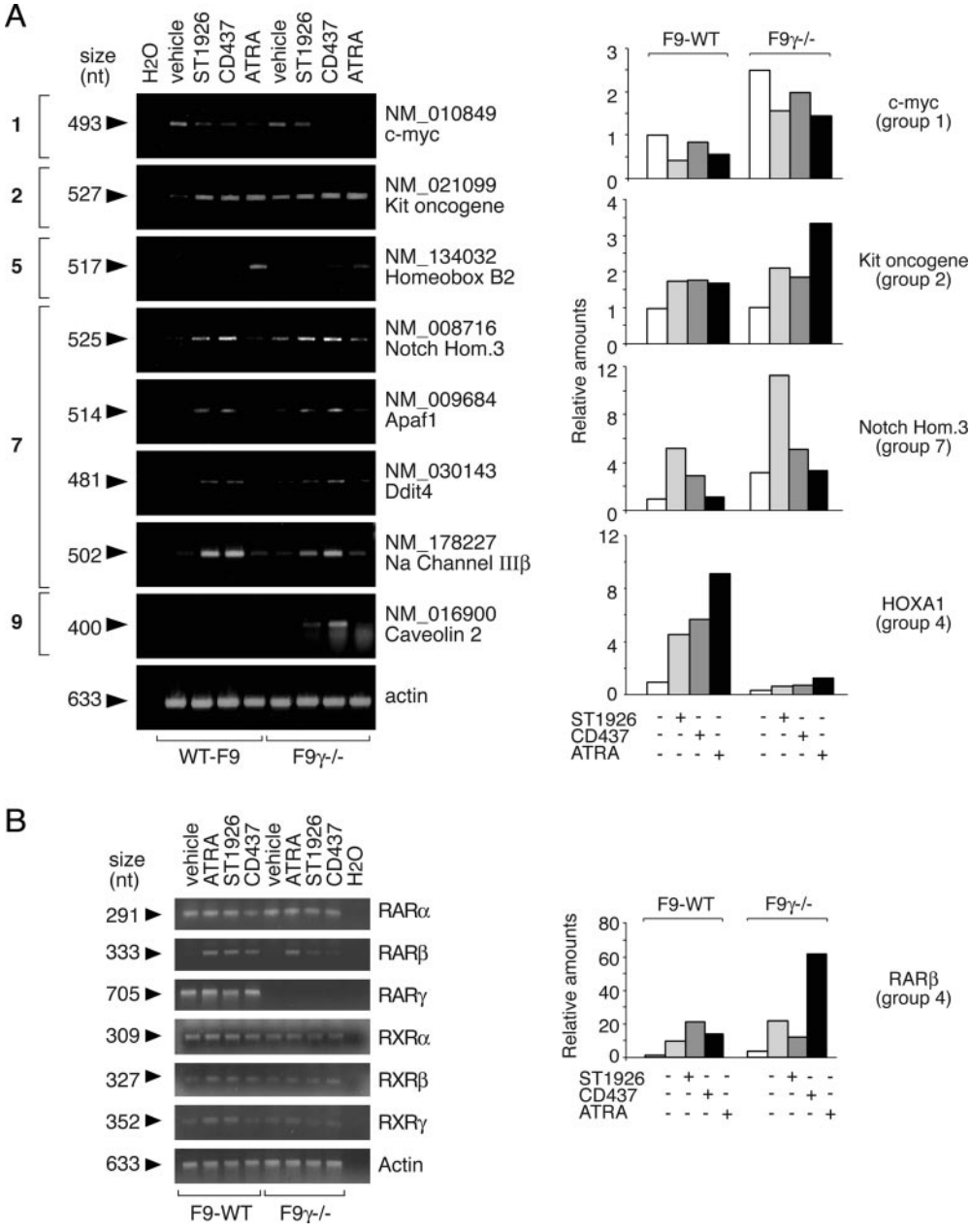

Fig. 8. PCR validation of the microarray results. A and B, total RNA was extracted from the indicated cell lines after incubation for 10 h with ATRA, ST1926, and CD437 (0.5 μM). Left, an equivalent amount of RNA (1 μg) was subjected to RT-PCR with couples of amplimers specific for the indicated genes. The PCR reactions were stopped between the 25th and 30th cycles according to the gene considered to ensure linear amplification ranges. PCR-amplified bands were electrophoresed in 1% agarose gels and stained with ethidium bromide. The size of the amplified bands (A and B) and the clusters (A) in which they were classified after microarray data analysis (Figs. 8 and 9) are indicated on the left. Right, real-time Taqman PCR of the indicated genes was performed using β-actin as an endogenous control. The data are expressed in fold-induction relative to vehicle treated F9-WT cells ($2^{-\Delta\Delta C_T}$). The results derive from two replicate CT determinations always with a variation coefficient lower than 2.5%.

Downloaded from molpharm.aspetjournals.org at ASPET Journals on June 3, 2022

Discussion

In this study, first we compared ST1926 and CD437 to ATRA for their ability to transactivate RARα, RARβ, and RARγ in COS-7 transfected cells. The data indicate that CD437 was a selective ligand of RARγ and a stronger agonist of the receptor than ATRA. ST1926 itself was a better RARγ transactivator than ATRA but lost RARγ selectivity. Both ST1926 and CD437 were poor RXR activators.

In F9 teratocarcinoma cells, we confirmed, in a native context, that ST1926 and CD437 were bona fide retinoids and had the potential to activate RARγ. As expected from classic retinoids with RARγ agonistic activity, low concentrations of the two RRMs were as effective as ATRA in inducing the cytodifferentiation of F9-WT but not F9γ−/− cells. The results obtained with whole-genome microarrays support the concept that ST1926 is endowed with classic retinoid activity.

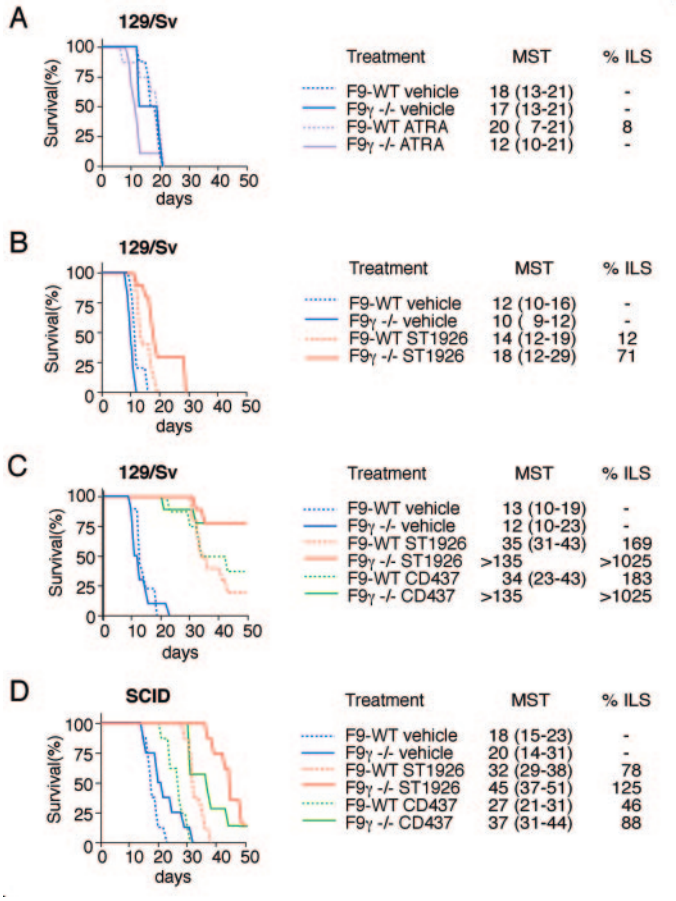

Fig. 9. In vivo effect of ST1926, CD437, and ATRA on the survival of animals transplanted with F9-WT and F9γ−/− tumors. F9-WT and F9γ−/− cells were inoculated (3×10^6/animal) i.p. into syngeneic 129/Sv (A–C) or SCID (D) mice (10 animals/experimental group). The graphs show Kaplan Meyer's survival curves. MST, median survival time expressed in days; the number in parentheses indicates the survival time range. %ILS, percentage increase in life span relative to the corresponding experimental group treated with vehicle. The value is calculated as follows: %ILS = (MST treated/MSTcontrol × 100) − 100. A, twelve hours after inoculation, animals were i.p. administered vehicle or ATRA (15 mg/kg), five times a week for 2 weeks. B, twelve hours after inoculation, animals were administered vehicle or ST1926 (30 mg/kg) orally, five times a week for 2 weeks. C, six hours after inoculation, animals were i.p. administered vehicle, ST1926, or CD437 (20 mg/kg), five times a week for 2 weeks. D, six hours after inoculation, SCID mice were i.p. administered vehicle ST1926 or CD437 (20 mg/kg) five times a week for 2 weeks.

ST1926 modulates the expression of a large proportion of the genes controlled by ATRA in F9-WT and F9γ−/− cells. A similar proportion of coregulated genes is observed in the responses specific for the F9-WT cellular context, where ATRA and RRM dependence is likely to be mediated by RARγ. These genes are of particular interest for the differentiation of teratocarcinoma cells along the parietal endoderm pathway.

The data obtained in the F9 model indicate that retinoid activity was unlikely to play a significant role in RRM-induced apoptosis, which is a primary determinant of ST1926 and CD437 antitumor activity. Indeed, the apoptotic action of RRMs is not shared by ATRA, strongly suggesting that programmed cell death is not a direct consequence of the retinoid-dependent cytodifferentiating effects as in NB4 leukemic cells (Giannì et al., 2000). Furthermore, unlike cytodifferentiation, apoptosis was independent of RARγ activation, as observed in F9-WT, F9γ−/−, and F9γ51 cells. Our results are consistent with the idea that ST1926 and CD437 activated not only the classic retinoid pathway but also a second signaling pathway. In cultures of F9 cells, the second pathway is prevalent and is at the basis of the apoptotic effect.

Similar to what we observed in NB4 myeloid leukemia cells (Garattini et al., 2004a), the earliest event associated with RRM-induced apoptosis in F9 cells is the elevation of cytosolic calcium. In NB4 cells, we demonstrated previously that calcium increases are not due to a net influx of the cation from the extracellular compartment and might be the result of RRM effects on the reuptake of the ion by the mitochondrion. Whatever the underlying mechanism, the rise in calcium is necessary for the programmed cell death activated by RRMs in NB4 and in F9 cells. In fact, in this last cell line, whereas ST1926 and CD437 were powerful calcium-mobilizing agents, ATRA and inactive RRMs were devoid of this activity. More importantly, chelation of intracellular calcium by BAPTA prevented ST1926-induced caspase activation, one of the hallmarks of apoptosis. Calcium mobilization was not influenced by RARγ, in that identical effects were observed in the F9-WT and F9γ−/− cell lines. Although the mobilization of calcium observed in RRM-treated F9 teratocarcinoma and NB4 cells is similar, the ensuing process of apoptosis is intrinsically different. In NB4 cells, apoptosis is very rapid and does not require gene expression or de novo protein synthesis. In contrast, the apoptotic response of F9 cells was slower and might therefore be dependent on gene transcription and protein synthesis. If this was indeed the case, genes relevant for the RRM-dependent apoptosis in F9 cells must be sought for among the large number of probes identified as specific and RARγ-independent targets of ST1926 (the genes controlled by ST1926, but not ATRA, in both F9-WT and F9γ−/− cells). This set of genes is of particular significance and deserves evaluation as to calcium-dependent transcriptional modulation.

The overall antitumor effect of RRMs may be the result not only of apoptotic but also of antiproliferative effects. To establish this point, we conducted studies with low and comparable concentrations of ST1926 or CD437 and ATRA. Under these conditions, the process of apoptosis activated by the two RRMs was delayed and the antiproliferative effects could be studied in a relatively clean situation. Our data demonstrate that ST1926 and CD437 treatments were associated with an early S and G_2M cell cycle block in both F9-WT and

Downloaded from molpharm.aspetjournals.org at ASPET Journals on June 3, 2022

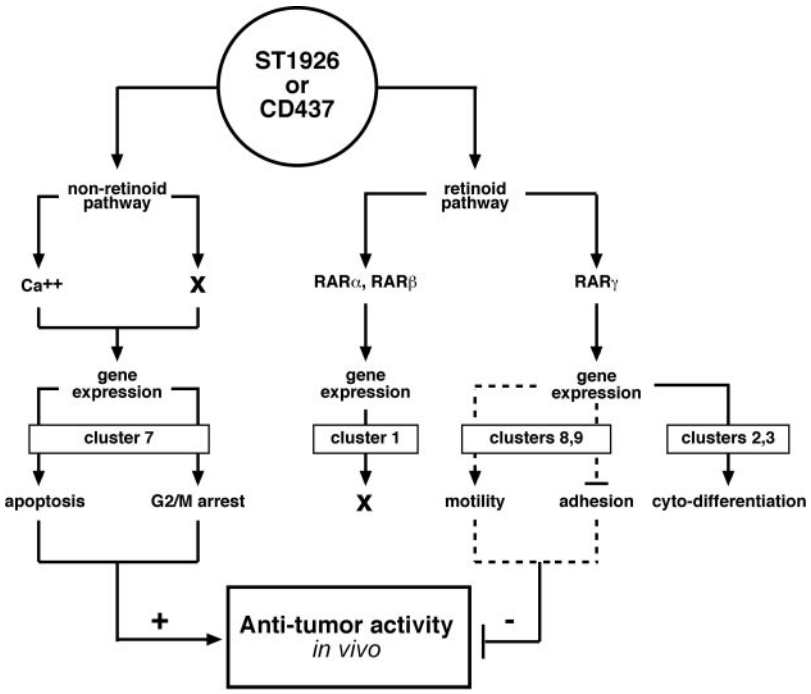

Fig. 10. Hypothetical scheme on the mechanisms underlying the pharmacological activity of RRMs in the F9 model. The scheme illustrates the various pathways activated by ST1926 and/or CD437 in F9 cells. Dashed lines indicate hypothetical processes activated by ST1926 based on the microarray data. The indication of clusters refers to the groups of genes determined with the microarray data analysis that may contain the determinants of the indicated processes.

F9γ−/− cells. The cell cycle block afforded by ATRA is different and consists of a G_1 arrest observed only after long exposures (3–4 days) (Li et al., 2004). The G_1 arrest caused by ATRA in both F9-WT and F9γ−/− cells suggests involvement of RARα and or RARβ. The assumption is in line with the observation that RARβ activation is a critical determinant of the growth arrest induced by ATRA in F9 cells (Faria et al., 1999; Zhuang et al., 2003).

Although RARγ is not a major determinant of RRMs' apoptotic and cytotoxic activity in vitro, the receptor seems to play an important role in the response of F9 tumor-bearing animals. Syngeneic and immunodeficient mice transplanted with F9γ−/− cells are more sensitive to RRMs than the corresponding counterparts inoculated with F9-WT cells. The phenomenon is not explained by differences in basal growth, in that the F9-WT and F9γ−/− untreated tumors grow in a similar fashion, show the same histological appearance, and are lethal to animals in approximately the same amount of time. Furthermore, the phenomenon is unlikely to reflect clonal variability between the F9-WT and F9γ−/− cells. In fact, animals transplanted with the two cell lines are equally insensitive to ATRA, whereas they respond equally well to intraperitoneal injection of other chemotherapeutic agents, such as cisplatin (M. M. Barzago and E. Garattini, unpublished observations). Although originally unexpected, this increased sensitivity may find an explanation in the profile of genes selectively modulated by ST1926 in either F9-WT or F9γ−/−. In fact, the cell type-specific effects observed on a number of genes controlling cell motility and angiogenic responses suggest relevance for the processes of invasion and metastasis. Overall, our data indicate that RARγ expression modulates some aspects of the host/tumor interaction unrelated to immune responses.

Figure 10 provides a summary and a rational interpretation of our observations. RRMs activated two distinct pathways in F9 cells. We defined as nonretinoid the actions exerted by ST1926 (and CD437) that were not shared by ATRA and that were likely to involve mechanisms unrelated to retinoic receptor activation. The nonretinoid pathway leads to G_2/M cell cycle arrest and apoptosis, which is mediated by a perturbation of calcium homeostasis. These two processes are likely to mediate a large proportion of the in vivo antitumor activity of both ST1926 and CD437. Although RARα and RARβ contribute to the genomic effects induced by ST1926 in F9 cells, activation of the two receptors does not seem to play a significant role in the overall antitumor activity of ST1926 and CD437 as well. Activation of RARγ by RRMs leads to cytodifferentiation; however, this phenomenon is unlikely to have any significance for the in vivo antineoplastic action of these compounds. In contrast, RARγ seems to have an important modulatory and negative role on the response to RRMs in vivo, perhaps by acting on genes involved in cell motility and adhesion.

In conclusion, the data presented provide the foundation for future studies aimed to define the functional relevance of the numerous genes modulated by RRMs. Our results also have far-reaching implications at the clinical level, in that they may orient the choice of target tumors. Indeed, if RARγ-related resistance is not limited to the F9 model, tumors with low or undetectable levels of the receptor would represent the primary targets against which to test ST1926 in phase II clinical trials. Finally, the genome-wide microarray data are a useful resource to design rational combinations of RRMs and other chemotherapeutics.

Acknowledgments

We thank Prof. Silvio Garattini and Dr. Mario Salmona for critical reading of the manuscript. We are also grateful to Dr. Beatrice Filippi for the help in the experiments involving the measurement of calcium at the single-cell level and to Felice Deceglie and Alessandro Soave for the artwork.

Downloaded from molpharm.aspetjournals.org at ASPET Journals on June 3, 2022

References

Altucci L and Gronemeyer H (2001) The promise of retinoids to fight against cancer. *Nat Rev Cancer* **1:**181–193.

Boylan JF, Lohnes D, Taneja R, Chambon P, and Gudas LJ (1993) Loss of retinoic acid receptor gamma function in F9 cells by gene disruption results in aberrant Hoxa-1 expression and differentiation upon retinoic acid treatment. *Proc Natl Acad Sci USA* **90:**9601–9605.

Bour G, Plassat JL, Bauer A, Lalavee S, and Rochette-Egly C (2005) Vinexin beta interacts with the non-phosphorylated AF-1 domain of retinoid receptor γ (RARγ) and represses RARγ-mediated transcription. *J Biol Chem* **280:**17027–17037.

Cao X, Liu W, Lin F. Li H, Kolluri SK, Lin B, Han YH, Dawson MI, Zhang XK (2004) Retinoid X receptor regulates Nur77/TR3-dependent apoptosis by modulating its nuclear export and mitochondrial targeting. *Mol Cell Biol* **24:**9705–9725.

Chun KH, Pfahl M, and Lotan R (2005) Induction of apoptosis by the synthetic retinoid MX3350–1 through extrinsic and intrinsic pathways in head and neck squamous carcinoma cells. *Oncogene* **24:**3669–3677.

Cincinelli R, Dallavalle S, Merlini L, Penco S, Pisano C, Carminati P, Giannini G, Vesci L, Gaetano C, Illy B, et al. (2003) A novel atypical retinoid endowed with proapoptotic and antitumor activity. *J Med Chem* **46:**909–912.

Dawson MI, Hobbs PD, Peterson VJ, Leid M, Lange CW, Feng KC, Chen Gq, Gu J, Li H, Kolluri SK, et al. (2001) Apoptosis induction in cancer cells by a novel analogue of 6-[3-(1-adamantyl)-4-hydroxyphenyl]-2-naphthalenecarboxylic acid lacking retinoid receptor transcriptional activation activity. *Cancer Res* **61:**4723–4730.

Delescluse C, Cavey MT, Martin B, Bernard BA, Reichert U, Maignan J, Darmon M, and Shroot B (1991) Selective high affinity retinoic acid receptor α or β-γ ligands. *Mol Pharmacol* **40:**556–562.

Deschamps J and van Nes J (2005) Developmental regulation of the Hox genes during axial morphogenesis in the mouse. *Development* **132:**2931–2942.

Faria TN, Mendelsohn C, Chambon P, and Gudas LJ (1999) The targeted disruption of both alleles of RARβ_2 in F9 cells results in the loss of retinoic acid-associated growth arrest. *J Biol Chem* **274:**26783–26788.

Fazi F, Travaglini L, Carotti D, Palitti F, Diverio D, Alcalay M, McNamara S, Miller WH Jr, Lo Coco F, Pelicci PG, et al. (2005) Retinoic acid targets DNA-methyltransferases and histone deacetylases during APL blast differentiation in vitro and in vivo. *Oncogene* **24:**1820–1830.

Garattini E, Giannì M, and Terao M (2004a) Retinoid related molecules an emerging class of apoptotic agents with promising therapeutic potential in oncology: pharmacological activity and mechanisms of action. *Curr Pharm Des* **10:**433–448.

Garattini E, Parrella E, Diomede L, Giannì M, Kalac Y, Merlini L, Simoni D, Zanier R, Ferrara FF, Chiarucci I, et al. (2004b) ST1926, a novel and orally active retinoid-related molecule inducing apoptosis in myeloid leukemia cells: modulation of intracellular calcium homeostasis. *Blood* **103:**194–207.

Garattini E and Terao M (2004) Atypical retinoids: an expanding series of anti-leukemia and anti-cancer agents endowed with selective apoptotic activity. *J Chemother* **16:**70–73.

Giannì M, Ponzanelli I, Mologni L, Reichert U, Rambaldi A, Terao M, and Garattini E (2000) Retinoid-dependent growth inhibition, differentiation and apoptosis in acute promyelocytic leukemia cells. Expression and activation of caspases. *Cell Death Differ* **7:**447–460.

Giannì M, Parrella E, Raska I Jr, Gaillard E, Nigro EA, Gaudon C, Garattini E, and Rochette-Egly C (2006) P38MAPK-dependent phosphorylation and degradation of SRC-3/AIB1 and RARalpha-mediated transcription. *EMBO (Eur Mol Biol Organ) J* **25:**739–751.

Jin F, Liu X, Zhou Z, Yue P, Lotan R, Khuri FR, Chung LW, and Sun SY (2005) Activation of nuclear factor-kappaB contributes to induction of death receptors and apoptosis by the synthetic retinoid CD437 in DU145 human prostate cancer cells. *Cancer Res* **65:**6354–6363.

Holmes WF, Dawson MI, Soprano RD, and Soprano KJ (2000) Induction of apoptosis in ovarian carcinoma cells by AHPN/CD437 is mediated by retinoic acid receptors. *J Cell Physiol* **185:**61–67.

Hsu CA, Rishi AK, Su-Li X, Gerald TM, Dawson MI, Schiffer C, Reichert U, Shroot B, Poirer GC, and Fontana JA (1997) Retinoid induced apoptosis in leukemia cells through a retinoic acid nuclear receptor-independent pathway. *Blood* **89:**4470–4479.

Kasturi J, Acharya R, and Ramanathan M (2003) An information theoretic approach for analyzing temporal patterns of gene expression. *Bioinformatics* **19:**449–458.

Knudsen S, Workman C, Sicheritz-Ponten T, and Friis C (2003) GenePublisher: automated analysis of DNA microarray data. *Nucleic Acids Res* **31:**3471–3476.

Li R, Faria TN, Boehm M, Nabel EG, and Gudas LJ (2004) Retinoic acid causes cell growth arrest and an increase in p27 in F9 wild type but not in F9 retinoic acid receptor beta2 knockout cells. *Exp Cell Res* **294:**290–300.

Lopez-Hernandez FJ, Ortiz MA, Bayon Y, and Piedrafita FJ (2004) Retinoid-related molecules require caspase 9 for the effective release of Smac and the rapid induction of apoptosis. *Cell Death Differ* **11:**154–164.

Mayo LD and Berberich SJ (1996) Wild-type p53 protein is unable to activate the mdm-2 gene during F9 cell differentiation. *Oncogene* **13:**2315–2321.

Marchetti P, Zamzami N, Joseph B, Schraen-Maschke S, Mereau-Richard C, Costantini P, Metivier D, Susin SA, Kroemer G, and Formstecher P (1999) The novel retinoid 6-[3-(1-adamantyl)-4-hydroxyphenyl]-2-naphtalene carboxylic acid can trigger apoptosis through a mitochondrial pathway independent of the nucleus. *Cancer Res* **59:**6257–6266.

Mologni L, Ponzanelli I, Bresciani F, Sardiello G, Bergamaschi D, Giannì M, Reichert U, Rambaldi A, Terao M, and Garattini E (1999) The novel synthetic retinoid 6-[3-adamantyl-4-hydroxyphenyl]-2-naphthalene carboxylic acid (CD437) causes apoptosis in acute promyelocytic leukemia cells through rapid activation of caspases. *Blood* **93:**1045–1061.

Pavlidis P and Noble WS (2001) Analysis of strain and regional variation in gene expression in mouse brain. *Genome Biol* **2:**RESEARCH0042.

Plassat J, Penna L, Chambon P, and Rochette-Egly C (2000) The conserved amphipatic alpha-helical core motif of RARgamma and RARalpha activating domains is indispensable for RA-induced differentiation of F9 cells. *J Cell Sci* **113:**2887–2895.

Ponzanelli I, Giannì M, Giavazzi R, Garofalo A, Nicoletti I, Reichert U, Erba E, Rambaldi A, Terao M, and Garattini E (2000) Isolation and characterization of an acute promyelocytic leukemia cell line selectively resistant to the novel antileukemic and apoptogenic retinoid 6-[3-adamantyl-4-hydroxyphenyl]-2-naphthalene carboxylic acid. *Blood* **95:**2672–2682.

Rishi AK, Zhang L, Boyanapalli M, Khadeer M, Inesi G, and Hussain A (2003) Identification and characterization of a cell cycle and apoptosis regulatory protein-1 as a novel mediator of apoptosis signaling by retinoid CD437. *J Biol Chem* **278:**33422–33435.

Rochette-Egly C and Chambon P (2001) F9 embryocarcinoma cells: a cell autonomous model to study the functional selectivity of RARs and RXRs in retinoid signaling. *Histol Histopathol* **16:**909–922.

Rochette-Egly C, Plassat JL, Taneja R, and Chambon P (2000) The AF-1 and AF-2 activating domains of retinoic acid receptor-alpha (RARalpha) and their phosphorylation are differentially involved in parietal endodermal differentiation of F9 cells and retinoid-induced expression of target genes. *Mol Endocrinol* **14:**1398–1410.

Saeed AI, Sharov V, White J, Li J, Liang W, Bhagabati N, Braisted J, Klapa M, Currier T, Thiagarajan M, et al. (2003) TM4: a free, open-source system for microarray data management and analysis. *Biotechniques* **34:**374–378.

Taneja R, Rochette-Egly C, Plassat JL, Penna L, Gaub MP, and Chambon P (1997) Phosphorylation of activation functions AF-1 and AF-2 of RAR alpha and RAR gamma is indispensable for differentiation of F9 cells upon retinoic acid and cAMP treatment. *EMBO (Eur Mol Biol Organ) J* **16:**6452–6465.

Sabichi AL, Xu H, Fischer S, Yang X, Steele VE, Kelloff GJ, Lotan R, and Clifford JL (2003) Retinoid receptor-dependent and independent biological activities of novel fenretinide analogues and metabolites. *Clin Cancer Res* **9:**4606–4613.

Sun SY, Yue P, Wu GS, El-Deiry WS, El-Deiry WS, Shroot B, Hong WK, and Lotan R (1999) Implication of p53 in growth arrest and apoptosis induced by the synthetic retinoid CD437 in human lung cancer cells. *Cancer Res* **59:**2829–2833.

Sun SY, Yue P, Chandraratna RA, Tesfaigzi Y, Hong WK, and Lotan R (2000a) Dual mechanisms of action of the retinoid CD437: nuclear retinoic acid receptor-mediated suppression of squamous differentiation and receptor-independent induction of apoptosis in UMSCC22B human head and neck squamous cell carcinoma cells. *Mol Pharmacol* **58:**508–514.

Sun SY, Yue P, Chen X, Hong WK, and Lotan R (2002) The synthetic retinoid CD437 selectively induces apoptosis in human lung cancer cells while sparing normal human lung epithelial cells. *Cancer Res* **62:**2430–2436.

Sun SY, Yue P, Hong WK, and Lotan R (2000b) Induction of Fas expression and augmentation of Fas/Fas ligand-mediated apoptosis by the synthetic retinoid CD437 in human lung cancer cells. *Cancer Res* **60:**6537–6543.

Ubezio P (1985) Microcomputer experience in analysis of flow cytometric DNA distributions. *Comput Programs Biomed* **19:**159–166.

Workman C, Jensen LJ, Jarmer H, Berka R, Gautier L, Nielser HB, Saxild HH, Nielsen C, Brunak S, and Knudsen S (2002) A new non-linear normalization method for reducing variability in DNA microarray experiments. *Genome Biol* **3:**research 0048.

Zhang Y, Dawson MI, Mohammad R, Rishi AK, Farhana L, Feng KC, Leid M, Peterson V, Zhang XK, Edelstein M, et al. (2002) Induction of apoptosis in retinoid-refractory acute myelogenous leukemia by a novel AHPN analog. *Blood* **100:**2917–2925.

Zhao X, Demary K, Wong L, Vaziri C, McKenzie AB, Eberlein TJ, and Spanjaard RA (2001) Retinoic acid receptor-independent mechanism of apoptosis of melanoma cells by the retinoid CD437 (AHPN). *Cell Death Differ* **8:**878–886.

Zhuang Y, Faria TN, Chambon P, and Gudas LJ (2003) Identification and characterization of retinoic acid receptor beta2 target genes in F9 teratocarcinoma cells. *Mol Cancer Res* **1:**619–630.

Zuco V, Zanchi C, Cassinelli G, Lanzi C, Supino R, Pisano C, Zanier R, Giordano V, Garattini E, and Zunino F (2004) Induction of apoptosis and stress response in ovarian carcinoma cell lines treated with ST1926, an atypical retinoid. *Cell Death Differ* **11:**280–289.

Address correspondence to: Enrico Garattini, Laboratory of Molecular Biology, Centro Catullo e Daniela Borgomainerio, Istituto di Ricerche Farmacologiche "Mario Negri", via Eritrea 62, 20157 Milano, Italy. E-mail: egarattini@marionegri.it

Downloaded from molpharm.aspetjournals.org at ASPET Journals on June 3, 2022

	Gene		Gene Ontology Annotation			Log$_2$ Ratio							
Cluster	Acc. No.	Name	GO Biological Process	GO Cellular Component	GO Molecular Function	WS1	WS2	WA1	WA2	GS1	GS2	GA1	GA2
1	NM_144841	orthodenticle homolog 2	anterior/posterior pattern formation;c	transcription factor complex	transcription factor activity	-2,99	-2,69	-1,47	-1,40	-2,66	-1,91	-1,56	-0,83
1	NM_178182	histone 1, H2ai				-2,05	-2,62	-2,75	-0,97	-1,90	-2,39	-0,62	-1,05
1	AK049305	clone:C330021E21			ATP dependent helicase activity	-2,10	-1,25	-1,65	-1,00	-1,19	-1,05	-0,56	-0,72
1	NM_009426	thyrotropin releasing hormone	cell-cell signaling	extracellular space;soluble fraction	thyrotropin-releasing hormone activit	-1,72	-2,10	-1,17	-1,18	-1,77	-1,19	-1,22	-0,79
1	NM_152895	jumonji, AT rich interactive domain 1B	regulation of transcription\, DNA-dep	nucleus	DNA binding	-1,34	-1,41	-0,61	-0,66	-1,46	-1,06	-1,78	-0,82
1	NM_153423	WAS protein family, member 2				-1,28	-0,94	-0,79	-0,66	-1,68	-0,88	-1,34	-0,97
1	NM_146125	inositol 1,4,5-trisphosphate 3-kinase A	myo-inositol metabolism	cellular_component unknown	1D-myo-inositol-trisphosphate 3-kina	-0,77	-0,56	-0,59	-0,46	-0,74	-0,61	0,33	-0,10
1	NM_175445	Ras association (RalGDS/AF-6) domain famil	neuropeptide signaling pathway			-0,99	-0,51	-0,91	-0,37	-0,81	-0,99	0,29	0,00
1	NM_177470	acetyl-Coenzyme A acyltransferase 2	fatty acid metabolism	mitochondrion	acetyl-CoA C-acyltransferase activity	-0,62	-0,71	-0,41	-0,55	-0,43	-0,66	-0,15	-0,12
1	A_51_P478544	Unknown				-0,94	-0,86	-0,51	-0,26	-0,67	-0,61	-0,02	0,26
1	NM_010068	DNA methyltransferase 3B	DNA methylation;imprinting	nuclear heterochromatin	ATP binding;DNA binding;methyltran	-0,56	-0,85	-0,87	-0,83	-1,15	-0,80	-0,33	-0,31
1	NM_139051	nuclear receptor subfamily 5, A1	cell-cell signaling;male gonad develo	transcription factor complex	steroid hormone receptor activity;tran	-1,02	-1,28	-0,64	-0,85	-0,99	-0,70	-0,76	-0,40
1	NM_010638	basic transcription element binding protein 1	regulation of transcription from Pol II	transcription factor complex	transcription factor activity	-1,04	-0,88	-0,68	-0,58	-0,04	-0,22	-0,96	-0,85
1	NM_008009	fibroblast growth factor binding protein 1	cell-cell signaling	extracellular space	heparin binding	-1,06	-0,92	-1,26	-0,89	-0,58	-0,34	-0,96	-0,37
1	NM_010849	myelocytomatosis oncogene (Myc)	cell cycle arrest;iron ion homeostasis	nucleus	protein binding;transcription factor ac	-1,28	-0,95	-0,92	-0,71	-0,55	-0,49	-0,96	-0,38
1	NM_009274	serine/arginine-rich protein specific kinase 2	protein amino acid phosphorylation		ATP binding;protein serine/threonine	-0,59	-1,12	-0,51	-0,75	-0,74	-0,72	-1,10	-0,73
1	NM_010639	kallikrein 6	proteolysis and peptidolysis	extracellular space	chymotrypsin activity;tissue kallikrein	-0,71	-1,13	-0,67	-0,76	-0,86	-0,55	-1,11	-0,42
1	NM_178383	transcription elongation factor B 3 bp1				-0,60	-0,71	-0,72	-0,58	-0,69	-0,30	-1,02	-0,67
1	NM_021366	Kruppel-like factor 13	regulation of transcription\, DNA-dep	transcription factor complex	DNA binding;RNA polymerase II tran	-0,92	-1,23	-0,78	-0,89	-0,85	-0,69	-1,07	-1,00
1	NM_181324	DEAD (Asp-Glu-Ala-Asp) box polypeptide 6	cell growth and/or maintenance	eukaryotic translation initiation factor	ATP dependent helicase activity;DNA	-0,87	-0,99	-0,70	-0,90	-0,72	-0,58	-1,48	-0,84
1	NM_010258	GATA binding protein 6				1,32	1,75	0,88	1,10	2,97	2,33	0,63	0,86
1	AK018112	clone:6330404C01				1,18	1,55	1,18	1,52	1,85	1,72	1,52	1,46
1	AK078597	clone:7030417P08				0,98	1,81	1,06	1,53	1,58	1,96	1,86	1,56
1	NM_001001881	RIKEN cDNA 2510009E07				1,36	1,77	1,84	1,92	1,80	0,31	-0,20	0,97
1	NM_010258	GATA binding protein 6				1,42	1,91	1,15	1,42	1,17	1,13	0,84	0,75
1	AK018112	adult male medulla oblongata cDNA				1,16	1,17	1,31	1,27	1,50	1,41	0,92	1,17
1	NM_011427	snail homolog 1	organogenesis	transcription factor complex	DNA binding	0,87	1,36	1,18	1,24	1,68	1,16	0,99	0,84
1	NM_146189	myosin binding protein C, fast-type	muscle contraction	cytoskeleton	structural constituent of cytoskeleton	1,46	2,24	1,56	1,71	1,92	1,58	0,67	0,86
1	BC025841	cDNA clone IMAGE:5149318				1,79	2,38	1,21	1,47	1,47	1,47	0,24	0,66
1	NM_019395	fructose bisphosphatase 1	gluconeogenesis	cytosol	fructose-bisphosphatase activity	1,78	1,85	1,35	1,37	2,39	1,49	1,09	0,44
1	NM_007483	ras homolog gene family,B	Rho protein signal transduction;cell	growth and/or maintenance	ATP binding;Rho small monomeric G	0,19	0,58	1,13	1,21	1,01	1,04	0,74	0,96
1	NM_022415	prostaglandin E synthase	prostaglandin metabolism	cytoplasm;extracellular space;integra	glutathione transferase activity;prosta	0,56	0,45	1,05	1,02	0,83	0,88	0,50	0,81
1	NM_019487	heme binding protein 2	circadian rhythm	cytoplasm;extracellular	binding	0,93	0,15	0,72	0,51	0,52	0,44	0,07	0,48
1	NM_139151	sperm associated antigen 4		integral to membrane;kinesin complex		1,17	0,49	0,87	0,54	0,72	0,69	-0,41	0,24
1	AK053542	clone:E130106L06				0,91	0,80	0,71	0,56	0,79	0,81	0,57	0,35
1	NM_172799	RIKEN cDNA 4932418K24				1,34	1,43	0,98	0,71	0,82	0,82	0,90	0,39
1	NM_145523	grancalcin	antimicrobial humoral response (sen	cytosol	calcium ion binding	0,90	1,20	0,78	0,94	0,52	0,85	0,77	0,74
1	TC986104	neprilysin-like peptidase gamma				1,71	1,44	1,34	1,15	1,11	1,11	0,01	0,45
1	NM_174850	RIKEN cDNA A930021H16				1,69	1,40	1,13	1,10	1,05	1,40	0,05	0,53
1	NM_172914	hypothetical protein 4933409I22				1,29	1,68	0,76	0,89	0,61	1,14	0,02	0,39
1	NM_016689	aquaporin 3	excretion;water transport	integral to plasma membrane;mitoch	porin activity;water channel activity	2,28	1,60	2,44	2,23	1,46	1,26	2,64	2,19
1	NM_198967	cDNA sequence BC023818				1,09	2,30	2,11	2,71	1,61	1,12	2,57	2,24
2	NM_007706	suppressor of cytokine signaling 2 (Socs2)	intracellular signaling cascade;positive regulation of neuron differentiation;regulation of body size;regulation of c			-2,07	-2,01	-1,26	-1,30	-0,42	-0,74	-0,46	-0,43
2	NM_030706	tripartite motif protein 2 (Trim2)	biological_process unknown	cytoplasm	myosin binding;zinc ion binding	-1,74	-1,46	-1,78	-1,65	-0,21	-1,11	-0,16	-0,77
2	NM_010849	myelocytomatosis oncogene (Myc)	cell cycle arrest;iron ion homeostasis	nucleus	protein binding;transcription factor ac	-1,39	-0,97	-1,16	-0,93	-0,17	-0,56	-0,61	-0,41
2	NM_177086	RIKEN cDNA 9630048M01		nucleus	RNA binding	-3,17	-2,47	-2,43	-2,03	-0,78	-0,67	0,04	-1,07
2	AK017820	clone:5730543M03	mitochondrial genome maintenance;	mitochondrial large ribosomal subuni	structural constituent of ribosome	-0,72	-0,60	-0,39	-0,16	0,67	0,72	0,21	0,09
2	NM_008168	glutamate receptor, ionotropic, kainate 5 (gan	potassium ion transport;synaptic tran	extracellular space;integral to membi	glutamate-gated ion channel activity;	-0,59	-0,55	-0,22	-0,03	0,42	0,42	0,37	0,02
2	NM_172338	RIKEN cDNA 4732437J24				-0,42	-0,46	-0,23	-0,23	0,26	0,03	-0,04	-0,09
2	NM_019443	NADH dehydrogenase 1 alpha subcomplex, 1	energy pathways	extracellular space;mitochondrion	NADH dehydrogenase (ubiquinone)	-0,24	-0,35	-0,26	-0,28	0,35	0,11	0,13	0,28
2	NM_008410	integral membrane protein 2B	biological_process unknown;neuroge	integral to plasma membrane;membi	ATP binding;structural molecule activ	-0,43	-0,20	-0,46	-0,19	0,55	0,26	0,18	-0,06
2	NM_023249	yippee-like 1				-0,32	-0,61	-0,25	-0,28	0,58	0,13	0,34	0,00
2	NM_145522	RIKEN cDNA 9530020D24				-0,60	-0,52	-0,22	-0,15	0,21	-0,04	0,45	0,12

2	NM_022409	zinc finger protein 296 (Zfp296)	regulation of transcription\, DNA-dep	transcription factor complex		-0,89	-0,95	-1,04	-1,11	0,08	-0,20	-0,04	-0,43
2	NM_025865	RIKEN cDNA 2310030G06				-1,24	-0,85	-0,83	-0,54	0,28	-0,43	0,29	-0,16
2	NM_028535	RIKEN cDNA 1700049E17	cell growth and/or maintenance	cytoplasm	catalytic activity	-0,91	-1,10	-0,82	-0,70	0,28	-0,25	0,32	-0,23
2	NM_009112	S100 calcium binding protein A10 (calpactin)	signal transduction	cytoplasm	calcium ion binding;receptor binding	-0,98	-0,54	-0,84	-0,68	0,07	-0,17	0,14	-0,03
2	NM_016888	UDP-GlcNAc:betaGal beta-1,3-N-acetylgluco	protein amino acid glycosylation	Golgi apparatus;integral to membran	N-acetyllactosaminide beta-1\,3-N-ac	-0,97	-0,71	-0,85	-0,60	-0,02	-0,42	0,21	-0,11
2	NM_028157	RIKEN cDNA 1700013B16				-0,39	-0,60	-0,52	-0,76	-0,22	-0,07	0,20	-0,13
2	AK036190	clone:9630044O09				-0,67	-0,24	-0,61	-0,44	0,22	0,06	-0,15	-0,01
2	NM_173047	carbonyl reductase 3	metabolism	cytosol	carbonyl reductase (NADPH) activity	-0,49	-0,29	-0,66	-0,73	0,62	0,07	0,09	-0,11
2	NM_010574	Iroquois related homeobox 2				-0,88	-0,48	-0,74	-0,49	0,37	-0,20	0,25	-0,14
2	NM_009434	pleckstrin homology-like domain, family A, me	imprinting;organogenesis	cytoplasm;integral to membrane	exo-alpha-sialidase activity	-0,74	-0,45	-0,42	-0,35	0,36	-0,19	0,28	-0,01
2	NM_009506	vascular endothelial growth factor C	angiogenesis;regulation of cell cycle	extracellular space;membrane	growth factor activity	-0,84	-0,59	-0,36	-0,68	0,34	-0,13	0,19	-0,19
2	NM_023140	thioredoxin-like 2	electron transport	chloroplast	electron transporter activity	-0,47	-0,23	-0,80	-0,63	0,54	0,77	0,24	-0,10
2	AK009303	putative Ly-6 superfamily member				-1,08	-0,55	-1,11	-0,87	0,70	0,40	-0,17	-0,43
2	AK050869	clone:D030027O06				0,57	0,26	0,39	0,52	-0,14	-0,07	0,07	0,15
2	NM_009594	v-abl Abelson murine leukemia oncogene 1				0,55	0,64	0,73	0,70	-0,04	-0,27	0,01	0,19
2	NM_153424	nephronophthisis 4 (juvenile) homolog (human)				0,58	0,56	0,68	0,56	0,17	0,34	-0,32	0,08
2	AK009365	clone:2310015K15				0,38	0,50	0,37	0,33	0,07	0,04	-0,19	0,01
2	BC030327	cDNA clone IMAGE:5375863)				0,38	0,31	0,25	0,34	0,15	-0,18	-0,18	-0,19
2	AK129447	mKIAA1815 protein.				0,48	0,24	0,23	0,40	-0,01	-0,18	-0,29	-0,06
2	NM_009864	cadherin 1	homophilic cell adhesion	extracellular space;integral to membr	calcium ion binding;calcium-depende	0,32	0,67	0,41	0,30	-0,30	0,01	-0,48	0,05
2	NM_175833	carnitine deficiency-associated gene expressed in ventricle 3				0,59	0,14	0,58	0,39	-0,57	-0,34	-0,44	0,04
2	NM_021414	RIKEN cDNA 4631427C17				0,62	0,15	0,54	0,40	-0,65	-0,29	-0,59	0,13
2	AK122431	mKIAA1058 protein.				0,69	0,36	0,37	0,26	-0,40	-0,16	-0,65	0,10
2	NM_013505	desmocollin 2	homophilic cell adhesion	cytoskeleton;extracellular space;inte	calcium ion binding	1,52	1,01	0,72	1,36	0,51	0,33	0,55	0,10
2	AK036172	clone:9630043L16				1,57	1,19	1,02	1,01	0,35	0,31	0,60	0,30
2	AF440735	cystatin SC mRNA, complete cds.		extracellular space	cysteine protease inhibitor activity	1,07	1,28	0,68	0,98	0,27	0,11	-0,02	-0,23
2	NM_023118	disabled homolog 2 (Drosophila)	cellular morphogenesis during differe	cytoplasm	cysteine-type endopeptidase activity	1,24	0,87	0,28	0,52	-0,23	-0,04	-0,05	-0,11
2	AK050862	clone:D030026N09				1,03	0,77	0,80	0,68	-0,02	-0,03	-0,17	0,06
2	1500006F24	unknown EST [1500006F24]				1,03	0,99	0,58	0,59	0,24	-0,24	-0,02	0,04
2	NM_198013	RIKEN cDNA C330016O16				0,99	0,97	1,44	1,32	-0,76	0,18	-1,10	0,27
2	NM_175485	RIKEN cDNA A230098A12				1,36	1,44	0,70	1,48	-0,42	0,13	-0,34	0,36
2	NM_026693	GABA(A) receptor-associated protein like 2	intra-Golgi transport;intracellular prot	Golgi membrane;cytoskeleton	ATP binding;actin binding;protein tra	0,76	0,98	1,23	1,15	0,09	-0,06	0,46	0,52
2	NM_011594	tissue inhibitor of metalloproteinase 2	biological_process unknown	extracellular matrix;extracellular spac	enzyme activator activity;metalloend	0,55	1,06	1,43	1,33	-0,09	-0,35	-0,07	0,30
2	NM_021099	kit oncogene (Kit)	autophosphorylation;cell differentiatio	extracellular space;integral to membr	ATP binding;protein serine/threonine	1,59	1,11	1,84	1,55	-0,55	-0,36	0,49	0,82
2	NM_010453	homeo box A5 (Hoxa5)	organogenesis;pattern specification;r	transcription factor complex	transcription factor activity	1,62	1,24	2,64	2,78	0,28	0,14	-0,43	-0,10
2	NM_007786	casein kappa (Csnk)	transport	extracellular space	transporter activity	2,36	2,00	2,34	2,84	0,00	1,10	0,76	1,61
2	A_51_P281078	Unknown				2,68	2,11	3,49	4,09	-0,81	-1,04	1,46	0,87
3	NM_175521	RIKEN cDNA 6430598A04				0,40	-0,15	0,80	0,41	-0,48	-0,57	-0,59	-0,17
3	NM_201637	RIKEN cDNA 5830451P18				0,11	0,23	-0,03	-0,04	-0,29	-0,29	-0,56	-0,18
3	AK028546	aryl hydrocarbon receptor nuclear translocato	protein-nucleus import\, translocation	cytoplasm;transcription factor comple	aryl hydrocarbon receptor nuclear tra	0,10	0,34	0,20	0,23	-0,15	-0,24	-0,41	-0,18
3	NM_009079	ribosomal protein L22 (Rpl22)	protein biosynthesis;ribosome bioger	cytosolic ribosome (sensu Eukarya)	RNA binding;heparin binding;structur	0,11	-0,05	0,08	0,28	-0,30	-0,27	-0,28	-0,08
3	BC055439	myosin, light polypeptide 9, regulatory	muscle development;regulation of mu	muscle myosin	calcium ion binding;structural constit	-0,04	0,05	0,20	0,25	-0,27	-0,29	-0,38	-0,12
3	NM_019919	transforming growth factor beta binding prote	TGFbeta receptor signaling pathway	extracellular matrix;extracellular spac	calcium ion binding;growth factor bin	0,37	0,32	0,05	0,16	-0,80	-0,42	-0,35	-0,05
3	NM_008480	laminin, alpha 1	cell adhesion;cell surface receptor lir	basal lamina;extracellular space;kine	ATP binding;cell adhesion molecule	0,60	-0,01	0,40	0,17	-1,62	-0,79	-1,52	-0,30
3	NM_146100	internexin neuronal intermediate filament prot	cytoskeleton organization and bioger	intermediate filament;kinesin comple	structural constituent of cytoskeleton	0,21	0,41	-0,04	0,01	-0,87	-0,95	-1,05	-0,50
3	AK172935	hypothetical protein kinase/Glutamine-rich region containing protein				0,74	0,79	0,25	-0,12	-0,78	-0,81	-1,04	-0,92
3	AJ278191	putative mc7 protein	mesoderm cell fate determination	integral to membrane;intracellular	zinc ion binding	0,61	0,47	0,33	0,31	-0,62	-0,44	-1,14	-0,26
3	AK011851	guanine nucleotide binding protein, alpha 13	G-protein coupled receptor protein si	heterotrimeric G-protein complex	heterotrimeric G-protein GTPase act	-0,93	-0,14	-0,61	-0,11	0,70	1,04	0,77	0,05
4	BC040800	kinesin family member 5B	microtubule-based movement;mitoch	kinesin complex	ATP binding;kinesin motor activity	0,51	0,60	-0,61	-0,33	0,09	0,05	-0,72	-0,59
4	NM_146200	translation initiation factor 3, subunit 8	translational initiation	eukaryotic translation initiation factor	translation initiation factor activity	0,41	0,50	-1,11	-0,83	0,31	-0,04	-0,89	-0,93
4	X17373	centrosomin A.	protein biosynthesis		translation initiation factor activity	0,50	1,03	-1,20	-0,95	0,05	-0,15	-0,76	-0,50
4	NM_172810	guanylate cyclase 1, soluble, beta 2				0,48	0,71	-0,89	-0,68	0,76	-0,11	-0,27	-0,81
4	BC026580	thyroid hormone receptor associated protein 3			receptor activity	0,27	0,35	-0,50	-0,48	0,56	0,03	-0,83	-0,88
4	NAP108333-1	Unknown				0,54	0,50	-0,42	-0,43	0,32	-0,06	-0,93	-0,51
4	NM_026249	RIKEN cDNA 4930429B21				0,34	0,88	-0,38	-0,12	0,37	0,52	-0,35	-0,54
4	NM_173363	translation initiation factor 5	protein biosynthesis		GTP binding;translation initiation fact	0,42	0,73	-0,50	-0,26	0,24	0,58	-0,76	-0,59
4	NM_145943	cDNA sequence BC031781				0,36	0,91	-0,77	-0,31	0,38	0,62	-0,57	-0,14

4	NM_054089	nuclear receptor coactivator 6 interacting protein			S-adenosylmethionine-dependent m	0,20	0,68	-0,77	-0,45	0,30	0,60	-0,53	-0,40
4	NM_194059	nanos homolog 3				0,18	-0,45	0,46	0,32	-0,18	-0,29	0,28	0,40
4	BC054732	zinc finger and BTB domain containing 9		nucleus	protein binding	-0,43	-0,41	0,56	0,42	-0,32	-0,11	-0,12	0,40
4	NM_029601	RIKEN cDNA 1700019E19				-0,42	-0,13	0,38	0,45	-0,45	-0,35	0,29	0,43
4	NM_138304	calmodulin-like 4			calcium ion binding	-0,22	-0,21	0,60	0,50	-0,24	-0,14	0,14	0,65
4	AK005136	clone:1500003N10				-0,23	0,06	0,49	0,67	-0,66	0,02	0,72	0,49
4	NM_009878	cyclin-dependent kinase inhibitor 2D (p19, inh	hearing;negative regulation of cell cy	cytoplasm	ATP binding;cyclin-dependent protei	-0,49	0,19	0,54	0,93	-0,20	-0,26	0,54	0,59
4	NM_011420	survival motor neuron	mRNA processing	cytoplasm;nucleus	RNA binding	-0,20	-0,17	0,72	0,70	-0,62	-0,01	0,16	0,41
4	NM_025953	RIKEN cDNA 1700019N12				-0,40	-0,58	0,52	0,54	-0,62	-0,36	0,14	0,71
4	NM_007872	DNA methyltransferase 3A , transcript variant	DNA methylation;imprinting;regulatio	extrachromosomal circular DNA;nucl	DNA (cytosine-5-)-methyltransferase	-0,15	-0,01	0,75	0,74	-0,74	-0,97	0,42	0,55
4	BC061227	cDNA clone MGC:74376 IMAGE:30312881				-0,55	-0,22	0,34	0,59	-0,07	-0,11	0,48	0,29
4	NM_025953	RIKEN cDNA 1700019N12				-0,38	-0,39	0,44	0,25	0,19	-0,43	0,75	0,48
4	NM_007408	adipose differentiation related protein	biological_process unknown	membrane	molecular_function unknown;recepto	-0,34	-0,19	0,52	0,69	-0,01	-0,49	0,45	0,29
4	NM_026753	RIKEN cDNA 1110019N10				-0,13	-0,05	0,44	0,69	-0,09	-0,26	0,41	0,14
4	NM_018854	RIKEN cDNA 0610009H04	metabolism	flagellum	binding	-0,49	0,09	0,32	0,31	-0,12	-0,45	0,33	0,27
4	NM_028889	EF hand domain containing 1			calcium ion binding	0,23	0,72	0,44	0,54	-0,12	-0,85	0,59	0,19
4	AK052718	phosphodiesterase 3A, cGMP inhibited	metabolism;signal transduction;trans	integral to membrane	cGMP-inhibited cyclic-nucleotide phc	0,21	0,12	0,31	0,36	-0,25	-0,58	0,80	0,28
4	NM_153196	ribokinase (Rbks)	ribose metabolism		ribokinase activity	0,24	-0,34	0,55	0,66	-0,38	-0,44	0,26	0,38
4	NM_009944	cytochrome c oxidase, subunit VIIa 1	electron transport	respiratory chain complex IV (sensu	cytochrome c oxidase activity;electro	0,39	-0,16	0,71	0,43	0,13	-0,30	0,88	0,74
4	NM_019831	zinc finger protein 261	development	integral to membrane	DNA binding	0,30	0,29	0,86	0,75	-0,55	-0,06	0,53	0,52
4	NM_009904	calmegin	proteolysis and peptidolysis	endoplasmic reticulum;extracellular s	calcium ion storage activity;subtilase	0,94	0,44	1,01	0,65	-0,29	-0,20	0,77	0,49
4	NM_007804	cut-like 2	regulation of transcription\, DNA-dep	kinesin complex;nucleus;ribosome	transcription factor activity	0,54	-0,14	1,03	1,06	0,23	0,06	1,03	0,60
4	NM_029335	RIKEN cDNA 1700026D08				0,78	0,17	1,30	1,43	0,24	-0,27	1,46	1,03
4	NM_011243	retinoic acid receptor, beta				1,12	1,14	2,29	2,44	1,75	1,21	3,41	2,80
4	NM_054044	G protein-coupled receptor 124	biological_process unknown;neurope	plasma membrane	G-protein coupled receptor activity;m	1,20	1,87	2,09	2,40	0,51	1,02	3,07	2,67
4	NM_013900	antigen p97 (melanoma associated)	iron ion homeostasis;iron ion transpo	extracellular space;integral to membi	ferric iron binding	0,29	0,76	1,29	1,50	0,44	0,29	1,52	1,00
4	NM_010449	homeo box A1	organogenesis;pattern specification;r	transcription factor complex	RNA polymerase II transcription fact	0,24	0,67	1,12	1,25	0,31	-0,03	1,79	1,08
4	NM_030244	RIKEN cDNA 2610524G09	biological_process unknown	cytoplasm	transcription co-activator activity	1,11	0,57	1,39	1,12	0,25	0,30	1,01	1,18
5	NM_175938	butyrophilin 2				-0,04	-0,29	0,84	0,75	0,05	-0,26	-0,01	-0,44
5	NM_172506	biregional cell adhesion molecule-related	regulation of myogenesis	integral to plasma membrane	molecular_function unknown	0,17	-0,57	0,83	0,53	-0,56	-0,13	-0,21	0,01
5	NM_153068	EH-domain containing 2			calcium ion binding	0,38	-0,20	0,90	0,65	-0,48	-0,08	-0,14	-0,41
5	XM_137117	similar to ADAMTS-14 precursor				-0,06	-0,26	0,49	0,54	-0,29	0,00	-0,34	0,02
5	NM_053198	sideroflexin 4	iron ion transport	integral to membrane;mitochondrion	cation transporter activity	-0,03	-0,15	0,46	0,40	-0,07	-0,04	-0,30	0,17
5	NM_206924	jumping translocation breakpoint				-0,47	-0,73	0,39	0,36	-0,30	-0,51	-0,33	0,07
5	NM_025577	RIKEN cDNA 2810428I15				-0,20	-0,32	0,38	0,17	-0,47	-0,35	-0,26	-0,03
5	NM_178635	UV radiation resistance associated gene	DNA repair	cytoplasm		-0,36	-0,30	0,28	0,35	-0,08	-0,10	-0,34	-0,02
5	NM_028306	heat shock protein 12B				-0,26	-0,26	0,16	0,18	-0,22	-0,18	-0,22	0,04
5	NM_025638	RIKEN cDNA 2610020H15	glycerol metabolism	extracellular space;extrachromosom	glycerophosphodiester phosphodiest	-0,18	0,07	0,44	0,52	0,00	-0,19	0,11	-0,09
5	NM_027985	MAD2 mitotic arrest deficient-like 2	mitotic spindle checkpoint	spindle pole body		0,07	0,36	0,44	0,55	0,18	0,03	0,06	0,04
5	NM_009943	cytochrome c oxidase, subunit VI a, polypepti	electron transport	extracellular space;respiratory chain	cytochrome c oxidase activity	0,22	-0,02	0,80	0,70	-0,03	-0,21	0,01	0,23
5	BC027663	cDNA clone IMAGE:1230948				0,37	0,11	0,86	0,76	0,26	0,28	0,60	0,40
5	NM_053246	docking protein 4	MAPKKK cascade;neurogenesis;trar	cellular_component unknown;cytopla	insulin receptor binding;transmembra	0,29	0,12	0,89	0,79	0,30	0,56	0,33	0,51
5	NM_007775	crystallin, gamma C	sensory organ development	cytoplasm	structural constituent of eye lens	0,04	0,02	0,74	0,87	-0,11	0,00	-0,09	0,23
5	NM_175527	RIKEN cDNA E330021D16	ubiquitin cycle		ubiquitin conjugating enzyme activity	0,20	0,24	0,90	0,99	-0,18	-0,03	-0,49	0,31
5	AK129195	mKIAA0709 protein.				0,47	0,30	1,07	0,95	-0,30	-0,03	-0,03	0,42
5	NM_010459	homeo box B4	organogenesis;pattern specification;r	transcription factor complex	transcription factor activity	0,42	-0,18	1,04	1,34	0,17	0,17	0,66	0,22
5	NM_008265	homeo box A4				0,62	0,10	1,17	1,45	-0,01	-0,23	0,20	-0,08
5	NM_008116	gamma-glutamyltransferase 1	glutathione biosynthesis;spermatoge	integral to plasma membrane	acyltransferase activity;gamma-gluta	0,27	0,59	1,29	1,49	0,21	-0,12	0,10	0,13
5	NM_013599	matrix metalloproteinase 9	collagen catabolism	extracellular matrix;extracellular spac	collagenase activity;gelatinase B acti	0,59	-0,08	1,71	1,46	-0,48	0,25	-0,07	0,51
5	NM_013599	matrix metalloproteinase 9	collagen catabolism	extracellular matrix;extracellular spac	collagenase activity;gelatinase B acti	0,61	-0,17	1,79	1,34	-0,04	-0,07	-0,01	0,30
5	NM_053254	transducin-like enhancer of split 6, homolog c	regulation of transcription\, DNA-dep	heterotrimeric G-protein complex;nuc	protein kinase activity	0,80	0,25	1,82	1,18	0,02	-0,35	0,48	0,37
5	NM_008267	homeo box B13	epidermal differentiation;pattern spec	transcription factor complex	transcription factor activity	1,03	0,35	1,64	1,63	-0,32	0,16	-0,31	0,21
5	XM_355671	similar to serine				0,89	0,16	2,31	2,14	-0,03	-0,06	0,81	1,10
5	NM_007702	cell death-inducing DNA fragmentation factor	apoptosis	cytosol	apoptosis regulator activity	0,92	1,43	2,58	2,49	0,03	0,19	1,07	1,44
5	NM_007811	cytochrome P450, family 26, subfamily a, poly	electron transport	endoplasmic reticulum;extracellular s	electron transporter activity;retinoic a	1,09	0,88	3,18	2,99	-0,99	-0,87	0,31	0,87
5	NM_008268	homeo box B5	organogenesis;pattern specification;r	transcription factor complex	transcription factor activity	0,18	1,32	2,76	2,87	-0,40	0,35	-0,07	1,56
5	NM_033268	actinin alpha 2	muscle contraction	actin filament;striated muscle thin fila	actin cross-linking activity;calcium ior	1,04	0,64	2,33	2,29	-0,27	0,40	0,54	1,25

5	NM_020572	aurora kinase C	cell cycle;protein amino acid phosphorylation		ATP binding;cAMP-dependent protei	0,91	0,52	2,52	2,32	-0,03	-0,12	0,38	1,03
5	NM_134032	homeo box B2	organogenesis;pattern specification;t	transcription factor complex	transcription factor activity	0,27	0,80	2,55	2,70	-0,33	-0,02	0,60	0,40
5	AK041376	weakly similar to SPINSTER-LIKE PROTEIN [Homo sapiens]		integral to membrane	serine protease inhibitor activity	0,41	0,93	1,62	1,76	0,40	0,21	0,31	0,16
5	NM_020572	aurora kinase C	cell cycle;protein amino acid phosphorylation		ATP binding;cAMP-dependent protei	0,51	-0,21	1,60	1,29	0,47	-0,16	0,80	0,37
5	NM_172822	RIKEN cDNA F630022B06		integral to membrane		-0,12	0,46	1,50	1,15	-0,14	0,20	0,84	0,16
5	NM_011081	phosphatidylinositol glycan, class A				0,36	0,43	-0,25	-0,09	0,19	0,25	0,44	0,24
5	AK129277	mKIAA1071 protein.				0,11	0,07	-0,32	-0,33	0,08	-0,03	-0,12	0,05
5	AK031289	clone:6030402G23				-0,08	-0,14	-0,45	-0,42	-0,11	-0,12	-0,01	-0,06
5	NM_010120	translation initiation factor 1A	translational initiation	eukaryotic 43S pre-initiation complex	translation initiation factor activity	-0,32	-0,13	-0,81	-0,64	-0,13	-0,18	-0,27	-0,08
6	NM_010415	diphtheria toxin receptor	EGF receptor signaling pathway;regu	extracellular space;integral to membr	growth factor activity;heparin binding	-0,25	-0,32	0,28	0,22	-0,31	-0,15	1,20	1,03
6	NM_013788	paternally expressed 12	cell growth and/or maintenance	extracellular	kinase activity	-0,39	-0,31	0,15	0,11	-0,50	-0,45	1,67	0,97
7	NM_010128	epithelial membrane protein 1	cell death;cell growth	extracellular space;integral to membr	structural constituent of eye lens	-2,92	-2,28	-0,75	-0,42	-2,16	-2,90	0,25	-0,11
7	NM_008059	G0/G1 switch gene 2 (G0s2)	cell cycle	integral to membrane		-0,76	-1,79	0,62	0,17	-2,50	-1,40	0,37	0,12
7	AK087493	hypothetical Dbl domain				-1,29	-1,80	0,69	0,49	-2,84	-1,74	-0,58	0,26
7	NM_013584	leukemia inhibitory factor receptor	cell surface receptor linked signal tra	extracellular space;integral to membr	ATP binding;hematopoietin/interferor	-1,24	-1,21	-0,06	-0,06	-1,50	-0,96	-0,94	-0,18
7	NM_028034	RIKEN cDNA 2410004F06				-1,03	-1,49	-0,10	-0,29	-1,12	-0,97	-0,75	-0,03
7	NM_027221	keratinocyte associated protein 3	biological_process unknown	extracellular space;integral to membrane		-0,89	-1,31	-0,06	-0,27	-1,28	-0,99	-0,69	-0,08
7	NM_010315	guanine nucleotide binding protein (G protein	G-protein coupled receptor protein si	heterotrimeric G-protein complex	heterotrimeric G-protein GTPase act	-0,85	-1,50	-0,21	-0,36	-1,19	-1,07	-0,65	-0,25
7	NAP057003-1	Unknown				-0,84	-1,48	-0,10	-0,43	-1,09	-1,13	-0,78	-0,29
7	NM_026630	RIKEN cDNA 2410116G06				-0,78	-1,49	0,08	-0,33	-1,84	-1,13	-0,54	-0,11
7	NM_011372	sialyltransferase 7	protein amino acid glycosylation	Golgi apparatus;extracellular space;i	sialyltransferase activity	-0,91	-0,78	-0,33	-0,40	-0,98	-0,83	-0,52	-0,24
7	AK019115	similar to RADIATED KERATINOCYTE MRN	biological_process unknown	intermediate filament;kinesin comple	structural constituent of cytoskeleton	-0,70	-0,98	-0,32	-0,37	-1,26	-0,91	-0,50	-0,02
7	NM_029394	sorting nexing 24	intracellular protein transport;intracel	cytoplasm	protein transporter activity	-1,08	-0,70	-0,03	0,26	-1,66	-1,20	-0,68	0,11
7	NM_016765	dimethylarginine dimethylaminohydrolase 2	arginine catabolism;nitric oxide biosy	extrachromosomal circular DNA	dimethylargininase activity	-1,00	-1,06	0,05	-0,10	-1,60	-1,42	-0,43	0,22
7	NM_009672	acidic nuclear phosphoprotein 32 family, mei	intracellular signaling cascade	cytoplasm;nuclear matrix	phosphatase inhibitor activity;protein	-1,00	-0,84	-0,24	0,01	-1,48	-1,33	-0,34	0,07
7	NM_029556	citrate lyase beta like	biological_process unknown	cellular_component unknown;glyoxys	lyase activity;molecular_function unk	-0,64	-1,11	0,36	0,05	-1,12	-0,97	-0,46	0,27
7	NM_172134	pyridoxal kinase	pyridoxine metabolism		pyridoxal kinase activity	-0,82	-1,29	0,15	-0,14	-1,23	-0,80	-0,57	0,03
7	AK019275	NG23 (G7D)				-0,76	-0,74	0,12	-0,08	-1,47	-0,93	-0,54	0,04
7	NM_025599	RIKEN cDNA 2610528E23	mRNA splicing	spliceosome complex	nucleic acid binding	-0,59	-0,99	0,01	-0,07	-1,32	-0,75	-0,34	0,17
7	AK011942	clone:2610300B10				-0,75	-1,03	0,03	0,00	-1,33	-0,74	-0,42	0,02
7	BC051474	similar to RAS, guanyl releasing protein 2				-1,49	-1,46	-0,48	-0,44	-0,94	-1,18	-0,21	-0,05
7	NM_175328	solute carrier family 6 , member 15				-1,67	-1,62	-0,51	-0,36	-1,15	-1,06	-0,67	-0,26
7	AK010436	clone:2410007B07				-1,41	-1,61	-0,61	-0,59	-1,40	-1,35	-0,70	-0,35
7	NM_011491	stanniocalcin 2	biological_process unknown	cellular_component unknown;extrace	hormone activity;molecular_function	-1,08	-1,27	-0,27	-0,46	-1,63	-1,50	-0,78	-0,33
7	NM_021454	CDC42 effector protein 5	JNK cascade;Rho protein signal tran	cytoplasm;plasma membrane	protein binding	-0,86	-1,70	-0,33	-0,67	-1,55	-1,49	-0,48	-0,17
7	NM_021454	CDC42 effector protein 5	JNK cascade;Rho protein signal tran	cytoplasm;plasma membrane	protein binding	-1,10	-1,47	-0,40	-0,66	-1,31	-1,40	-0,27	-0,14
7	NM_133851	nucleolar and spindle associated protein 1	cell growth and/or maintenance	extracellular	binding	-1,80	-1,37	-0,34	-0,04	-1,72	-1,33	-0,03	0,02
7	NM_133873	DNA segment, Chr 4, Wayne State University 114				-1,90	-1,72	0,10	0,01	-0,87	-1,19	0,29	-0,02
7	AI121041	clone IMAGE:1498252 5'.				-1,56	-2,12	0,03	-0,16	-1,06	-1,40	0,24	0,25
7	NM_027189	gem (nuclear organelle) associated protein 7				-0,93	-1,66	-0,04	-0,42	-0,89	-0,98	-0,30	0,10
7	NM_024198	glutathione peroxidase 7	response to oxidative stress	chloroplast;extracellular space	glutathione peroxidase activity	-0,91	-1,43	-0,05	-0,10	-1,09	-1,25	-0,04	-0,08
7	NM_016662	Max dimerization protein 3	regulation of transcription\, DNA-dep	transcription factor complex	protein binding;transcription factor ac	-0,70	-1,20	0,39	-0,30	-0,92	-1,07	0,34	0,07
7	NM_010858	myosin, light polypeptide 4	cytoskeleton organization and bioger	myosin	calcium ion binding	-0,36	-1,18	0,30	-0,13	-0,82	-0,83	0,12	0,15
7	NM_153513	L259				-0,90	-0,93	0,13	0,03	-0,66	-1,14	0,09	-0,08
7	NM_030749	RIKEN cDNA 1810057E01	protein folding	endoplasmic reticulum;extracellular s	chaperone activity	-0,68	-1,19	0,19	-0,15	-0,66	-0,93	-0,23	-0,03
7	NM_133679	crystallin, zeta -like 1			alcohol dehydrogenase activity\, zinc	-0,84	-1,19	0,17	0,15	-0,80	-1,09	-0,16	0,12
7	AK008577	hypothetical EF-hand structure containing protein				-1,24	-1,43	-0,05	-0,18	-0,52	-0,83	0,33	0,12
7	NM_153596	transmembrane protein 17				-1,31	-1,00	-0,17	-0,03	-0,68	-0,85	-0,08	-0,08
7	NM_029522	G-protein signalling modulator 2 (AGS3-like, (	G-protein coupled receptor protein signaling pathway		GTPase activator activity	-1,08	-0,93	-0,28	-0,15	-0,32	-0,87	0,21	-0,06
7	NM_026821	DNA segment, Chr 4, Brigham & Women's Genetics 0951				-1,00	-1,15	-0,28	-0,47	-0,61	-1,16	0,01	-0,21
7	NM_053261	inositol (myo)-1(or 4)-monophosphatase 2	myo-inositol metabolism;phosphate r	cellular_component unknown	myo-inositol-1(or 4)-monophosphata	-0,84	-1,13	-0,34	-0,41	-0,77	-1,02	0,00	-0,07
7	NM_027592	RIKEN cDNA 4921516M08			ATP binding	-1,33	-0,99	0,02	0,49	-1,16	-1,25	0,00	0,24
7	NM_207522	cDNA sequence BC067068				-1,09	-1,00	0,05	0,22	-1,08	-0,93	-0,10	0,21
7	AK017341	contactin associated protein-like 2	cell adhesion	integral to membrane	cell adhesion molecule activity	-0,86	-0,82	-0,08	0,46	-1,11	-0,84	0,14	0,25
7	NM_025566	RIKEN cDNA 2600017J23				-1,07	-0,65	-0,17	0,16	-1,01	-0,96	0,06	0,07
7	NM_020510	frizzled homolog 2	G-protein coupled receptor protein si	extracellular space;integral to plasma	G-protein coupled receptor activity;fr	-0,97	-1,12	-0,09	-0,31	-1,74	-0,93	0,13	-0,23
7	NM_025533	nitric oxide synthase interacting protein	cell growth and/or maintenance	cytoplasm	zinc ion binding	-1,07	-1,45	-0,08	-0,22	-1,65	-0,82	0,55	-0,09

7	NM_025495	RIKEN cDNA 1700022C02				-1,32	-1,26	-0,35	-0,15	-1,26	-0,94	0,26	-0,16
7	NM_022021	Cdk5 and Abl enzyme substrate 1	G1/S transition of mitotic cell cycle;cy	nucleus;virion	cyclin-dependent protein kinase\, intr	-1,35	-0,80	-0,31	-0,05	-1,59	-0,91	0,33	-0,01
7	BC061948	RIKEN cDNA 2610014F08				-0,95	-1,01	0,06	0,17	-1,26	-0,39	-0,01	0,03
7	NM_025545	aprataxin	biological_process unknown	nucleoplasm	metal ion binding	-0,92	-0,69	0,01	0,20	-1,58	-0,43	0,30	0,19
7	NM_144526	RIKEN cDNA 6720460F02				-0,98	-1,66	0,71	0,43	-1,65	-1,47	0,03	0,28
7	BC049694	clone MGC:58593 IMAGE:6705916				-1,41	-1,36	0,29	0,38	-1,54	-1,62	-0,31	0,09
7	NM_008624	muscle and microspikes RAS	RAS protein signal transduction;mus	plasma membrane	ATP binding;RAS small monomeric (	-0,90	-0,81	0,66	0,88	-1,30	-0,92	-0,48	0,29
7	NM_013917	pituitary tumor-transforming 1	DNA repair;chromosome segregatior	cytoplasm;nucleus	transcription factor activity	-0,55	-0,94	0,52	0,35	-1,83	-0,99	0,03	0,00
7	NM_176835	RIKEN cDNA 2810451A06		integral to membrane		-0,95	-1,25	0,44	0,52	-2,00	-0,68	-0,19	0,37
7	NM_008278	hydroxyprostaglandin dehydrogenase 15	prostaglandin metabolism		15-hydroxyprostaglandin dehydroger	-0,99	-0,40	0,98	0,91	-0,83	-0,80	0,02	0,59
7	NM_008278	hydroxyprostaglandin dehydrogenase 15	prostaglandin metabolism		15-hydroxyprostaglandin dehydroger	-0,73	-0,41	0,62	1,00	-0,89	-0,97	0,33	0,76
7	NM_194342	expressed sequence AI551766				-1,01	-1,05	0,20	0,22	-0,63	-0,56	-0,48	-0,09
7	NM_010841	metallothionein-like 5, testis-specific	spermatogenesis	cytoplasm		-0,99	-0,76	0,29	0,05	-1,01	-0,68	-0,57	-0,02
7	NM_026015	RIKEN cDNA 2610510L01			nucleic acid binding	-0,40	-0,87	0,33	0,12	-0,76	-0,41	-0,16	0,06
7	AK013564	clone:2900019O16				-0,50	-0,88	0,14	0,28	-0,91	-0,46	-0,29	0,05
7	NAP097103-001	Unknown				-0,40	-0,88	0,29	0,11	-0,63	-0,71	-0,26	0,28
7	CL212473	clone G041F08				-0,64	-0,84	0,28	0,17	-0,93	-0,63	-0,50	0,27
7	NM_019986	hyaluronic acid binding protein 4	signal transduction	integral to endoplasmic reticulum me	G-protein coupled receptor activity	-0,47	-0,66	0,21	0,14	-0,93	-0,95	-0,41	-0,07
7	NM_011570	testis derived transcript	electron transport	cytoskeleton	electron transporter activity	-0,39	-0,44	-0,13	0,35	-0,69	-0,65	-0,11	0,17
7	NM_027288	mannosidase, beta A, lysosomal	carbohydrate metabolism;glycoprote	lysosome	beta-mannosidase activity	-0,66	-0,42	0,01	0,40	-1,09	-0,73	-0,17	0,03
7	BC046478	clone IMAGE:5324476				-0,65	-0,62	-0,03	0,05	-0,78	-0,73	-0,50	-0,11
7	NM_010171	coagulation factor III (F3)	blood coagulation	extracellular space;integral to membi	blood coagulation factor activity;hem	-0,77	-0,83	0,00	-0,01	-0,70	-0,50	-0,44	0,00
7	AK009757	PIRIN		nucleus		-0,65	-0,61	-0,12	-0,07	-0,74	-0,69	-0,19	0,17
7	NM_028137	RIKEN cDNA 5730528L13	cell growth and/or maintenance	integral to membrane		-0,75	-0,51	-0,35	-0,10	-0,85	-0,62	-0,40	0,02
7	NM_010261	Rab acceptor 1 (prenylated)				-0,41	-0,99	0,16	-0,14	-0,52	-0,62	-0,04	0,03
7	AK122501	mKIAA1389 protein.				-0,47	-0,75	0,03	-0,21	-0,47	-0,73	-0,04	-0,25
7	BC057072	clone IMAGE:5696235				-0,37	-0,92	-0,12	-0,26	-0,57	-0,80	0,08	-0,11
7	AF223568	frataxin pseudogene				-0,40	-0,54	-0,01	0,03	-0,83	-0,50	-0,32	-0,07
7	BC065162	clone MGC:90084 IMAGE:6402921				-0,31	-0,68	0,05	-0,25	-0,59	-0,50	-0,15	-0,19
7	BC026773	clone MGC:25733 IMAGE:3982549				-0,81	-1,10	0,06	0,06	-0,73	-0,24	-0,10	0,26
7	NM_025902	RIKEN cDNA 1500009M05	microtubule-based process	microtubule associated complex	motor activity	-0,88	-1,01	0,09	0,22	-0,78	-0,59	-0,26	0,29
7	AK015271	clone:4930431J08				-0,88	-1,02	0,10	-0,03	-0,72	-0,64	-0,20	0,17
7	NM_146059	RIKEN cDNA 2410075B13				-0,75	-0,94	-0,03	-0,02	-0,58	-0,49	-0,14	-0,05
7	NM_015740	biogenesis of lysosome-related organelles co	biological_process unknown	membrane	2\,3-dihydro-2\,3-dihydroxybenzoate	-0,63	-0,79	-0,04	-0,04	-0,45	-0,57	-0,01	0,06
7	NM_025462	RIKEN cDNA 1810009K13	proteolysis and peptidolysis	hydrogenase complex	S-adenosylmethionine-dependent m	-0,68	-0,79	0,01	-0,20	-0,68	-0,36	0,06	0,04
7	AK003786	nitrogen fixation gene 1	protein complex assembly;sulfur ami	cytosol;extracellular space;mitochon	lyase activity;transaminase activity	-0,88	-0,96	-0,02	0,06	-0,47	-0,52	0,11	0,22
7	AK004044	RNA component of mitochondrial RNAase P, 1				-0,88	-0,99	-0,18	-0,03	-0,65	-0,31	0,11	0,05
7	NM_023873	RIKEN cDNA C030018L16	cell growth and/or maintenance	cytoplasm	catalytic activity	-0,84	-0,89	-0,17	0,02	-0,71	-0,60	0,20	0,03
7	AK011942	clone:2610300B10				-0,97	-0,78	-0,20	-0,01	-0,55	-0,52	0,09	0,03
7	NM_028185	U7 snRNP-specific Sm-like protein LSM11	mRNA splicing	small nucleolar ribonucleoprotein cor	pre-mRNA splicing factor activity	-0,65	-1,17	-0,13	-0,27	-0,77	-0,65	0,05	0,08
7	NM_019394	melanoma inhibitory activity	cell-matrix adhesion;extracellular ma	extracellular space	growth factor activity	-1,03	-0,90	-0,32	-0,14	-0,58	-0,73	0,09	0,17
7	AK037208	hypothetical Tetratricopeptide repeat (TPR)	structure containing protein			-0,92	-1,11	-0,27	-0,20	-0,57	-0,48	0,05	0,19
7	AK045323	similar to OPA-INTERACTING PROTEIN OIP5				-0,70	-1,01	0,30	0,43	-0,60	-0,53	-0,14	0,24
7	NM_177731	RIKEN cDNA C130073F10				-0,81	-0,81	0,31	0,42	-0,79	-0,80	0,09	0,37
7	NM_023209	PDZ binding kinase	peptidyl-serine phosphorylation;pepti	cellular_component unknown;integra	ATP binding;protein binding;protein s	-0,83	-0,80	0,18	0,45	-0,85	-0,73	-0,13	0,39
7	NM_008612	menage a trois 1	cell cycle;regulation of transcription\,	nucleus		-0,81	-0,70	0,05	0,11	-0,63	-0,79	-0,25	0,08
7	NM_028002	RIKEN cDNA 2310069P03	biological_process unknown	mitochondrion	molecular_function unknown;peroxid	-0,80	-0,59	0,14	0,21	-0,50	-0,57	-0,19	-0,07
7	NM_025581	RIKEN cDNA 2810433K01	development	membrane	catalytic activity	-0,67	-0,64	0,26	0,28	-0,65	-0,59	-0,05	0,24
7	NM_139063	muted	pigmentation;vesicle-mediated transport		protein binding	-0,78	-0,75	0,09	0,12	-0,84	-0,54	-0,14	0,20
7	NAP017720-001	Unknown				-0,66	-0,79	0,13	0,23	-0,85	-0,75	-0,02	0,29
7	AK005556	clone:1600028I17				-0,57	-0,60	0,12	0,05	-0,52	-0,52	0,10	0,18
7	NM_025768	GH regulated TBC protein 1	circulation	extracellular	hormone activity	-0,56	-0,70	0,23	-0,05	-0,51	-0,58	-0,04	0,11
7	AK011315	RIKEN cDNA 2610005D18				-0,50	-0,78	-0,02	0,19	-0,60	-0,61	-0,11	0,00
7	AK050586	clone:C920006O11				-0,53	-0,71	0,50	0,47	-0,28	-0,34	-0,14	0,14
7	NM_020031	prefoldin 5	protein folding	prefoldin complex	chaperone activity	-0,46	-0,79	0,05	0,15	-0,64	-0,40	0,00	0,53
7	AK006006	CASM (LSM1 PROTEIN) homolog	mRNA splicing	small nucleolar ribonucleoprotein cor	pre-mRNA splicing factor activity	-0,41	-0,63	-0,10	0,05	-0,67	-0,35	-0,08	0,25
7	NM_025755	RIKEN cDNA 4933428G09				-0,57	-0,58	-0,06	0,09	-0,44	-0,33	0,02	0,32

7	NM_007627	cholecystokinin B receptor	G-protein coupled receptor protein si	integral to membrane	gastrin receptor activity;neuropeptide	-0,40	-0,57	0,06	0,09	-0,52	-0,31	0,11	0,25
7	AK018089	clone:6230416A05				-0,86	-0,62	-0,03	0,23	-0,59	-0,49	0,03	0,37
7	NM_026981	RIKEN cDNA 1810033A06				-0,77	-0,71	0,04	0,17	-0,44	-0,31	-0,03	0,25
7	NM_145475	ceramide kinase	ceramide metabolism;protein kinase	membrane fraction	ceramide kinase activity;diacylglycer	-0,72	-0,49	-0,04	0,24	-0,73	-0,26	0,17	0,20
7	NM_175287	RIKEN cDNA A430005L14				-0,33	-0,62	-0,05	0,00	-0,21	-0,68	0,22	0,00
7	NM_033080	DNA segment, Chr 7, Roswell Park 2 comple	proteolysis and peptidolysis	extrachromosomal circular DNA	aspartic-type endopeptidase activity	-0,48	-0,71	0,01	-0,08	-0,21	-0,66	0,08	-0,04
7	AK029271	SYNAPTONEMAL COMPLEX PROTEIN SC65 homolog		nucleus		-0,71	-0,55	-0,17	0,00	-0,29	-0,48	0,28	0,02
7	AK038662	clone:A230053F13				-0,59	-0,46	0,02	0,08	-0,66	-0,52	0,30	0,20
7	NM_201244	coatomer protein complex, subunit gamma				-0,55	-0,62	-0,09	-0,15	-0,53	-0,48	0,36	0,08
7	NM_026503	RIKEN cDNA 1110058L19	DNA repair	membrane	theta DNA polymerase activity	-0,60	-0,43	-0,08	-0,07	-0,53	-0,36	0,43	0,03
7	NM_008344	insulin-like growth factor binding protein 6	regulation of cell growth	extracellular space	insulin-like growth factor binding;rece	-0,55	-0,59	0,04	-0,13	-0,46	-0,25	-0,21	0,09
7	NM_013865	N-myc downstream regulated gene 3	cell differentiation;negative regulatior	cytoplasm	catalytic activity;molecular_function u	-0,44	-0,49	0,14	0,09	-0,48	-0,21	-0,14	0,22
7	NM_144805	RIKEN cDNA 9030407H20		integral to membrane		-0,45	-0,22	-0,04	0,02	-0,44	-0,20	0,01	0,19
7	NM_026502	RIKEN cDNA 1110004E09	metabolism	ribosome	oxidoreductase activity	-0,44	-0,33	-0,07	0,13	-0,30	-0,40	0,00	0,25
7	NM_029976	DNA segment, Chr 11, ERATO Doi 497	negative regulation of transcription	transcription factor complex	double-stranded RNA binding	-0,49	-0,39	-0,11	0,21	-0,42	-0,21	0,11	0,15
7	NM_025757	RIKEN cDNA 4933439F18	biological_process unknown	membrane	protein transporter activity	-0,69	-0,23	-0,02	0,20	-0,33	-0,34	0,05	0,07
7	NM_026543	RIKEN cDNA 3010026O09				-0,40	-0,51	0,27	0,11	-0,42	-0,01	0,17	-0,01
7	AK090016	clone:G430060N02				-0,47	-0,50	0,18	0,27	-0,53	-0,17	0,22	0,24
7	NM_144873	ubiquitin-like, containing PHD and RING finge	regulation of transcription\, DNA-dependent		DNA binding	-0,33	-0,51	0,34	0,16	0,08	-0,50	0,37	0,16
7	NM_025582	RIKEN cDNA 2810405K02	protein amino acid phosphorylation	integral to membrane	kinase activity	-0,52	-0,64	0,28	0,08	-0,15	-0,69	0,19	0,17
7	NM_025397	RIKEN cDNA 1110030J09	regulation of transcription\, DNA-dep	mitochondrion	transcription factor activity	-0,57	-0,42	0,07	0,09	-0,30	-0,55	0,29	0,23
7	NM_027954	RIKEN cDNA 1700013H19	development	membrane	catalytic activity	-0,40	-0,50	0,07	0,39	-0,13	-0,43	-0,05	0,07
7	NM_199199	expressed sequence AI316787				-0,37	-0,43	0,14	0,30	-0,33	-0,14	-0,01	0,36
7	BC029863	clone MGC:36861 IMAGE:4460168				-0,50	-0,43	0,25	0,21	-0,25	-0,27	-0,07	0,33
7	NM_145956	c6.1a protein	biological_process unknown;cellular	integral to plasma membrane		-0,68	-0,36	0,20	0,28	-0,20	-0,32	0,34	0,25
7	NM_023831	RIKEN cDNA 1500035H01				-0,72	-0,54	0,11	0,34	-0,20	-0,28	0,20	0,15
7	NM_153138	Wiskott-Aldrich syndrome protein interacting	actin filament-based movement;actin	actin cytoskeleton	actin binding;profilin binding	-0,38	-0,21	-0,01	0,26	-0,12	-0,18	0,25	0,16
7	NM_080555	phosphatidic acid phosphatase type 2B	germ-cell migration;lipid metabolism	integral to membrane	protein phosphatase activity	-0,36	-0,38	0,10	0,20	-0,14	-0,40	0,32	0,11
7	NM_009805	CASP8 and FADD-like apoptosis regulator, tr	induction of apoptosis;proteolysis and	peptidolysis	apoptosis regulator activity	-0,40	-0,41	0,07	0,16	0,01	-0,29	0,11	0,12
7	AK033738	weakly similar to HAI-2 RELATED SMALL PROTEIN				-0,28	-0,38	0,51	0,36	-0,49	-0,45	0,12	0,26
7	AI323028	clone IMAGE:477222 5'				-0,29	-0,40	0,25	0,20	-0,32	-0,42	-0,07	0,18
7	AK014035	clone:3110009M16				-0,29	-0,67	0,30	0,10	-0,42	-0,42	0,12	0,23
7	NM_011973	renal tumor antigen	protein amino acid phosphorylation	cytoplasm	ATP binding;protein serine/threonine	-0,03	-0,41	0,28	0,12	-0,43	-0,30	0,02	0,43
7	NM_172562	transcriptional adaptor 2 (ADA2 homolog, yeast)-like				-0,15	-0,31	0,18	0,01	-0,22	-0,37	0,07	-0,11
7	NM_175244	RIKEN cDNA 1700064K09	ubiquitin cycle	intracellular	ubiquitin-protein ligase activity	-0,25	-0,28	0,15	-0,02	-0,30	-0,10	0,18	-0,03
7	NM_145368	RIKEN cDNA C730036D15	protein targeting		acyltransferase activity	-0,26	-0,06	0,13	0,07	-0,30	-0,31	0,03	0,11
7	NM_025319	RIKEN cDNA 0610009B22	ER to Golgi transport;nonselective ve	Golgi apparatus;endoplasmic reticul	intracellular transporter activity	-0,11	-0,09	0,17	0,29	-0,14	-0,14	0,06	0,13
7	NM_007607	carbonic anhydrase 4	one-carbon compound metabolism;p	extracellular space;membrane	carbonate dehydratase activity;zinc i	-0,26	-0,10	0,03	0,36	-0,40	-0,28	0,11	0,28
7	NM_011110	phospholipase A2, group V	lipid catabolism	extracellular space	calcium ion binding;calcium-depende	-0,25	-0,22	0,27	0,28	-0,61	-0,13	0,16	0,19
7	NM_025329	RIKEN cDNA 0610012D17	microtubule-based movement	membrane	dynein ATPase activity	-0,39	-0,24	0,28	0,20	-0,52	-0,28	0,18	0,16
7	NM_008102	GTP cyclohydrolase 1	tetrahydrobiopterin biosynthesis	mitochondrion	GTP cyclohydrolase I activity	-1,24	-1,25	0,24	-0,08	-0,72	-0,58	1,27	0,80
7	NM_008189	guanylate cyclase activator 1a	signal transduction;vision	synaptic vesicle	ATP binding;calcium ion binding;calc	-0,74	-1,28	0,34	0,13	-1,14	-0,56	0,49	0,47
7	AK013071	clone:2810410L24				-0,59	-1,26	0,45	0,09	-0,56	-0,67	0,18	0,38
7	NM_172148	cDNA sequence BC028440				-1,01	-1,04	-0,04	-0,12	-0,77	-0,71	0,68	0,48
7	AK008705	clone:2210011C24				-0,75	-0,69	-0,08	-0,21	-0,63	-0,89	0,63	0,31
7	NM_174996	DNA segment, Chr 4, ERATO Doi 22				-0,76	-0,78	-0,12	-0,12	-0,77	-0,82	0,26	0,12
7	AF176530	F-box protein FBX15		SCF ubiquitin ligase complex	protein binding	-0,76	-0,42	0,04	0,29	-0,44	-0,92	0,27	0,10
7	NAP030482-1	Unknown				-0,63	-0,65	0,07	0,30	-0,40	-0,77	0,12	0,13
7	NM_023844	junction adhesion molecule 2	cell-cell adhesion	extracellular space;integral to plasma	cell adhesion molecule activity	-1,18	-0,77	0,02	0,46	-0,37	-0,71	0,35	0,27
7	AK020068	weakly similar to SUMO-1 SPECIFIC PROTE	protein modification	integral to membrane	cysteine-type peptidase activity	-1,23	-0,13	0,10	0,50	-0,70	-0,60	0,32	0,29
7	NM_022879	myosin, light polypeptide 7, regulatory	cytoskeleton organization and bioger	myosin	calcium ion binding;myosin ATPase	-0,90	0,02	0,23	0,68	-0,52	-0,75	0,55	0,46
7	NM_025539	nudix (nucleoside diphosphate linked moiety	biological_process unknown;nucleob	cellular_component unknown;cytopla	bis(5'-nucleosyl)-tetraphosphatase (a	-0,81	-0,06	-0,01	0,44	-0,50	-0,76	0,25	0,41
7	NM_021426	RIKEN cDNA C030019F02	cell growth and/or maintenance	extracellular space;integral to membr	peptidyl-dipeptidase A activity	-0,19	-0,14	0,16	0,18	-0,61	-0,52	0,60	0,42
7	NM_020259	Hedgehog-interacting protein	carbohydrate metabolism;lung develo	extracellular space;integral to plasma	protein binding;scavenger receptor a	-0,64	-0,16	0,21	0,31	-0,35	-0,77	0,69	0,25
7	NM_008043	frequently rearranged in advanced T-cell lym	cell growth and/or maintenance	extracellular	kinase activity	-0,64	-0,17	0,20	0,26	-0,25	-0,65	0,83	0,48
7	NM_008043	frequently rearranged in advanced T-cell lym	cell growth and/or maintenance	extracellular	kinase activity	-0,38	-0,55	0,18	0,37	-1,27	-0,59	0,74	0,59
7	NM_008631	metallothionein 4	biological_process unknown	cytoplasm	copper ion binding;zinc ion binding	-0,79	-0,45	-0,21	0,12	-0,85	-0,92	0,21	0,36

7	NM_010581	CD47 antigen	integrin-mediated signaling pathway	extracellular space;integral to membr	catalytic activity	-0,99	-0,32	-0,22	0,15	-1,30	-0,77	0,36	0,31
7	NM_016890	dynactin 3	microtubule-based movement;mitosis	dynactin complex;microtubule associ	molecular_function unknown;structur	-0,81	-0,27	-0,17	0,48	-0,73	-0,28	0,38	0,34
7	NM_019432	protein distantly related to to the gamma subu	ion transport	integral to membrane	calcium channel activity;voltage-gate	-0,91	-0,32	-0,20	-0,09	-0,70	-0,32	0,80	0,41
7	NM_178616	proteasome 26S subunit, non-ATPase, 11				0,65	0,02	-0,49	-0,78	0,04	0,31	-0,19	-0,45
7	XM_205178	expressed sequence C77370				0,44	0,36	-0,60	-0,30	-0,17	0,08	-0,85	-0,37
7	NM_010686	lysosomal-associated protein transmembrane	transport	integral to membrane;lysosome	nucleobase transporter activity	0,20	0,11	-0,36	-0,53	-0,11	0,16	-0,87	-0,24
7	NM_010897	neurofibromatosis 1				0,56	0,16	-0,18	-0,09	0,67	0,84	-0,97	-0,29
7	AK011193	clone:2600013D04				1,13	0,48	0,12	-0,29	0,60	0,51	-0,34	-0,03
7	NM_146035	mannoside acetylglucosaminyltransferase 2				0,69	0,15	-0,17	-0,41	0,56	0,54	-0,42	-0,18
7	NM_009469	Unc-51 like kinase 1	protein amino acid phosphorylation	cytosol	ATP binding;protein serine/threonine	0,94	0,22	-0,17	-0,46	0,60	0,84	-0,47	-0,14
7	BC035522	similar to hypothetical protein MGC955				0,75	0,22	0,05	-0,24	0,32	0,39	-0,52	-0,32
7	AK010350	ES cells cDNA, actin-associated protein palladin				0,44	0,07	-0,11	-0,28	0,41	0,37	-0,60	-0,63
7	AK039124	clone:A230098N07				0,35	0,06	-0,28	-0,40	0,41	0,09	-0,51	-0,46
7	BB021877	clone 5330407N12				0,54	0,55	-0,41	-0,32	0,37	0,19	-0,51	-0,23
7	NM_016721	IQ motif containing GTPase activating protein	small GTPase mediated signal transd	actin filament	GTPase inhibitor activity;Ras GTPas	0,57	0,51	-0,22	-0,28	0,44	0,27	-0,30	-0,23
7	NM_138671	cDNA sequence BC004012	ATP metabolism;electron transport;p	cytosol;extrachromosomal circular D	NAD+ kinase activity	0,39	0,06	-0,11	-0,02	0,38	0,31	-0,18	-0,15
7	AK086050	clone:D830050G17				0,52	0,30	-0,10	-0,10	0,51	0,27	-0,26	-0,09
7	NM_009876	cyclin-dependent kinase inhibitor 1C	cell cycle arrest	extracellular;nucleus	cyclin-dependent protein kinase inhil	0,20	0,42	-0,13	0,04	0,34	0,38	-0,53	-0,14
7	NM_153800	Rho GTPase activating protein 22				0,17	0,26	-0,37	-0,26	0,30	0,33	-0,36	-0,16
7	AB093226	mKIAA0308 protein				0,36	0,03	-0,16	-0,16	0,10	0,05	-0,15	-0,20
7	AK129483	mKIAA3018 protein				0,42	0,34	-0,12	-0,37	0,23	0,10	-0,18	-0,14
7	NM_146131	pre-B-cell leukemia transcription factor interacting protein 1		membrane		0,19	0,19	-0,13	-0,32	0,36	0,45	0,12	-0,16
7	NM_009905	CDC-like kinase	protein amino acid phosphorylation	nucleus	ATP binding;protein serine/threonine	0,58	0,75	0,04	0,19	0,65	0,53	-0,16	0,03
7	NM_175205	RIKEN cDNA 4632419I22				0,42	0,67	0,03	0,35	0,73	0,57	0,00	-0,04
7	AK034138	weakly similar to ETAA16 PROTEIN				0,55	0,42	0,08	0,20	0,44	0,60	0,07	0,03
7	NM_011665	ubiquitin-conjugating enzyme E2I	ubiquitin-dependent protein catabolism		ubiquitin conjugating enzyme activity	0,55	0,39	0,14	0,23	0,38	0,43	-0,16	0,04
7	NM_144530	RIKEN cDNA 5730454B08	DNA repair	nuclear heterochromatin	nucleic acid binding	0,45	0,69	-0,24	0,04	0,36	0,45	-0,22	-0,04
7	NM_025958	RIKEN cDNA 2210404G23				0,55	0,71	0,12	0,15	0,46	0,49	-0,48	0,03
7	BC057363	expressed sequence AI316828				0,62	0,65	-0,17	-0,04	0,54	0,51	-0,53	0,00
7	NM_009144	secreted frizzled-related sequence protein 2	development	extracellular space;membrane	transmembrane receptor activity	0,54	0,56	-0,03	-0,03	0,72	0,28	-0,42	-0,14
7	AK046153	N-TERMINAL ACETYLTRANSFERASE COMPLEX ARD1 SUBUNIT homolog				0,67	0,40	-0,08	0,14	0,57	0,25	-0,10	-0,19
7	AK014742	OXIDOSQUALENE CYCLASE homolog	biological_process unknown;electron	cellular_component unknown	copper ion binding;electron transport	0,38	0,64	0,01	0,03	0,76	0,36	-0,10	0,02
7	NM_133753	RIKEN cDNA 1300002F13				0,40	0,34	-0,02	0,08	0,79	0,39	0,05	-0,11
7	NM_007738	procollagen, type VII, alpha 1	cell adhesion	collagen type VII;extracellular space;	extracellular matrix structural constitu	0,32	0,46	0,12	0,09	0,52	0,54	-0,17	-0,05
7	NM_013783	mel transforming oncogene-like 1	proteolysis and peptidolysis	Golgi apparatus;endoplasmic reticulu	neprilysin activity;zinc ion binding	0,23	0,33	-0,02	-0,05	0,65	0,50	-0,13	0,00
7	NM_008974	protein tyrosine phosphatase 4a2	protein amino acid dephosphorylatio	soluble fraction	prenylated protein tyrosine phosphat	0,23	0,60	-0,12	-0,06	0,57	0,40	-0,02	-0,52
7	XM_136222	similar to hypothetical protein MGC10120				0,54	0,32	-0,09	-0,01	0,53	0,78	-0,15	0,11
7	NM_030218	RIKEN cDNA 9130017N09	cell growth and/or maintenance	extracellular	binding	0,31	0,59	0,13	-0,14	0,64	0,85	-0,09	-0,01
7	AK036375	clone:9830001H06				0,24	0,42	-0,10	-0,09	0,59	0,67	0,13	0,12
7	NM_011647	tuberous sclerosis 2	negative regulation of cell cycle	cytosol;nucleus;plasma membrane	GTPase activator activity;receptor bi	0,44	0,41	-0,20	-0,38	0,79	0,59	-0,09	-0,17
7	NM_145587	SH3-binding kinase	biological_process unknown;protein	cellular_component unknown	ATP binding;protein serine/threonine	0,62	0,54	-0,40	-0,35	0,53	0,71	0,04	-0,11
7	NM_008797	pyruvate carboxylase	biotin metabolism;gluconeogenesis;li	mitochondrion	ATP binding;biotin binding;manganes	0,46	0,59	-0,07	-0,25	0,48	0,66	0,22	-0,19
7	BC021494	RIKEN cDNA 1110004P15				1,22	0,65	-0,30	-0,43	0,21	0,55	-1,35	-0,33
7	NM_175341	muscleblind-like 2			nucleic acid binding	0,76	0,56	-0,30	-0,25	0,43	0,65	-1,11	-0,44
7	NM_021515	adenylate kinase 1	ATP metabolism;cell cycle arrest	cytoplasm;plasma membrane	ATP binding;adenylate kinase activit	1,73	0,56	0,00	-0,53	0,69	0,91	-0,80	-0,31
7	NM_153798	polymerase (RNA) II (DNA directed) polypeptide B				0,80	0,74	-0,29	-0,11	0,78	0,99	-0,49	-0,12
7	NM_153057	DNA segment, Chr 7, ERATO Doi 156				0,89	0,95	-0,03	-0,13	0,95	0,81	-0,40	-0,21
7	AK006449	nasopharyngeal epithelium specific protein 1				0,66	0,78	-0,20	-0,12	0,95	0,71	-0,37	-0,30
7	AK030917	clone:5830454P10				1,15	0,84	-0,15	-0,31	0,99	0,72	-0,57	-0,33
7	NM_178600	vitamin K epoxide reductase complex, subunit 1				1,33	0,88	0,05	-0,21	0,55	1,07	-0,09	-0,42
7	AK010453	pyrimidine synthesis protein CAD (fragment)	'de novo' pyrimidine base biosynthes	aspartate carbamoyltransferase com	transferase activity	0,93	0,88	-0,35	-0,36	0,26	1,27	-0,35	-0,17
7	NM_177960	isopentenyl-diphosphate delta isomerase	carotenoid biosynthesis;cholesterol b	peroxisome	isopentenyl-diphosphate delta-isome	0,86	0,82	0,06	-0,03	0,51	0,41	-0,23	0,25
7	AK084657	disintegrin-like and metalloprotease (reprolysin type) with thrombospondin type 1 motif, 2				0,93	0,96	-0,07	0,20	0,42	0,69	0,01	-0,06
7	NM_153762	ring finger protein 26				0,79	1,00	-0,17	-0,06	0,43	0,77	-0,34	0,33
7	XM_127312	expressed sequence C78339				0,83	0,76	0,01	0,11	0,55	0,88	-0,44	0,17
7	NM_133673	torsin family 1, member B	biological_process unknown;protein t	endoplasmic reticulum;extracellular s	ATP binding	0,94	0,87	-0,15	0,05	0,52	0,97	-0,37	0,13
7	NM_199017	RIKEN cDNA 9230110C19				0,58	1,00	0,06	0,35	0,88	1,06	-0,41	0,17

7	NM_177372	RIKEN cDNA E130315B21				0,61	0,68	0,05	0,23	0,76	0,92	-0,19	0,15
7	NM_007597	calnexin	protein secretion	endoplasmic reticulum membrane;ex	calcium ion storage activity;chaperon	0,71	1,01	-0,26	0,06	0,75	0,66	-0,25	-0,10
7	ENSMUST00000	BC031754 zinc finger protein 60				0,74	1,24	-0,45	0,26	0,82	0,79	-0,31	0,09
7	NM_153798	polymerase (RNA) II (DNA directed) polypeptide B				0,98	0,89	-0,18	-0,02	0,67	1,04	-0,56	-0,14
7	NM_016910	protein phosphatase 1D magnesium-depende	protein amino acid dephosphorylatio	protein serine/threonine phosphatase	CTD phosphatase activity;calcium-de	1,00	1,03	-0,08	0,03	0,75	1,05	-0,54	0,04
7	NM_030167	RIKEN cDNA 4632404H22	SRP-dependent cotranslational mem	ribosome	RNA binding	0,85	0,76	-0,14	-0,03	0,55	1,20	-0,20	-0,07
7	NM_007508	ATPase, H+ transporting, V1 subunit A, isofo	ATP biosynthesis;energy coupled pr	integral to plasma membrane;proton	ATP-binding and phosphorylation-de	0,79	0,90	-0,26	0,04	0,30	1,00	-0,62	-0,12
7	BC037239	BCL2-associated athanogene 4	apoptosis;biological_process unknow	cellular_component unknown;cytosol	apoptosis regulator activity;chaperon	1,39	0,98	0,20	-0,02	0,54	0,64	-0,53	-0,01
7	NM_030721	acyl-Coenzyme A oxidase 3	electron transport;fatty acid beta-oxi	peroxisomal matrix	pristanoyl-CoA oxidase activity	0,94	0,63	0,36	0,31	0,69	0,80	-0,79	-0,08
7	NM_009572	zinc fingers and homeoboxes protein 1	regulation of transcription\, DNA-dep	transcription factor complex	transcription factor activity	0,86	0,89	0,28	0,49	0,75	0,68	-0,72	0,07
7	NM_172759	RIKEN cDNA 9030624L02		extracellular space	carboxylic ester hydrolase activity	1,36	0,98	0,20	-0,75	1,22	1,94	-1,45	-0,36
7	BC058991	a disintegrin-like and metalloprotease (reprolysin type) with thrombospondin type 1		motif, 7		1,14	0,66	-0,50	-0,46	0,61	1,92	-0,40	-0,40
7	NM_009465	AXL receptor tyrosine kinase	protein amino acid phosphorylation;r	extracellular space;integral to membr	ATP binding;protein serine/threonine	1,06	1,48	-0,82	-0,46	0,63	1,63	-0,70	-0,31
7	X56974	MMETSB2 mRNA for external transcribed sp	ribosome biogenesis	cytosolic small ribosomal subunit (sensu Eukarya)		1,59	1,35	-0,13	-0,22	1,63	1,82	-0,54	-0,31
7	NM_013690	endothelial-specific receptor tyrosine kinase	cell-cell adhesion;cell-cell signaling;c	extracellular space;integral to plasma	ATP binding;protein serine/threonine	1,72	1,14	-0,01	0,06	1,82	1,88	-0,75	-0,45
7	NM_011075	ATP-binding cassette, sub-family B (MDR/TA	transport	integral to membrane	ATP-binding cassette (ABC) transpo	1,59	1,28	-0,27	-0,17	2,29	2,08	-0,17	-0,15
7	S60315	DMR-B15=myotonic dystrophy kinase	protein amino acid phosphorylation	kinesin complex	ATP binding;protein serine/threonine	1,57	1,71	0,11	0,06	2,38	1,76	-0,48	-0,13
7	NAP112463-1	Unknown				1,33	0,52	0,15	-0,29	1,84	1,59	-0,33	-0,26
7	NM_133779	phosphatidylinositol glycan, class T	transport	membrane	transporter activity	1,80	0,44	0,11	-0,69	2,15	2,16	-0,14	-0,31
7	NM_019423	elongation of very long chain fatty acids (FEN	fatty acid biosynthesis;very-long-cha	endoplasmic reticulum;integral to me	transferase activity\, transferring grou	1,80	1,13	-0,01	-0,22	1,50	1,28	0,08	-0,13
7	NM_031867	taste receptor, type 1, member 1	G-protein coupled receptor protein si	extracellular space;integral to plasma	electron transporter activity;metabotr	1,89	1,14	-0,03	-0,05	1,21	1,45	-0,08	0,02
7	NM_007932	endoglin	angiogenesis;cell adhesion;heart de	extracellular space;integral to membr	binding;cell adhesion molecule activi	1,77	1,41	-0,02	-0,12	1,31	1,94	-0,21	0,05
7	NM_009964	crystallin, alpha B	muscle contraction;protein folding;re	cytoplasm	heat shock protein activity;structural	2,12	1,04	0,10	-0,34	1,69	1,81	-0,24	-0,08
7	TC996139	Unknown				1,73	0,67	0,16	-0,35	1,83	1,09	0,08	-0,10
7	NM_172994	RIKEN cDNA 6330548O06	signal transduction	protein phosphatase type 2A comple	protein phosphatase type 2A\, intrins	1,92	0,94	0,02	-0,44	1,41	1,06	-0,28	-0,08
7	NM_016811	diacylglycerol kinase, alpha	intracellular signaling cascade;protei	cytoplasm	calcium ion binding;diacylglycerol bi	1,07	1,44	0,25	0,40	1,38	0,94	-0,10	-0,08
7	NM_019498	olfactomedin 1	development	endoplasmic reticulum;extracellular s	structural molecule activity	1,32	0,86	0,58	0,34	1,17	0,85	-0,15	-0,05
7	NM_028954	RIKEN cDNA 4933417E01				1,39	0,96	0,54	0,38	1,16	1,35	0,13	0,28
7	AK129197	mKIAA0711 protein.				1,38	1,07	0,79	0,58	1,36	1,26	-0,05	-0,04
7	ENSMUST00000	GLYCOPHORIN.				1,49	0,76	0,13	0,06	1,27	1,34	-0,30	-0,07
7	NM_027902	transmembrane serine protease 6	proteolysis and peptidolysis	extracellular;plasma membrane	chymotrypsin activity;trypsin activity	1,26	0,80	0,24	0,10	1,64	1,26	-0,23	-0,27
7	NM_011250	retinoblastoma-like 2	negative regulation of cell cycle;regu	transcription factor complex	DNA binding;protein binding	1,24	0,91	0,25	0,20	1,33	1,29	-0,16	0,09
7	NM_007557	bone morphogenetic protein 7	TGFbeta receptor signaling pathway	extracellular space	cytokine activity;growth factor activity	1,26	1,19	0,42	0,28	1,31	1,37	-0,37	0,05
7	BC013089	E26 avian leukemia oncogene 1, 5' domain	immune response;negative regulatio	membrane;nucleus	RNA polymerase II transcription fact	1,09	0,83	-0,16	0,38	1,54	1,33	0,10	0,13
7	NM_178787	RIKEN cDNA A930037G23				0,96	0,97	0,11	0,29	1,71	1,81	-0,07	0,08
7	NM_010043	desmin (Des)	muscle development	intermediate filament;kinesin comple	structural constituent of cytoskeleton	1,07	0,75	0,37	0,14	1,22	1,76	-0,32	0,28
7	NM_016693	mitogen-activated protein kinase kinase kinas	activation of JUNK;protein amino aci	cytoplasm	ATP binding;MAP kinase kinase kina	0,83	1,26	0,27	0,50	1,41	1,57	-0,23	0,30
7	BC066165	wingless-type MMTV integration site 9A				1,21	1,34	0,39	0,58	1,50	1,71	-0,19	0,29
7	BC051549	cDNA clone IMAGE:5256461				1,32	1,24	-0,01	0,28	1,55	1,84	-0,55	0,24
7	NM_172451	UDP-N-acetyl-alpha-D-galactosamine:polype	O-linked glycosylation	Golgi apparatus	polypeptide N-acetylgalactosaminyltr	1,28	1,32	0,15	0,20	1,15	1,92	-0,46	0,17
7	NM_146257	solute carrier family 29 (nucleoside transporte	biological_process unknown;transpo	cellular_component unknown;integra	molecular_function unknown;nucleos	1,66	0,99	0,07	-0,10	0,97	1,22	-0,41	-0,08
7	AK014608	hypothetical Cytochrome c family heme-bindi	electron transport		electron transporter activity	1,66	1,06	0,04	0,09	0,77	0,93	-0,60	0,03
7	NM_012048	polymerase (DNA directed), kappa	DNA repair	extrachromosomal circular DNA		1,75	1,54	0,09	0,12	1,16	1,00	-0,34	-0,13
7	NM_009855	CD80 antigen	defense response	extracellular space;integral to membr	receptor activity	1,43	1,46	-0,19	0,12	1,06	0,74	-0,42	0,38
7	NM_027960	dipeptidase 3	proteolysis and peptidolysis	microsome	dipeptidyl-peptidase activity;membra	1,20	1,44	0,15	0,30	0,56	1,12	0,01	0,23
7	NM_080563	ring finger protein 144		integral to membrane;nucleus		1,45	1,50	-0,12	0,42	0,76	1,18	-0,14	0,23
7	AK086540	programmed cell death 6 interacting protein	apoptosis;signal transduction	cytosol	signal transducer activity	1,24	1,48	0,26	0,46	0,93	1,05	-0,33	0,00
7	NM_175259	RIKEN cDNA 9330132O05				1,24	1,19	0,28	0,33	0,77	1,07	-0,59	0,27
7	NM_020275	tumor necrosis factor receptor superfamily, m	apoptosis;signal transduction	integral to membrane	receptor activity	1,10	0,60	-0,04	-0,18	0,90	1,26	-0,69	-0,03
7	NM_027988	NADPH oxidase organizer 1	intracellular signaling cascade;super	cellular_component unknown;cytosol	electron transporter activity;superoxi	0,99	0,61	0,11	0,02	1,25	1,35	-0,41	-0,01
7	NM_023529	membrane-spanning 4-domains, subfamily A,	defense response	integral to membrane	receptor activity;receptor signaling pr	1,16	0,75	-0,02	-0,09	1,24	1,33	-0,57	-0,11
7	NM_008519	leukotriene B4 receptor 1	G-protein coupled receptor protein si	extracellular space;integral to membr	leukotriene receptor activity	0,68	0,74	-0,07	0,09	1,34	1,47	-0,78	0,10
7	A_52_P335218	Unknown				1,31	1,45	-0,26	-0,20	1,61	1,50	-0,35	0,18
7	NM_177688	hypothetical protein E130307C13				1,49	1,45	-0,17	-0,01	1,25	1,57	-0,34	0,24
7	NM_023396	RIKEN cDNA 2410012A13	cell cycle arrest	cytoplasm;integral to membrane		1,51	1,04	0,09	-0,18	1,30	0,97	-0,18	0,03
7	NM_011173	protein S (alpha)				1,52	1,03	0,12	-0,06	1,36	1,13	0,07	0,13
7	NM_134033	cDNA sequence BC018601				1,25	0,96	0,08	0,04	1,20	0,92	0,06	0,08

7	NM_025821	calcium regulated heat stable protein 1	intracellular signaling cascade;regula	cytoplasm	DNA binding;signal transducer activit	1,33	0,83	-0,18	-0,32	1,18	1,02	-0,31	-0,25
7	NM_025821	calcium regulated heat stable protein 1	intracellular signaling cascade;regula	cytoplasm	DNA binding;signal transducer activit	1,36	0,80	-0,18	-0,36	1,24	1,01	-0,23	-0,26
7	NM_025821	calcium regulated heat stable protein 1	intracellular signaling cascade;regula	cytoplasm	DNA binding;signal transducer activit	1,40	0,87	0,01	-0,38	1,27	1,07	-0,31	-0,28
7	NM_025821	calcium regulated heat stable protein 1	intracellular signaling cascade;regula	cytoplasm	DNA binding;signal transducer activit	1,39	0,84	-0,05	-0,37	1,30	1,06	-0,33	-0,30
7	NM_025821	calcium regulated heat stable protein 1	intracellular signaling cascade;regula	cytoplasm	DNA binding;signal transducer activit	1,40	0,84	-0,02	-0,37	1,28	1,03	-0,34	-0,27
7	NM_025821	calcium regulated heat stable protein 1	intracellular signaling cascade;regula	cytoplasm	DNA binding;signal transducer activit	1,36	0,86	-0,02	-0,39	1,22	1,01	-0,28	-0,28
7	NM_025821	calcium regulated heat stable protein 1	intracellular signaling cascade;regula	cytoplasm	DNA binding;signal transducer activit	1,39	0,81	-0,07	-0,34	1,24	1,02	-0,31	-0,26
7	NM_025821	calcium regulated heat stable protein 1	intracellular signaling cascade;regula	cytoplasm	DNA binding;signal transducer activit	1,41	0,85	-0,09	-0,30	1,30	1,01	-0,36	-0,25
7	NM_025821	calcium regulated heat stable protein 1	intracellular signaling cascade;regula	cytoplasm	DNA binding;signal transducer activit	1,38	0,85	-0,06	-0,32	1,29	1,03	-0,33	-0,28
7	NM_173731	3-hydroxymethyl-3-methylglutaryl-Coenzyme A lyase-like 1				1,05	0,97	-0,14	-0,13	1,76	1,11	-0,38	0,30
7	NM_026731	protein phosphatase 1, regulatory (inhibitor) subunit 14A				1,14	0,94	0,40	0,27	1,21	0,94	0,83	0,40
7	NM_009522	wingless-related MMTV integration site 3A (W	cell-cell signaling;frizzled-2 signaling	extracellular matrix;extracellular spac	receptor binding	0,96	1,11	0,51	0,30	1,06	0,67	0,31	0,50
7	NM_175474	RIKEN cDNA A230106M15				0,43	1,06	-0,08	0,11	1,27	0,98	0,34	0,19
7	NM_025907	RIKEN cDNA 1600013P15	actin cytoskeleton organization and t	actin filament	S-adenosylmethionine-dependent m	0,80	1,34	0,02	0,18	1,06	0,64	0,41	0,12
7	BC059873	3-hydroxy-3-methylglutaryl-Coenzyme A reductase				0,80	0,92	0,05	0,11	0,85	0,73	0,08	0,09
7	BC006717	cDNA clone MGC:12151 IMAGE:3711012				0,86	0,79	0,26	0,29	0,71	0,60	0,06	0,22
7	NM_019708	short coiled-coil protein	intracellular protein transport	muscle myosin	muscle motor activity	1,07	1,03	0,28	0,15	0,91	0,65	0,00	0,17
7	NM_021411	RAB37	intracellular protein transport;small G	secretory granule	RAB small monomeric GTPase activ	0,92	0,92	0,39	0,56	0,93	0,99	0,20	0,08
7	AK036882	2P DOMAIN K+ CHANNEL TWIK-2 homolog	potassium ion transport	membrane fraction;voltage-gated pot	inward rectifier potassium channel ac	0,81	1,15	-0,11	0,08	0,48	1,12	0,35	0,12
7	NM_019585	espin (Espn), transcript variant 6	parallel actin filament bundle formati	actin cytoskeleton;brush border;ciliur	ATP binding;actin bundling activity	0,98	0,80	0,12	0,04	0,87	0,99	-0,05	0,05
7	NM_009283	signal transducer and activator of transcriptio	NIK-I-kappaB/NF-kappaB cascade;S	cytoplasm;nucleus	hematopoietin/interferon-class (D200	1,05	0,92	0,16	0,09	0,80	1,00	0,04	-0,02
7	NM_031183	trans-acting transcription factor 6 (Sp6)				0,97	1,01	-0,03	-0,02	0,94	1,05	0,16	0,30
7	XM_142415	similar to OBOX4 (LOC235841)				1,00	1,06	0,06	0,20	0,91	1,08	0,16	0,06
7	NM_031183	trans-acting transcription factor 6				1,26	0,33	0,05	-0,14	0,93	1,26	0,15	-0,14
7	NM_172257	cDNA sequence BC023957				1,34	0,38	0,22	-0,29	1,22	0,95	0,10	-0,13
7	NM_011176	suppression of tumorigenicity 14 (colon carci	amino acid activation;cell migration;p	extracellular;extrinsic to plasma mem	ATP binding;chymotrypsin activity;tR	1,42	0,64	0,06	-0,29	0,82	0,99	-0,21	0,00
7	NM_172205	suprabasin	biological_process unknown	cytoplasm	molecular_function unknown	1,08	0,48	0,05	-0,20	0,99	0,77	-0,08	0,01
7	NM_033590	protocadherin gamma subfamily A, 7	cell adhesion		calcium ion binding	1,20	0,70	0,26	-0,11	0,72	1,00	0,20	-0,08
7	NM_011399	solute carrier family 25 , member 17	mitochondrial transport	integral to membrane;mitochondrial i	binding;carrier activity	0,74	0,64	-0,07	0,01	1,42	0,99	0,28	0,16
7	NM_029097	RIKEN cDNA 1110012E06	cation transport;metabolism	integral to membrane	ATPase activity\, coupled to transme	0,77	0,64	-0,11	-0,20	1,22	0,74	0,12	-0,18
7	AK081230	similar to N-TYPE CALCIUM CHANNEL POF	calcium ion transport;sodium ion tran	voltage-gated calcium channel comp	ATP binding;calcium ion binding;volta	0,80	0,58	-0,08	-0,06	1,28	0,92	-0,01	-0,22
7	NM_008427	potassium inwardly-rectifying channel, subfamily J, member 4				0,95	0,61	-0,04	-0,24	1,57	0,60	0,28	-0,14
7	NM_010112	embryonal Fyn-associated substrate	cell adhesion	cytoplasm	SH3-domain binding;cell adhesion m	0,79	0,73	-0,07	-0,01	1,37	1,03	-0,18	0,06
7	NM_027185	differentially expressed in FDCP 6			calcium ion binding	1,02	0,87	-0,09	-0,17	1,17	1,05	-0,16	-0,06
7	NM_147778	COMM domain containing 3				0,87	0,80	0,05	0,12	1,19	0,74	-0,03	-0,21
7	NM_144534	RIKEN cDNA 1110001E17		integral to membrane		0,95	0,73	-0,01	-0,02	1,07	0,75	-0,06	-0,09
7	NM_007789	chondroitin sulfate proteoglycan 3	heterophilic cell adhesion	extracellular matrix;extracellular spac	calcium ion binding;hyaluronic acid b	0,84	0,76	0,17	-0,03	1,20	0,44	-0,11	-0,02
7	NM_153119	expressed sequence AI840980				0,68	0,41	0,18	0,10	1,09	0,85	-0,21	0,00
7	NM_139154	Rab40c	protein transport;small GTPase mediated signal transduction		RAB small monomeric GTPase activ	0,71	0,34	0,09	-0,11	0,84	0,49	-0,10	0,01
7	AK004470	clone:1190003J15				0,80	0,45	0,06	-0,05	0,79	0,65	0,08	-0,01
7	NM_146168	expressed sequence AW146242				0,82	0,52	0,23	-0,22	0,85	0,67	0,07	-0,01
7	NM_027840	RIKEN cDNA 9130017C17	intracellular protein transport;intracellular signaling cascade		protein transporter activity	0,35	1,16	-0,34	0,05	1,19	1,23	-0,41	0,28
7	XM_357374	similar to alpha-2u-globulin IV precursor				0,81	1,37	-0,39	0,01	1,42	1,21	-0,48	0,13
7	NAP102507-1	Unknown				0,93	1,47	-0,13	-0,03	0,83	1,17	-0,94	0,14
7	NM_133187	RIKEN cDNA 1110032E23	carbohydrate metabolism	integral to membrane;intermediate fil	dopamine-beta-monooxygenase acti	0,75	1,52	-0,49	0,12	1,03	1,68	-0,79	-0,12
7	NM_009810	caspase 3	induction of apoptosis;proteolysis an	caspase complex	caspase activity	0,92	1,51	-0,53	0,12	0,79	1,21	-0,08	0,14
7	NM_011521	syndecan 4	biological_process unknown	extracellular space;integral to membr	cytoskeletal protein binding	1,16	1,54	-0,38	-0,02	0,96	1,32	-0,26	-0,03
7	AK009638	clone:2310035N15				1,15	1,76	-0,29	0,33	0,79	1,21	-0,36	0,03
7	TC1058052	T00741 NADH2 dehydrogenase acyl carrier chain, mitochondrial - human				0,96	1,53	-0,16	0,46	1,14	1,32	-0,24	-0,02
7	AK020483	clone:9430072K23				1,04	2,18	-0,80	0,11	0,76	0,88	-0,11	-0,20
7	NM_010234	FBJ osteosarcoma oncogene	DNA methylation;inflammatory respo	cytoplasm;nucleus	specific RNA polymerase II transcrip	0,91	2,14	-0,80	-0,06	1,07	1,28	-0,32	-0,98
7	AK077083	clone:4933402D05				1,09	1,62	-0,55	-0,52	0,68	1,24	0,36	-0,41
7	NM_178682	RIKEN cDNA 4933426M11		integral to membrane		1,25	1,84	-0,27	0,07	1,09	1,00	0,22	-0,09
7	NM_010904	neurofilament, heavy polypeptide				0,93	1,59	-0,60	-0,15	1,22	0,66	0,18	-0,13
7	NM_053124	SWI/SNF related, actin dependent regulator c	chromatin assembly/disassembly;chr	nucleus	ATP dependent helicase activity;DNA	0,87	1,52	-0,27	-0,23	0,91	0,72	0,01	0,12
7	NM_053124	SWI/SNF related, actin dependent regulator c	chromatin assembly/disassembly;chr	nucleus	ATP dependent helicase activity;DNA	0,80	1,53	-0,41	-0,24	0,92	0,71	-0,02	0,10
7	BC048857	integrin alpha V				1,28	1,53	-0,37	-0,25	0,90	0,97	-0,10	0,08

7	NM_178421	nanos homolog 1				0,91	2,09	-0,45	0,12	1,03	1,40	0,60	0,08
7	NM_026169	RIKEN cDNA 1200004M23	small GTPase mediated signal transd	cytoskeleton	small GTPase regulatory/interacting	0,84	1,54	-0,43	-0,18	1,07	1,66	0,56	-0,25
7	NM_019874	DnaJ (Hsp40) homolog, subfamily B, membe	response to stress	cytoplasm	heat shock protein activity	1,06	0,39	0,02	-0,17	0,96	1,69	0,09	0,06
7	NM_011521	syndecan 4	biological_process unknown	extracellular space;integral to membr	cytoskeletal protein binding	1,25	0,15	-0,15	-0,31	1,35	1,35	-0,25	-0,13
7	AK080468	axotrophin				0,73	0,71	-0,42	0,15	0,86	1,58	-0,11	-0,36
7	XM_133920	RIKEN cDNA 2410012C07				0,64	0,51	-0,44	-0,17	0,99	1,29	-0,14	-0,27
7	AK017869	weakly similar to SIGNAL RECOGNITION PARTICLE 72 KDA PROTEIN				0,62	0,67	-0,40	-0,29	0,99	1,61	0,18	0,00
7	NM_019427	erythrocyte protein band 4.1-like 4b	biological_process unknown;transpo	cellular_component unknown;cytoske	molecular_function unknown;structur	0,88	0,95	-0,47	-0,49	1,23	1,49	0,28	-0,20
7	AK030285	decay accelerating factor 1	complement activation\, classical pat	extracellular space;integral to membr	aspartic-type endopeptidase activity	1,02	0,31	-0,47	-0,71	1,15	1,03	-0,16	-0,17
7	NM_007569	B-cell translocation gene 1, anti-proliferative				0,67	0,27	-0,59	-0,80	1,25	1,36	0,18	-0,28
7	NM_183156	zinc finger protein 455				0,87	0,82	-0,04	-0,10	1,78	1,09	0,51	-0,10
7	NM_175313	RIKEN cDNA A130022J15		extracellular space		0,67	1,00	-0,16	0,03	1,46	1,13	0,47	-0,07
7	AK011873	clone:2610204B21				0,76	0,85	-0,20	0,05	1,68	1,32	0,46	0,09
7	NM_008243	macrophage stimulating 1 (hepatocyte growth	blood coagulation;embryo implantati	extracellular matrix;extracellular spac	calcium ion binding;chymotrypsin act	1,16	0,67	0,24	-0,08	1,66	1,11	0,30	-0,05
7	NM_001001980	RIKEN cDNA 3732412D22				0,64	1,26	-0,40	0,11	1,54	1,17	-0,11	-0,32
7	AK010453	pyrimidine synthesis protein CAD homolog	'de novo' pyrimidine base biosynthes	aspartate carbamoyltransferase com	transferase activity	0,84	1,04	-0,45	-0,50	1,37	1,16	-0,14	-0,27
7	BC054112	clone IMAGE:30015653				0,88	1,01	-0,46	-0,19	1,32	1,14	-0,11	-0,14
7	AK051500	clone:D130053F06				0,77	1,05	-0,57	-0,20	1,60	1,11	0,14	-0,19
7	NM_028712	RAP2B				0,75	1,26	-0,81	-0,39	1,52	1,02	0,11	-0,35
7	NM_146067	RIKEN cDNA C530044N13	protein amino acid dephosphorylatio	protein serine/threonine phosphatase	protein serine/threonine phosphatase	0,66	1,26	-0,75	-0,34	1,36	1,02	0,18	-0,30
7	NM_177407	calcium/calmodulin-dependent protein kinase	protein amino acid phosphorylation	calcium/calmodulin-dependent protei	ATP binding;calcium/calmodulin-dep	1,37	1,13	-0,06	-0,16	1,31	0,70	0,41	-0,23
7	NM_133880	platelet-activating factor acetylhydrolase 2	lipid catabolism	2-acetyl-1-alkylglycerophosphocholir	2-acetyl-1-alkylglycerophosphocholir	0,98	1,24	-0,29	-0,20	1,55	0,91	0,28	-0,20
7	NM_172295	cDNA sequence BC037703				1,09	1,02	-0,50	-0,04	1,11	0,90	0,07	-0,17
7	NM_018775	TBC1 domain family, member 8	biological_process unknown;positive	cellular_component unknown;membr	calcium ion binding;molecular_functi	1,28	1,15	-0,46	0,07	1,05	0,65	0,07	-0,14
7	AK009163	clone:2310005C01				0,94	1,21	-0,35	-0,03	1,07	0,60	0,09	-0,26
7	NM_011033	poly A binding protein, cytoplasmic 2	mRNA polyadenylation		poly(A) binding	-0,03	0,55	-0,59	-0,61	0,93	0,96	-0,50	-0,36
7	BC022630	cDNA sequence BC022630				0,31	0,87	-0,50	-0,25	0,87	1,02	0,00	-0,02
7	NM_026640	expressed sequence AW413625				0,36	0,50	-0,31	-0,04	0,84	0,79	-0,33	-0,16
7	NM_015742	myosin IXb	cytoskeleton organization and bioger	kinesin complex;myosin	ATP binding;GTPase activator activit	0,46	0,58	-0,44	-0,53	1,00	0,69	0,22	-0,26
7	NM_009469	Unc-51 like kinase 1	protein amino acid phosphorylation	cytosol	ATP binding;protein serine/threonine	0,77	0,76	-0,46	-0,23	1,24	0,72	0,17	-0,36
7	NM_010945	neutral sphingomyelinase activation associat	ceramide metabolism;signal transduc	cytoplasm;soluble fraction	death receptor adaptor protein activit	0,33	0,57	-0,30	-0,14	0,91	0,66	0,27	-0,06
7	AI464795	clone IMAGE:719887 5'.				0,57	0,58	-0,03	0,00	1,07	0,68	0,09	-0,01
7	NM_172742	expressed sequence BB128963				0,59	0,78	-0,22	-0,03	0,93	0,72	0,24	0,00
7	AK033138	WWP1 (FRAGMENT) homolog	protein ubiquitination	cellular_component unknown	ubiquitin-protein ligase activity	0,66	0,83	-0,23	-0,19	1,18	0,80	0,42	-0,02
7	NM_009423	Tnf receptor associated factor 4	apoptosis;development;proteolysis a	kinesin complex;nucleus	astacin activity;receptor activity;zinc	0,69	0,95	-0,35	-0,16	1,05	0,67	0,57	0,02
7	AK122456	mKIAA1146 protein.	intracellular signaling cascade;male	cellular_component unknown	molecular_function unknown;transcri	0,80	0,53	-0,07	-0,35	0,96	0,74	0,39	0,02
7	AK040826	MEMBRANE-ASSOCIATED NUCLEIC ACID BINDING PROTEIN homolog			nucleic acid binding	0,59	0,87	-0,14	-0,17	0,77	0,14	-0,08	-0,34
7	CL211492	clone M016D07				0,47	1,11	-0,45	-0,14	0,80	0,37	0,09	-0,04
7	NM_030563	cDNA sequence BC004022	DNA recombination		DNA binding	0,58	0,89	-0,39	-0,11	0,75	0,51	-0,04	-0,33
7	NM_013873	sulfotransferase family 4A, member 1	steroid metabolism;sulfur metabolism	cytoplasm	sulfotransferase activity	1,25	1,07	0,90	0,71	1,66	1,20	0,56	0,44
7	NM_025674	transcription factor 19	regulation of transcription\, DNA-dep	mitochondrion;transcription factor co	transcription factor activity	1,06	1,12	0,21	0,40	2,05	1,54	0,77	0,21
7	AK004989	clone:1300013F15				0,83	1,19	0,46	0,19	2,09	1,45	0,53	0,20
7	NM_011328	secretin	pancreatic juice secretion	extracellular space	hormone activity	1,24	1,93	0,34	0,60	2,11	1,18	0,96	0,31
7	AK006434	clone:1700027L20				1,43	1,56	0,31	0,38	1,80	1,48	0,81	0,27
7	AK085092	telomerase RNA component	telomerase-dependent telomere mai	telomerase holoenzyme complex	template for synthesis of G-rich strar	1,19	1,73	0,35	0,73	1,86	1,66	0,52	0,24
7	AK036288	clone:9630053P03				0,77	1,75	0,28	0,09	1,78	2,10	0,03	0,20
7	AK016443	hypothetical D-galactoside/L-rhamnose binding	SUEL lectin domain containing pro	integral to membrane	sugar binding	0,90	1,78	0,66	0,27	1,97	1,73	0,03	0,60
7	NM_007557	bone morphogenetic protein 7	TGFbeta receptor signaling pathway	extracellular space	cytokine activity;growth factor activity	1,16	2,29	0,10	0,62	1,72	1,68	-0,18	0,25
7	BC057682	clone IMAGE:3596174				1,08	2,09	0,04	0,45	2,18	1,30	-0,05	0,31
7	AK122448	mKIAA1112 protein.				1,55	1,87	-0,07	0,37	1,92	1,39	0,30	0,00
7	NM_025961	glycine amidinotransferase (L-arginine:glycine	creatine biosynthesis;transport	membrane;mitochondrial intermembr	glycine amidinotransferase activity;re	1,49	1,94	0,04	0,25	2,12	1,59	-0,05	0,28
7	NM_007398	adenosine deaminase	immune response;purine ribonucleos	cytoplasm	adenosine deaminase activity	1,64	2,21	-0,10	0,31	2,25	1,97	0,19	0,03
7	NM_007670	cyclin-dependent kinase inhibitor 2B (p15, inh	negative regulation of cell cycle;regu	cytoplasm	cyclin-dependent protein kinase inhit	1,48	2,01	-0,34	0,10	1,96	1,90	0,06	0,11
7	AK043908	similar to death effector domain-containing ar	apoptosis	nucleus	DNA binding;apoptosis regulator acti	1,65	2,51	0,16	0,88	1,27	1,70	0,08	0,38
7	NM_146140	translocation associated membrane protein 1-like 1		integral to membrane		1,79	2,10	0,39	0,87	1,22	2,16	-0,09	0,50
7	NM_007955	protein tyrosine phosphatase, receptor type, \	protein amino acid dephosphorylatio	extracellular space;integral to membr	protein tyrosine phosphatase activity	1,37	1,99	0,02	0,25	0,73	1,97	-0,01	0,57
7	NM_009400	tumor necrosis factor receptor superfamily, m	anti-apoptosis	extracellular space;integral to membr	receptor activity	1,50	2,05	-0,05	-0,10	1,07	1,76	0,01	0,12

7	AK033431	clone:9030024J15				1,35	2,36	-0,33	0,26	1,74	1,41	-0,37	-1,09
7	AK090111	clone:G430136C21				0,45	2,04	0,12	-0,14	2,49	1,79	-0,54	-0,27
7	XM_125685	hypothetical protein 4732470K04				1,05	1,89	-0,55	0,84	2,01	1,92	-0,95	0,45
7	NM_007420	adrenergic receptor, beta 2	G-protein coupled receptor protein si	integral to plasma membrane	beta2-adrenergic receptor activity	1,57	1,95	-0,58	-0,15	1,60	1,50	-1,08	0,02
7	NM_153098	CD109 antigen		extracellular space	endopeptidase inhibitor activity	1,51	2,06	-0,36	0,04	2,05	2,40	-0,56	0,01
7	XM_149659	RIKEN cDNA 1110030H18	transport	membrane	transporter activity	1,43	2,57	-0,25	0,00	1,58	1,97	-0,13	0,19
7	AK028313	solute carrier family 25 (mitochondrial) 3	transport	integral to membrane;mitochondrial i	binding	2,23	2,49	0,21	0,54	1,00	1,38	-0,88	0,01
7	NM_178771	RIKEN cDNA C630013N10			protein binding	1,68	2,15	-0,14	0,11	1,45	1,08	-0,05	-0,06
7	AK129335	mKIAA1340 protein.				1,62	1,77	0,10	0,17	1,36	1,17	0,13	0,12
7	NM_019570	REV1-like	DNA repair	extrachromosomal circular DNA	transferase activity	1,78	2,45	-0,51	-0,03	1,54	0,97	-0,07	0,37
7	NM_172716	RIKEN cDNA 2310035N15				1,45	2,38	-0,26	0,26	1,11	1,04	-0,06	0,33
7	AK084988	clone:D430021N24				1,98	2,58	-0,24	0,23	1,74	1,67	-0,05	0,26
7	NM_201639	desmuslin , transcript variant 1				1,95	2,66	-0,04	0,13	1,37	1,65	-0,21	0,07
7	NAP037823-1	Unknown				2,24	2,60	-0,23	0,21	1,43	1,84	0,31	0,25
7	AK018076	clone:6230400I06				2,28	2,19	-0,04	0,04	1,42	1,65	-0,10	0,12
7	NM_178679	zinc finger protein 365				2,34	1,74	-0,10	-0,27	1,31	1,55	-0,42	0,09
7	NM_080428	F-box and WD-40 domain protein 7, archipela	N signaling pathway;protein ubiquitin	Golgi apparatus;endoplasmic reticul	protein binding;transcription factor ac	1,98	2,37	-0,63	-0,10	1,15	1,33	-0,11	-0,21
7	XM_143807	similar to alpha-2u-globulin IV precursor - mouse				1,66	2,10	-0,53	-0,31	1,58	1,44	-0,25	0,14
7	NM_021493	RIKEN cDNA 4933428G20	intracellular signaling cascade	membrane	Rho GTPase activator activity	1,86	2,04	-0,35	-0,32	1,38	1,54	-0,46	-0,20
7	BC026653	RIKEN cDNA A430096B05 gene	binding of sperm to zona pellucida;ce	membrane	cell adhesion molecule activity	1,90	0,68	0,26	-0,05	1,14	1,51	-0,80	0,18
7	NM_011729	excision repair ,complementation group 5	nucleotide-excision repair	mitochondrion;nucleus	endonuclease activity;single-strande	2,03	1,35	0,27	0,18	0,94	1,47	-0,96	0,07
7	NM_022654	leucine-rich and death domain containing	amino acid activation;signal transduc	cytoplasm	ATP binding;tRNA ligase activity	2,16	1,27	0,49	0,20	0,94	1,43	-0,73	-0,01
7	NM_011173	protein S (alpha)				1,72	1,40	0,36	0,16	1,15	1,30	-0,74	0,18
7	NM_009521	wingless-related MMTV integration site 3 (Wr	cell growth and/or maintenance;cell-c	extracellular matrix;extracellular spac	extracellular matrix structural constitu	1,53	1,32	0,05	0,18	0,75	1,65	-0,79	0,35
7	NM_175124	RIKEN cDNA 1300004K21				1,88	1,60	-0,30	-0,07	0,75	1,41	-1,06	0,04
7	NM_023396	RIKEN cDNA 2410012A13	cell cycle arrest	cytoplasm;integral to membrane		1,81	1,83	0,02	0,30	0,99	1,31	-0,82	0,27
7	NM_026662	phosphoribosyl pyrophosphate synthetase 2	nucleoside metabolism;ribonucleosid	cytoplasm	lipoate-protein ligase B activity;magn	1,94	1,76	0,10	0,13	1,02	1,34	-0,64	-0,05
7	NM_153484	thyrotroph embryonic factor , transcript varian	positive regulation of transcription fro	transcription factor complex	double-stranded DNA binding;protein	1,95	1,45	0,05	0,07	0,82	1,56	-0,65	-0,03
7	NM_029100	selenoprotein N, 1				1,70	1,08	0,54	0,49	1,35	1,92	-0,27	0,14
7	NM_178939	RIKEN cDNA 1110004D19				1,56	1,05	0,30	0,33	1,56	1,60	-0,29	-0,01
7	AK014912	clone:4921517L17				1,88	1,47	0,49	0,85	1,33	1,91	-0,15	0,04
7	AK051380	cyclin L	cell cycle;cytokinesis;regulation of tra	nuclear cyclin-dependent protein kina	cyclin-dependent protein kinase\, intl	1,90	1,63	0,44	0,51	1,51	1,55	-0,83	-0,07
7	NM_013564	insulin-like 3	physiological processes	extracellular	hormone activity	2,26	1,43	0,94	0,62	1,40	1,40	-0,59	-0,03
7	BB133117	clone 9830005L03				3,04	4,70	-0,19	0,55	2,99	3,61	0,86	0,24
7	AK036408	Similar to apolipoprotein L		integral to membrane		2,66	4,25	-0,08	0,69	2,14	4,19	-0,01	0,36
7	NM_178680	cardiomyopathy associated 4				2,65	2,86	-0,05	0,17	3,45	3,14	-0,17	0,21
7	NM_020043	neighbor of Punc E11 (Nope)	cell adhesion	integral to plasma membrane	cell adhesion molecule activity	3,09	3,64	-0,43	0,18	3,39	3,01	-0,27	0,06
7	BC025830	RIKEN cDNA 4732466D17	proteolysis and peptidolysis	extracellular space	metallopeptidase activity	2,11	3,74	-0,28	0,69	2,69	3,30	0,41	0,19
7	NM_172759	RIKEN cDNA 9030624L02		extracellular space	carboxylic ester hydrolase activity	2,54	3,58	-0,63	0,00	3,33	3,58	0,51	-0,07
7	AK014503	transformation related protein 73	apoptosis;cell growth and/or mainten	nucleus	DNA binding;translation regulator act	2,91	4,18	-1,18	-0,91	5,00	3,95	0,91	-0,30
7	NM_178763	RIKEN cDNA A030007D23		nucleus		1,94	3,83	-1,28	-0,76	3,51	2,89	0,10	-0,25
7	BC058636	sodium channel, voltage-gated, type III, beta				2,32	3,18	-0,91	-0,51	4,31	3,01	1,63	-0,21
7	NM_152804	polo-like kinase 2	cell cycle;protein amino acid phosph	phosphorylase kinase complex	ATP binding;DNA binding;protein ser	2,46	3,61	-0,79	-0,27	3,46	2,52	1,38	-0,07
7	NM_172524	RIKEN cDNA 9530066K23		integral to membrane		2,46	1,97	1,05	-0,35	2,27	2,78	-0,87	0,59
7	NM_011322	sodium channel, voltage-gated, type I, beta	sodium ion transport;synaptic transm	extracellular space;integral to membr	voltage-gated sodium channel activit	2,65	1,65	0,49	0,14	1,76	1,98	-0,31	0,38
7	NM_133683	transmembrane protein 19		integral to membrane		2,24	1,79	0,05	-0,13	1,97	2,05	-0,37	-0,10
7	NM_023631	RIKEN cDNA 2310003G12	electron transport	peroxisome	aldehyde oxidase activity;electron ca	2,13	1,29	0,16	0,16	1,95	2,16	-0,15	0,08
7	NM_031393	synaptotagmin-like 1	proton transport	membrane fraction	hydrogen-exporting ATPase activity\,	2,11	2,13	0,22	0,40	2,10	2,90	-0,66	0,40
7	NM_007955	protein tyrosine phosphatase, receptor type, \	protein amino acid dephosphorylation	extracellular space;integral to membr	protein tyrosine phosphatase activity	2,19	1,75	0,31	0,27	1,67	2,49	-0,55	0,29
7	NM_148937	phospholipase C, delta 4	acrosome reaction;intracellular signa	intracellular	1-phosphatidylinositol-4\,5-bisphosph	1,79	1,71	0,25	0,12	1,85	2,10	-0,76	0,12
7	NM_175324	RIKEN cDNA 5730439E10				1,78	1,55	0,41	0,35	1,87	2,42	-0,75	0,12
7	NM_133902	serine dehydratase-like	amino acid metabolism		lyase activity	2,31	1,98	0,93	0,54	1,80	2,17	-0,77	0,19
7	NM_007570	B-cell translocation gene 2, anti-proliferative (	DNA repair;negative regulation of ce	extracellular	transcription factor activity	2,80	1,90	-0,57	-0,59	1,04	2,15	-1,15	-0,15
7	NM_007570	B-cell translocation gene 2, anti-proliferative (	DNA repair;negative regulation of ce	extracellular	transcription factor activity	2,54	1,87	-0,59	-0,68	2,03	1,65	-0,41	-0,44
7	NM_007570	B-cell translocation gene 2, anti-proliferative (	DNA repair;negative regulation of ce	extracellular	transcription factor activity	2,33	1,40	-0,34	-0,80	1,47	1,75	-0,68	-0,25
7	NM_008317	hyaluronidase 1	carbohydrate metabolism		hyaluronoglucosaminidase activity	3,36	2,66	0,35	0,24	1,86	2,45	-1,50	-0,21
7	NM_008317	hyaluronidase 1	carbohydrate metabolism		hyaluronoglucosaminidase activity	3,34	2,67	0,11	0,45	1,51	2,50	-1,77	-0,10

7	NM_010235	fos-like antigen 1	positive regulation of cell proliferatior	cytoplasm;nucleus	transcription factor activity	2,39	2,13	-0,26	-0,04	1,78	2,46	-1,29	0,01
7	NM_030143	DNA-damage-inducible transcript 4-like (Ddit4	immune response	membrane	zinc ion binding	2,65	2,30	-0,40	-0,40	2,19	2,18	-0,92	-0,24
7	NM_175398	RIKEN cDNA 6530418L21				2,53	2,69	-0,08	0,16	1,83	2,11	-0,59	0,20
7	ENSMUST00000	Unknown				2,54	2,58	0,16	0,32	2,02	2,34	-0,39	0,25
7	NM_172295	cDNA sequence BC037703				3,03	2,95	-0,19	0,23	1,90	2,13	-0,86	-0,13
7	AK050890	clone:D030030M23				2,40	3,21	-0,32	0,30	1,22	2,72	-0,52	0,20
7	NM_011075	ATP-binding cassette, member 1B (Abcb1b)	transport	integral to membrane	ATP-binding cassette (ABC) transpo	2,13	3,18	-0,03	0,56	2,10	2,78	-0,93	0,48
7	NM_011322	sodium channel, voltage-gated, type I, beta	sodium ion transport;synaptic transm	extracellular space;integral to membi	voltage-gated sodium channel activit	2,97	2,37	0,47	0,53	1,82	2,48	-0,69	0,62
7	NM_010786	mouse 3T3 cell double minute 2 (Mdm2)	protein catabolism;protein ubiquitinat	membrane;nucleus	ATP binding;protein binding;ubiquitin	2,47	2,40	0,17	0,69	1,10	2,33	-0,44	0,41
7	NM_172205	suprabasin	biological_process unknown	cytoplasm	molecular_function unknown	2,99	2,88	0,30	0,16	1,93	3,55	-0,74	0,15
7	NM_178227	sodium channel, voltage-gated, type III, beta	sodium ion transport	integral to membrane	voltage-gated sodium channel activit	3,79	3,36	-0,09	0,10	2,40	3,10	-0,85	0,27
7	NM_008240	forkhead box J1	pattern specification;regulation of tra	transcription factor complex	transcription factor activity	3,61	2,03	-0,50	0,07	2,00	2,10	0,23	-0,01
7	NM_009684	apoptotic protease activating factor 1 (Apaf1)	brain development;caspase activatio	cytosol	ATP binding;apoptotic protease activ	2,44	3,28	-0,36	0,22	2,04	1,94	0,17	0,36
7	AK005731	clone:1700007K13				2,64	3,47	0,00	0,42	2,56	2,28	0,48	0,27
7	NM_009521	wingless-related MMTV integration site 3 (Wr	cell growth and/or maintenance;cell-(	extracellular matrix;extracellular spac	extracellular matrix structural constitu	2,93	3,22	0,20	0,03	1,75	2,42	0,58	0,18
7	NM_028263	RIKEN cDNA 2610306H15				2,89	2,19	0,43	1,11	2,63	3,16	0,27	-0,40
7	NM_181728	ADP-ribosyltransferase 3	protein amino acid ADP-ribosylation	extracellular space	NAD(P)+-arginine ADP-ribosyltransfe	2,33	2,09	-0,59	0,55	3,39	2,85	-0,49	0,08
7	NM_010430	hypermethylated in cancer 1	development;regulation of transcripti	nucleus	DNA binding;protein binding	1,86	1,94	0,46	0,47	2,50	1,26	0,51	-0,12
7	NM_010090	dual specificity phosphatase 2	protein amino acid dephosphorylatio	cytoplasm;nucleus	CTD phosphatase activity;MAP kinas	1,61	1,25	0,38	0,20	2,85	1,76	0,55	0,18
7	NM_010464	homeo box C13				1,79	1,72	0,02	0,18	2,73	1,74	1,21	0,02
7	NM_021487	potassium voltage-gated channel, member 1-like		integral to membrane		1,66	1,94	-0,15	0,13	2,16	2,01	0,89	0,15
7	NM_175438	aldehyde dehydrogenase 4 family, member A	proline catabolism	mitochondrial matrix	1-pyrroline-5-carboxylate dehydroge	1,30	1,79	-0,01	0,13	2,25	2,08	0,73	0,18
7	Z27088	relaxin precursor	physiological processes	extracellular space	hormone activity	2,00	1,75	0,09	0,09	2,60	2,07	0,53	0,21
7	BC043473	RIKEN cDNA 1300015B04				1,46	1,81	-0,17	-0,08	2,69	1,87	0,49	-0,08
7	NM_198885	scleraxis				1,02	1,90	0,05	0,31	2,66	2,50	0,14	0,29
7	NM_010800	muscle, intestine and stomach expression 1 (	G-protein coupled receptor protein si	membrane;nucleus	DNA binding;protein binding	2,05	2,24	0,13	0,64	2,84	2,09	0,07	0,28
7	AK003161	clone:1100001F07	development	mitochondrion	cytochrome c oxidase activity	1,91	2,07	0,29	0,58	3,18	2,83	0,12	-0,01
7	NM_010479	heat shock protein 1A				1,82	2,06	-0,05	0,19	3,16	2,78	1,28	0,37
7	NM_010479	heat shock protein 1A				1,95	2,78	-0,04	0,39	3,44	2,84	1,22	0,38
7	NM_022032	PERP, TP53 apoptosis effector	induction of apoptosis	Golgi apparatus;extracellular space;i	structural constituent of eye lens	1,78	2,82	-0,78	-0,14	3,28	2,68	0,80	-0,11
7	NM_183152	RIKEN cDNA 6330514A18				1,93	2,55	-0,17	0,03	3,53	2,59	0,58	-0,02
7	AK033569	weakly similar to NA+-GLUCOSE COTRANS	transport	membrane	transporter activity	1,72	1,54	-0,01	-0,30	3,75	2,47	0,99	-0,15
7	NM_009283	signal transducer and activator of transcriptio	NIK-I-kappaB/NF-kappaB cascade;S	cytoplasm;nucleus	hematopoietin/interferon-class (D200	1,02	1,71	-0,07	0,29	1,54	1,74	0,35	0,02
7	BC022653	sirtuin 4				1,19	1,55	0,03	0,18	2,06	1,67	0,40	0,31
7	NM_016910	protein phosphatase 1D magnesium-depende	protein amino acid dephosphorylatio	protein serine/threonine phosphatase	CTD phosphatase activity;calcium-de	0,78	1,52	-0,37	0,27	1,85	1,31	0,28	-0,03
7	NM_175388	RIKEN cDNA 2900057K09				1,10	1,84	-0,38	0,04	1,62	1,23	0,48	-0,01
7	NM_008999	RAB23, member RAS oncogene family	intracellular protein transport;neurog	late endosome	ATP binding;RAB small monomeric (	0,88	1,74	-0,39	-0,04	2,04	1,47	0,65	0,03
7	NM_029519	RIKEN cDNA 5830461H18	small GTPase mediated signal transduction		ATP binding;RAS small monomeric (	1,45	2,39	-0,45	0,10	1,82	1,27	0,70	-0,02
7	NM_007857	desert hedgehog	cell-cell signaling;pattern specificatio	extracellular space	peptidase activity;signal transducer a	1,39	2,32	-0,51	0,08	1,94	1,83	0,52	0,39
7	NM_023061	melanoma cell adhesion molecule	heterophilic cell adhesion	extracellular space;integral to membi	cell adhesion molecule activity	1,67	1,60	-0,74	-0,75	1,78	1,78	0,26	0,06
7	NM_134076	abhydrolase domain containing 4	aromatic compound metabolism;proteolysis and peptidolysis		aminopeptidase activity	1,42	1,56	-0,39	-0,40	1,49	1,83	0,49	-0,25
7	NM_133234	Bcl-2 binding component 3	induction of apoptosis;negative regul	mitochondrial membrane	apoptosis activator activity;catalytic a	1,09	1,53	-0,64	-0,48	1,82	1,68	0,71	-0,24
7	NM_013750	pleckstrin homology-like domain, family A, member 3		integral to membrane	exo-alpha-sialidase activity	1,46	1,45	-0,35	-0,57	1,63	1,25	0,46	-0,22
7	NM_177013	RIKEN cDNA 6332401O19				1,14	2,29	-0,71	-0,78	1,41	1,77	0,15	-0,61
7	NM_054087	solute carrier family 19 (thiamine transporter)	G-protein coupled receptor protein si	integral to membrane;plasma membi	folate transporter activity;folic acid bi	1,54	1,97	-0,74	-1,03	2,40	1,71	0,75	-0,20
7	NM_133641	rhotekin				1,41	1,11	-0,26	-0,55	2,36	1,78	0,31	-0,14
7	NM_010764	mannosidase 2, alpha B1	carbohydrate metabolism	lysosome	alpha-mannosidase activity	0,98	1,22	-0,46	-0,47	2,59	1,70	0,50	-0,36
7	BC016221	clone MGC:28766 IMAGE:4485843				0,59	1,27	-0,79	-0,54	2,11	1,66	0,64	-0,38
7	BQ043793	clone IMAGE:5683160 5'				0,80	1,11	-1,17	-0,92	1,96	1,84	0,73	-0,63
7	NAP105291-1	Unknown				1,03	1,41	-0,29	-0,14	2,38	1,17	0,71	-0,25
7	NM_172574	RIKEN cDNA E030024M05				1,02	1,82	-0,75	-0,38	2,09	1,30	0,47	-0,20
7	AK029268	similar to X-LINKED ECTODYSPLASIN-A RE	programmed cell death		tumor necrosis factor receptor activit	1,44	1,82	-0,74	-0,46	1,99	1,44	0,52	-0,33
7	AK046574	KINESIN SUPERFAMILY PROTEIN 1C hom	microtubule-based process	kinesin complex	ATP binding;microtubule motor activi	0,65	1,39	-0,62	-0,24	1,69	1,39	0,16	-0,11
7	NM_010016	decay accelerating factor 1	complement activation\, classical pat	extracellular space;integral to membi	aspartic-type endopeptidase activity	0,88	1,55	-0,86	-0,35	1,75	1,48	0,30	0,09
7	AK049134	similar to X-LINKED ECTODYSPLASIN-A RI	programmed cell death		tumor necrosis factor receptor activit	0,92	0,99	-0,60	-0,46	1,80	1,08	0,45	-0,15
7	NM_134087	expressed sequence AA409316 (AA409316)				0,97	1,30	-0,74	-0,65	2,02	1,30	0,39	-0,32
7	AK038651	clone:A230052H18				0,88	1,23	-0,40	-0,28	1,98	1,51	0,22	-0,17

7	NM_009846	CD24a antigen (Cd24a)	cell differentiation;defense response;	extracellular space;plasma membrane		1,12	1,20	-0,54	-0,53	2,18	1,53	0,24	0,04
7	NM_009831	cyclin G1	cytokinesis;mitosis;regulation of CDK	nuclear cyclin-dependent protein kina	cyclin-dependent protein kinase\, intr	0,85	1,45	-0,80	-0,46	1,56	0,98	0,83	0,08
7	AK050940	clone:D030041E15				1,32	3,34	-0,72	0,01	2,07	2,05	0,79	-0,21
7	BC023116	cell growth regulator with EF hand domain 1	cell cycle arrest	extracellular space	calcium ion binding	1,25	2,20	-0,33	0,02	2,91	2,10	1,01	0,00
7	NM_030143	DNA-damage-inducible transcript 4-like (Ddit4	immune response	membrane	zinc ion binding	1,48	2,39	-0,73	-0,33	2,39	1,69	1,08	-0,08
7	AK076567	clone:4921513I01				1,61	2,62	-0,71	-0,24	2,78	1,88	0,86	-0,17
7	NM_080854	solute carrier family 34 (sodium phosphate), r	phosphate transport	apical plasma membrane;brush bord	sodium-dependent phosphate transp	1,23	2,45	-0,26	-0,39	2,43	2,46	0,50	-0,22
7	NM_025727	kelch-like 10		nucleus	DNA binding;protein binding	2,13	1,85	0,07	-0,12	2,35	1,99	-0,07	-0,01
7	BC049768	cDNA clone MGC:58861				2,16	2,19	-0,05	-0,01	2,32	2,11	0,22	0,05
7	Z37110	cyclin G	cytokinesis;mitosis;regulation of CDK	nuclear cyclin-dependent protein kina	cyclin-dependent protein kinase\, intr	1,83	2,28	-0,61	-0,09	1,87	1,64	0,15	-0,09
7	NM_015763	lipin 1	adipocyte differentiation;lipid metabo	nucleus	molecular_function unknown	2,06	2,32	-0,54	-0,45	1,94	2,21	0,42	-0,16
7	NM_183168	pyrimidinergic receptor P2Y, G-protein coupled, 6 (P2ry6)				2,43	2,24	-0,28	-0,41	2,70	2,11	0,38	-0,74
7	NM_015763	lipin 1	adipocyte differentiation;lipid metabo	nucleus	molecular_function unknown	2,15	2,80	-0,81	-0,29	2,72	1,94	0,53	-0,21
7	NM_015763	lipin 1	adipocyte differentiation;lipid metabo	nucleus	molecular_function unknown	2,16	2,80	-0,67	-0,24	2,85	2,15	0,43	-0,17
7	NM_021897	transformation related protein 53 inducible nu	induction of apoptosis;response to st	nucleolus	apoptosis activator activity	2,10	2,94	-0,71	-0,62	2,65	2,12	0,58	-0,01
7	NM_008716	Notch gene homolog 3	N signaling pathway;cell differentiatio	extracellular space;integral to plasma	ATP binding;calcium ion binding;prot	2,24	2,51	-0,92	-0,72	2,96	1,46	0,64	-0,58
8	AK009823	LEUCYL TRNA SYNTHETASE homolog	amino acid activation;protein amino a	cytoplasm	protein prenyltransferase activity	2,61	2,39	0,03	0,11	-2,22	-0,39	-0,56	0,48
8	NM_013507	translation initiation factor 4, gamma 2	cell cycle arrest;cell death;regulation	eukaryotic translation initiation factor	RNA binding;translation initiation fact	4,64	3,66	0,00	0,20	-0,30	-0,24	0,50	1,09
8	AK034776	clone:9430036F11				4,43	2,68	0,61	-0,37	-0,12	0,00	1,40	0,72
8	AK079548	clone:A230054D04				0,65	0,73	-0,51	-0,41	-0,68	-0,30	-1,29	-0,80
8	NM_020494	DEAD (Asp-Glu-Ala-Asp) box polypeptide 24	RNA metabolism	cytoplasm	ATP dependent helicase activity;DNA	0,80	0,71	-0,57	-0,45	-0,33	0,01	-1,18	-0,36
8	AK009316	SKI PROTO-ONCOGENE homolog	cell growth and/or maintenance;limb	cytoplasm;transcriptional repressor c	protein binding	0,30	0,47	-0,22	-0,23	-0,18	-0,31	-0,63	-0,46
8	NM_144959	SWI/SNF related, actin dependent regulator of chromatin, a3				0,47	0,40	-0,29	-0,10	-0,70	-0,29	-0,74	-0,10
8	AK043052	clone:A730051E03				0,52	0,35	-0,20	0,15	-0,21	-0,28	-0,20	-0,36
8	NM_177089	RIKEN cDNA B230378H13				0,48	0,63	-0,36	-0,30	-0,32	-0,22	-0,02	-0,27
8	AK083741	clone:D030073N12				1,04	0,61	-0,06	-0,40	0,33	-0,14	-0,22	-0,31
8	AK122429	mKIAA1046 protein.				1,25	0,67	-0,33	-0,41	0,09	0,31	-0,45	0,09
8	AK083642	clone:D030058I23				0,89	0,73	-0,13	-0,06	-0,28	-0,21	-0,96	-0,64
8	TC1029980	Unknown				1,17	1,05	-0,11	0,01	-0,06	0,09	-1,07	-0,35
8	NM_199196	DNA segment, Chr 11, ERATO Doi 530				0,77	1,31	-0,49	-0,17	0,13	-0,34	0,27	0,27
8	NM_009386	tight junction protein 1	intracellular signaling cascade	adherens junction;tight junction	protein binding	0,52	0,57	0,15	-0,02	0,27	0,09	-0,18	-0,18
8	NM_010476	hydroxysteroid (17-beta) dehydrogenase 7	steroid biosynthesis	extracellular space;integral to membr	estradiol 17 beta-dehydrogenase act	0,56	0,56	0,07	0,14	0,16	0,00	-0,22	0,01
8	BC022649	cytidine deaminase				0,59	0,75	0,20	0,26	0,29	0,25	0,27	0,05
8	NM_008737	neuropilin	angiogenesis;axon guidance;cell adh	extracellular space;integral to membr	cell adhesion molecule activity;protei	0,48	0,99	0,10	0,30	0,00	0,19	-0,02	0,13
8	NM_181517	importin 7 (Ipo7)	protein-nucleus import		histone binding	1,12	0,91	0,05	-0,16	0,02	0,36	-0,37	0,35
8	AK078120	protein tyrosine phosphatase 4a1	protein amino acid dephosphorylation	soluble fraction	prenylated protein tyrosine phosphat	0,84	0,93	-0,11	0,02	0,23	0,27	-0,38	0,11
8	NM_011631	tumor rejection antigen gp96		endoplasmic reticulum;extracellular s	ATP binding;calcium ion binding;hea	1,09	1,06	0,08	0,06	0,08	-0,11	-0,42	-0,06
8	NM_133227	nucleoporin 155	nucleocytoplasmic transport	mitochondrial outer membrane;nucle	nucleocytoplasmic transporter activit	1,24	0,72	0,21	-0,12	0,13	0,06	-0,58	0,17
8	AF068198	activity-dependent neuroprotective protein	neuropeptide signaling pathway;regu	nucleus	neuropeptide hormone activity;transc	1,06	0,89	0,31	0,34	-0,22	0,11	-0,35	0,13
8	AK032821	clone:6720458D05				1,29	0,88	0,30	0,17	-0,31	0,18	-0,27	-0,09
8	NM_012010	translation initiation factor 2, subunit 3, struct	translational elongation		GTP binding;translation elongation fa	1,45	1,14	0,15	0,05	-0,17	0,16	-0,40	0,45
8	AK016689	ubiquitination factor E4B, UFD2 homolog	protein ubiquitination;ubiquitin-depen	cytoplasm;ubiquitin ligase complex	protein binding;ubiquitin conjugating	1,40	0,99	-0,09	-0,14	0,29	0,18	0,08	0,22
8	NM_018856	cyclin L2 , transcript variant 2	cell cycle		cyclin-dependent protein kinase\, intr	1,20	0,80	0,26	0,19	0,12	-0,03	0,25	0,31
8	AK079302	3-HYDROXY-3-METHYLGLUTARYL-COENZ	cholesterol biosynthesis	endoplasmic reticulum;integral to me	hydroxymethylglutaryl-CoA reductas	1,10	1,16	0,21	0,41	0,06	0,48	-0,45	0,34
8	NM_134033	cDNA sequence BC018601				1,49	1,06	0,20	0,19	0,42	0,58	-0,28	0,50
8	NM_026556	RIKEN cDNA 6720463E02	biological_process unknown;microtul	cellular_component unknown;dynein	microtubule motor activity;molecular_	1,42	1,04	0,32	0,00	0,52	0,42	0,11	-0,15
8	NM_177595	RIKEN cDNA 9430023B20				1,55	0,99	0,32	-0,09	0,76	0,38	0,18	-0,09
8	BI646741	clone IMAGE:5320025 5'				1,42	1,43	-0,07	-0,03	0,38	0,07	-0,43	-0,27
8	XM_144142	RIKEN cDNA 1810045K06				1,09	1,31	-0,03	0,20	0,27	0,42	-0,07	0,00
8	TC1029926	BC035974 DEAD/H (Asp-Glu-Ala-Asp/His) box polypeptide 15				1,04	1,07	0,19	0,32	0,46	0,43	-0,25	0,17
8	NM_029763	RIKEN cDNA 3010019O03	transcription	DNA-directed RNA polymerase III co	DNA-directed RNA polymerase activ	1,07	1,07	-0,40	0,27	0,40	0,44	0,01	0,10
8	BC054362	cDNA sequence BC010304				0,84	1,11	-0,16	0,05	0,53	0,22	-0,02	0,07
8	NM_146157	RIKEN cDNA C230096C10				0,90	1,04	-0,13	0,07	0,43	0,36	-0,12	0,03
8	AK085149	PROTEIN TRANSPORT PROTEIN SEC61 G	protein targeting;regulation of transcr	endoplasmic reticulum membrane;int	protein translocase activity;transcript	1,52	1,39	-0,10	0,47	0,49	0,85	0,09	0,05
8	NM_026887	adaptor-related protein complex 1, sigma 2 su	endocytosis;intracellular protein trans	AP-1 adaptor complex;Golgi trans fa	protein transporter activity	0,99	0,92	0,25	0,58	0,59	0,52	0,31	0,30
8	NM_175511	RIKEN cDNA A130092J06				0,93	1,30	0,46	0,47	0,11	0,70	0,04	0,33
8	NM_015751	ATP-binding cassette, sub-family E , member	electron transport	membrane	ATP-binding cassette (ABC) transpo	2,50	2,44	0,19	0,27	-0,57	-0,15	0,20	1,11

8	NM_022997	vacuolar protein sorting 35	secretory pathway;vacuolar protein p	integral to membrane	protein transporter activity	2,57	2,54	-0,03	0,22	0,07	0,30	0,45	0,94
8	AK129403	mKIAA1601				2,15	3,09	0,11	0,64	-0,41	0,22	0,27	1,25
8	NM_024181	DnaJ (Hsp40) homolog, subfamily C, membe	electron transport	endoplasmic reticulum;mitochondrion	chaperone activity;electron transport	1,51	2,68	-0,08	0,47	-0,41	0,30	0,47	0,74
8	NM_145942	3-hydroxy-3-methylglutaryl-Coenzyme A synt	C21-steroid hormone biosynthesis;a	cytoplasm;transcription factor comple	hydroxymethylglutaryl-CoA synthase	2,83	2,27	0,43	0,44	-0,69	0,14	-0,89	0,66
8	NM_010771	matrin 3		nucleus	RNA binding	2,97	3,04	-0,15	0,32	-0,45	0,05	-0,29	0,79
8	AK049446	NUCLEAR TRANSPORT RECEPTOR homolog				2,80	2,67	-0,22	0,11	-0,14	0,24	-0,56	0,24
8	NM_009457	ubiquitin-activating enzyme E1, Chr X	DNA replication;ubiquitin cycle;ubiqu	cytoplasm	ligase activity;ubiquitin activating enz	2,91	2,39	0,08	0,23	-0,04	0,43	-0,53	0,45
8	NM_177732	solute carrier family 35, member D1				2,90	2,48	0,40	0,32	0,14	1,75	-0,24	0,13
8	NM_011112	poly (A) polymerase alpha	mRNA processing;transcription	nucleus	RNA binding;polynucleotide adenylyl	1,57	1,96	-0,12	0,27	-0,34	0,04	-1,13	0,04
8	NM_028727	RIKEN cDNA 4632412I24	biological_process unknown;proteoly	mRNA cleavage factor complex	ATP binding;carboxypeptidase A act	1,82	2,64	0,09	0,55	-0,31	0,11	-0,62	0,50
8	NM_007399	a disintegrin and metalloprotease domain 10	proteolysis and peptidolysis	extracellular space;integral to membr	metalloendopeptidase activity;zinc io	1,52	1,54	0,24	0,69	-0,58	-0,08	0,44	0,42
8	NM_181517	importin 7	protein-nucleus import		histone binding	1,80	1,62	0,11	0,18	-0,94	0,25	-0,37	0,48
8	NM_010891	septin 2	cell cycle;cytokinesis	contractile ring	ATP binding;GTPase activity	1,95	2,06	0,15	0,35	-0,75	-0,18	-0,26	0,74
8	NM_145985	archain 1	intracellular protein transport	clathrin vesicle coat		2,10	2,08	0,15	0,42	-0,54	0,22	-0,03	0,51
8	AY256848	FATH protein				1,88	1,03	0,31	-0,08	-0,17	0,35	-0,89	0,03
8	AK047094	TANKYRASE-RELATED PROTEIN (FRAGMENT) homolog				1,78	2,30	-0,20	0,18	0,16	0,49	0,92	1,21
8	AK033268	ETHANOLAMINE KINASE (EC 2.7.1.82) homolog			kinase activity;transferase activity	2,14	2,50	0,28	0,75	0,74	0,67	0,61	0,60
8	NM_012048	polymerase (DNA directed), kappa	DNA repair	extrachromosomal circular DNA		1,70	2,29	0,41	0,48	0,67	0,88	0,83	0,61
8	NM_175540	ectodysplasin A2 isoform receptor	programmed cell death		tumor necrosis factor receptor activit	2,07	2,66	-0,36	-0,06	0,48	0,98	0,79	0,28
8	NM_007832	deoxycytidine kinase	pyrimidine nucleotide metabolism	mitochondrion;nucleus	ATP binding;deoxycytidine kinase ac	2,00	1,87	0,24	0,30	0,29	0,57	-0,22	0,61
8	NM_028744	phosphatidylinositol 4-kinase type 2 beta	biological_process unknown	cytoplasm	inositol/phosphatidylinositol kinase a	1,31	1,56	0,40	0,44	0,75	0,67	0,09	0,54
8	NM_032008	sarcolemma associated protein	muscle contraction	integral to membrane	catalytic activity	1,40	1,81	0,37	0,41	0,56	0,45	0,34	0,65
8	BC060128	poly (A) polymerase alpha				1,47	1,73	0,00	0,34	-0,05	0,24	0,30	0,29
8	AK122429	mKIAA1046 protein				1,40	1,79	-0,36	-0,12	0,02	0,63	0,03	0,22
8	NM_010884	N-myc downstream regulated gene 1				-2,42	-2,35	-1,28	-1,03	-1,02	-1,19	-0,37	-0,49
8	NM_176933	dual specificity phosphatase 4	protein amino acid dephosphorylatio	nucleus	CTD phosphatase activity;myosin ph	-2,04	-1,59	-0,89	-0,79	-0,32	-0,88	-0,17	-0,30
8	NM_013549	histone 2, H2aa1				-2,39	-3,30	-0,51	-1,30	-1,56	-1,75	-0,53	-1,04
8	AK006938	clone:1700072H12				-0,69	-0,44	0,18	0,28	0,35	0,34	-0,30	0,11
8	NM_145987	hypothetical protein MGC37938				-0,20	-0,17	0,27	0,27	0,58	0,39	0,29	0,13
8	AK009476	hypothetical RNA-binding region RNP-1 containing protein				-0,11	-0,22	0,27	0,13	0,30	0,28	0,12	0,22
8	AK008384	clone:2010110K18				-0,32	-0,13	0,34	0,55	0,44	0,23	0,23	0,18
8	NM_024176	Dr1 associated protein 1 (negative cofactor 2	negative regulation of transcription fr	negative cofactor 2 complex	transcription co-repressor activity;tra	-0,44	-0,76	0,34	0,23	-0,07	0,10	0,22	0,56
8	AK045923	WDC146 homolog	transport		transporter activity	-0,37	-0,78	0,29	0,16	0,05	-0,23	0,05	0,07
8	NM_028218	RIKEN cDNA 2210409E12	RNA elongation from Pol II promoter	transcription elongation factor compl	translation elongation factor activity	-0,47	-0,70	0,33	0,25	-0,25	-0,11	0,04	0,16
8	NM_026035	mitochondrial ribosomal protein L55	biological_process unknown	cellular_component unknown	molecular_function unknown;structur	-0,64	-0,81	0,14	0,07	0,01	-0,33	0,39	0,21
8	NM_029236	RIKEN cDNA 4930556P03		mitochondrion		-0,58	-0,63	0,09	0,06	0,14	-0,36	0,21	0,00
8	NM_025977	RIKEN cDNA 2510048L02	cell growth and/or maintenance	cytoplasm	ATP binding;catalytic activity	-0,33	-0,36	0,21	0,11	0,17	-0,15	0,19	0,04
8	BC004695	zinc finger protein 64	development;regulation of transcripti	transcription factor complex	DNA binding	-0,47	-0,45	0,16	0,13	0,15	0,01	0,03	0,04
8	NM_145546	general transcription factor IIB				-0,39	-0,45	0,25	0,16	0,15	-0,12	0,04	0,09
8	NM_021534	peroxisomal membrane protein 4	biological_process unknown	cellular_component unknown;integra	molecular_function unknown	-0,32	-0,41	0,22	0,18	0,04	-0,15	-0,03	-0,03
8	BC046229	RIKEN cDNA 2010305K11				-0,12	-0,12	0,05	0,12	0,04	0,05	0,23	0,14
8	NM_009478	uroporphyrinogen decarboxylase	heme biosynthesis	chloroplast	uroporphyrinogen decarboxylase act	-0,55	-0,44	0,02	-0,15	0,17	-0,12	0,32	0,18
8	NM_018827	cytokine receptor-like factor 1		extracellular space	receptor activity	-0,34	-0,45	-0,01	-0,07	0,00	-0,07	-0,01	0,28
8	NM_133869	choline/ethanolaminephosphotransferase 1	phospholipid biosynthesis	integral to membrane	transferase activity	-0,33	-0,55	-0,04	-0,16	0,00	-0,08	0,07	0,05
8	NM_022318	popeye domain containing 2	biological_process unknown	integral to membrane		-0,28	-0,53	0,02	-0,12	0,01	-0,05	0,08	0,06
8	BC019757	histone 1, H4i				-1,78	-0,90	-0,20	0,11	0,22	0,42	0,12	0,14
8	NM_027250	RIKEN cDNA 2010305A19				-0,96	-0,92	0,22	0,22	0,07	-0,44	0,60	0,15
8	AK005805	clone:1700010A01				-0,56	-1,07	0,36	-0,07	0,51	-0,07	0,31	-0,16
8	NM_017377	UDP-Gal:betaGlcNAc beta 1,4- galactosyltrar	oligosaccharide biosynthesis	Golgi apparatus;integral to membran	N-acetyllactosamine synthase activit	-0,55	-0,76	-0,21	-0,22	-0,02	-0,07	0,16	-0,16
8	NM_025689	RIKEN cDNA 5730568A12	protein amino acid dephosphorylatio	protein serine/threonine phosphatase	manganese ion binding	-0,67	-0,90	0,04	-0,06	0,04	0,04	0,30	0,15
8	NM_146176	CCR4-NOT transcription complex, subunit 3				-0,55	-0,82	0,01	-0,16	0,37	0,25	0,41	-0,01
8	NM_194346	ring finger protein 31				-0,49	-0,70	0,01	-0,18	0,11	0,22	-0,07	-0,06
8	NM_028047	RIKEN cDNA 1500002O20			ATP binding	-0,46	-0,66	0,20	0,03	0,12	0,27	-0,01	0,14
8	AK085605	clone:D630045M09				-0,87	-0,97	-0,12	0,04	-0,23	-0,14	-0,16	0,06
8	NM_029631	RIKEN cDNA 1810013B01			catalytic activity	-0,73	-1,05	-0,11	-0,11	-0,18	0,16	-0,27	0,08
8	NM_133759	zinc finger and BTB domain containing 3		nucleus	protein binding	-0,63	-0,54	-0,09	0,04	-0,27	-0,15	-0,07	0,07
8	NM_018811	abhydrolase domain containing 2	biological_process unknown	cellular_component unknown;integra	hydrolase activity;molecular_function	-0,65	-0,68	-0,02	0,03	-0,17	-0,09	-0,41	-0,09

8	AK004937	hypothetical GroEL-like chaperone, ATPase domain structure containing protein				-0,79	-0,75	-0,06	-0,04	0,22	0,10	-0,09	0,03
8	NM_028908	RIKEN cDNA 4933403G14				-1,06	-0,62	-0,12	0,02	0,05	0,06	-0,15	0,09
8	TC1053155	X07687 ORFI				-0,78	-1,34	0,16	-0,21	-0,53	-0,27	-0,22	0,05
8	AK002723	clone:0610031G08				-0,84	-1,00	0,00	-0,13	-0,56	-0,25	-0,08	0,03
8	NM_026366	RIKEN cDNA 5830445C04				-1,15	-0,88	-0,11	-0,13	-0,16	-0,42	-0,32	-0,25
8	NM_011780	a disintegrin and metalloprotease domain 23	central nervous system development	integral to plasma membrane	integrin binding;metalloendopeptidas	-0,75	-0,75	-0,23	-0,14	-0,28	-0,46	-0,53	-0,28
8	NM_153162	thioredoxin reductase 3	oxidized glutathione reduction;thiore	cytoplasm;microsome	arsenate reductase (glutaredoxin) ac	-0,63	-1,08	-0,21	-0,44	-0,32	-0,39	-0,23	-0,26
8	AK122413	mKIAA0978 protein.				-0,58	-0,83	-0,36	-0,44	-0,19	-0,33	-0,12	-0,16
8	NM_026840	platelet-derived growth factor receptor-like	transmembrane receptor protein tyro	integral to membrane	platelet-derived growth factor\, beta-r	-1,20	-1,58	-0,46	-0,45	-0,90	-0,28	-0,17	-0,10
8	NM_007974	coagulation factor II receptor-like 1	G-protein coupled receptor protein si	extracellular space;integral to plasma	purinergic nucleotide receptor activity	-1,60	-1,47	-0,70	-0,47	-0,39	-0,16	-0,34	0,01
8	NM_009638	cysteine-rich secretory protein 1	biological_process unknown	extracellular		-1,56	-1,41	-0,63	-0,40	-0,50	-0,74	-0,14	-0,03
8	NM_133218	glucocorticoid induced gene 1	regulation of transcription\, DNA-dep	extracellular		-1,19	-1,45	-0,32	-0,39	-0,30	-0,43	-0,81	-0,45
8	NM_025730	RIKEN cDNA 4921513O20	protein amino acid phosphorylation	cytoplasm	ATP binding;protein serine/threonine	-1,07	-0,99	-0,71	-0,53	-0,53	-0,51	-0,62	-0,23
8	NM_178218	histone 3, H2a				-1,76	-1,67	0,21	0,38	-0,79	-0,58	0,24	0,32
8	NM_007933	enolase 3, beta muscle	glycolysis	phosphopyruvate hydratase complex	magnesium ion binding;phosphopyru	-1,28	-0,63	-0,39	-0,01	-0,25	-0,13	0,03	0,18
8	NM_026251	RIKEN cDNA 4930424G05	development	transcription factor complex	DNA binding	-1,23	-1,01	-0,16	0,08	-0,05	-0,15	0,14	-0,38
8	NM_010825	myeloid ecotropic viral integration site-related	eye morphogenesis;negative regulat	transcription factor complex	specific RNA polymerase II transcrip	-1,18	-0,84	-0,14	-0,05	0,02	-0,49	0,19	-0,26
8	NM_026505	BMP and activin membrane-bound inhibitor, h	TGFbeta receptor signaling pathway	integral to membrane		-1,15	-1,21	-0,44	-0,30	-0,24	-0,66	0,00	-0,26
8	NM_026505	BMP and activin membrane-bound inhibitor, h	TGFbeta receptor signaling pathway	integral to membrane		-1,33	-1,00	-0,48	-0,36	-0,25	-0,73	-0,05	-0,26
8	NM_026505	BMP and activin membrane-bound inhibitor, h	TGFbeta receptor signaling pathway	integral to membrane		-1,41	-1,06	-0,40	-0,29	-0,49	-0,71	0,00	-0,23
8	NM_026505	BMP and activin membrane-bound inhibitor, h	TGFbeta receptor signaling pathway	integral to membrane		-1,38	-1,13	-0,51	-0,30	-0,47	-0,46	0,00	-0,30
8	NM_011636	phospholipid scramblase 1	phospholipid scrambling	integral to membrane	calcium ion binding	-1,18	-1,17	-0,39	-0,39	-0,45	-0,67	0,11	-0,05
8	NM_011636	phospholipid scramblase 1	phospholipid scrambling	integral to membrane	calcium ion binding	-1,04	-1,26	-0,32	-0,49	-0,58	-0,53	0,02	-0,12
8	NM_026080	mitochondrial ribosomal protein S24	protein biosynthesis	mitochondrial small ribosomal subun	structural constituent of ribosome	-0,90	-1,10	-0,42	-0,35	-0,47	-0,76	0,51	0,16
8	NM_024215	RIKEN cDNA 3110024A21	regulation of transcription\, DNA-dep	nucleus	DNA binding	-1,18	-1,26	-0,25	-0,58	-0,78	-0,59	0,65	0,14
9	BC059192	integrin beta 4				0,61	1,14	-0,50	-0,33	2,90	1,94	0,42	-0,18
9	BC059192	integrin beta 4				0,65	1,25	-0,50	-0,27	3,01	2,16	0,28	-0,16
9	NM_145143	membrane protein, palmitoylated 4 (MAGUK	biological_process unknown;intracell	cellular_component unknown	molecular_function unknown	-0,24	0,24	-0,10	0,43	2,20	2,26	1,04	0,32
9	NM_016900	caveolin 2	endocytosis	caveola;integral to membrane	molecular_function unknown;structur	-0,41	0,67	-0,49	0,09	2,09	2,42	0,25	0,88
9	AK002434	similar to keratin K7, type II, epithelial, 55K	cytoskeleton organization and bioger	intermediate filament;kinesin comple	structural constituent of cytoskeleton	0,17	0,35	0,13	0,28	2,00	1,40	-0,15	0,09
9	NM_026239	RIKEN cDNA 9030603L14		integral to membrane		0,53	0,33	-0,09	0,04	2,01	1,57	0,17	-0,15
9	NM_007987	tumor necrosis factor receptor superfamily, m	apoptosis;immune response;signal tr	extracellular space;integral to membr	transmembrane receptor activity	0,62	0,70	0,10	0,08	1,98	1,04	-0,07	0,15
9	NM_028807	RIKEN cDNA 1200009I06				0,68	0,66	0,20	0,13	1,87	1,39	-0,04	0,09
9	AK015217	hypothetical G-protein beta WD-40 repeats c	microtubule-based process	microtubule associated complex	calcium ion binding	0,61	0,73	0,06	-0,06	1,91	1,43	-0,20	0,10
9	NM_018805	heparan sulfate (glucosamine) 3-O-sulfotrans	protein amino acid sulfation	integral to plasma membrane	heparin-glucosamine 3-O-sulfotransf	0,67	0,43	-0,09	-0,13	1,75	1,15	0,31	0,08
9	NM_170684	copine VII				0,93	0,37	0,10	-0,13	1,64	1,17	0,10	-0,09
9	NM_146126	sorbitol dehydrogenase 1	sorbitol metabolism	extrachromosomal circular DNA	L-iditol 2-dehydrogenase activity;alcc	0,97	0,36	0,47	0,33	1,29	1,79	-0,18	0,31
9	NM_001001309	integrin alpha 8				0,50	0,74	-0,19	0,03	1,79	1,80	-0,38	0,22
9	AK017732	PROTEIN AD-016 (PROTEIN CGI-116) (X0009) homolog				0,37	0,54	0,24	0,36	1,52	1,61	-0,41	0,43
9	NM_153142	RIKEN cDNA A330108F03				0,60	0,33	-0,28	-0,04	1,50	1,97	0,46	-0,21
9	BC020030	Rho guanine nucleotide exchange factor 16				0,96	0,61	-0,06	-0,11	2,17	1,99	0,67	-0,02
9	NM_145447	cDNA sequence BC011209				0,69	0,94	0,24	0,28	1,78	1,28	0,38	0,08
9	NM_175369	RIKEN cDNA 4933415L06				0,89	0,63	0,09	0,35	1,73	1,58	0,96	0,24
9	NM_013755	glycogenin 1	glycogen biosynthesis	soluble fraction	glycogenin glucosyltransferase activi	0,69	0,81	0,24	0,19	1,55	1,67	0,84	-0,06
9	J00623	MUSRGEB3 18S ribosomal RNA gene				0,29	0,05	-0,69	-0,91	2,58	1,79	0,72	-0,46
9	NM_013822	jagged 1	N signaling pathway;angiogenesis;ce	extracellular space;integral to membr	Notch binding;calcium ion binding;gr	-0,43	0,48	-1,55	-0,89	2,02	1,91	0,23	-0,50
9	NM_021472	ribonuclease, RNase A family 4 , transcript variant 1			pancreatic ribonuclease activity	0,33	-0,13	-0,66	-0,65	1,46	1,61	-0,72	-0,31
9	NM_021472	ribonuclease, RNase A family 4 , transcript variant 1			pancreatic ribonuclease activity	0,38	-0,43	-0,35	-0,64	1,35	1,39	-0,43	-0,25
9	NM_008767	solute carrier family 22 , member 18	anion transport;electron transport;tet	extracellular space;integral to plasma	organic anion transporter activity;tetr	0,38	0,81	-0,63	-0,38	1,51	1,78	-0,57	-0,18
9	TC1070053	ZN84_HUMAN Zinc finger protein 84				0,42	0,00	-0,23	-0,45	0,89	0,72	0,00	-0,39
9	NM_010516	cysteine rich protein 61	cell proliferation;patterning of blood v	extracellular space	insulin-like growth factor binding;rece	0,22	0,22	-0,01	0,01	1,23	0,70	-0,09	-0,52
9	NM_054093	ubiquitin protein ligase E3B	ubiquitin cycle	ubiquitin ligase complex	ubiquitin-protein ligase activity	0,41	0,14	-0,40	-0,44	1,21	1,20	0,50	-0,24
9	NM_198167	cDNA sequence BC026370				0,37	0,50	-0,37	-0,31	1,28	0,94	0,20	-0,13
9	NM_178900	expressed sequence AI325941				0,38	0,32	0,14	0,03	0,66	0,95	-0,01	0,05
9	NM_011890	sarcoglycan, beta (dystrophin-associated gly	membrane organization and biogene	cytoskeleton;integral to plasma mem	structural constituent of muscle	0,48	0,56	0,15	0,13	1,06	0,86	0,33	0,02
9	NM_031159	apolipoprotein B editing complex 1	cytidine to uridine editing;lipoprotein	integral to plasma membrane	hydrolase activity;zinc ion binding	0,52	0,38	0,22	0,16	1,13	0,85	-0,15	-0,10
9	NM_026436	RIKEN cDNA 1810054O13				0,68	0,10	0,48	0,07	1,32	1,01	0,11	0,01

9	NM_177716	expressed sequence AI836003				0,41	0,54	-0,07	0,04	1,38	1,22	0,23	0,06
9	AK019871	clone:5031410B04			nucleic acid binding	0,17	0,48	-0,15	0,18	1,35	1,05	0,10	0,11
9	AK016443	hypothetical D-galactoside/L-rhamnose binding		integral to membrane	sugar binding	0,17	0,24	-0,08	0,00	1,16	0,92	0,14	0,12
9	NM_020034	histone 1, H1b	nucleosome assembly	nucleosome;nucleus	DNA binding	-0,34	0,44	0,07	0,07	1,18	1,23	-0,26	0,19
9	NM_022883	lipin 3		nucleus		-0,09	-0,12	0,00	0,17	0,80	1,06	-0,05	0,10
9	NM_028780	transmembrane 9 superfamily member 1	transport	extracellular space;integral to membr	transporter activity	-0,09	0,03	-0,04	-0,07	0,88	0,32	0,22	-0,09
9	NM_025653	RIKEN cDNA 3110001I22		extracellular	calcium ion binding	-0,43	0,15	-0,22	-0,03	0,93	0,55	0,15	0,08
9	NM_028298	RIKEN cDNA 2700038I16				-0,17	-0,17	-0,18	0,07	0,98	0,67	0,31	0,10
9	NM_138646	Hermansky-Pudlak syndrome 4 homolog (hur	melanocyte differentiation;organelle o	cytoplasmic vesicle		0,00	0,07	0,15	0,09	0,58	0,51	-0,04	-0,08
9	NM_007705	cold inducible RNA binding protein		nucleus	RNA binding	-0,01	0,28	-0,02	0,18	0,75	0,61	0,16	0,12
9	NM_009079	ribosomal protein L22	protein biosynthesis;ribosome bioger	cytosolic ribosome (sensu Eukarya)	RNA binding;heparin binding;structur	0,28	0,24	0,18	-0,06	0,62	0,54	0,19	0,10
9	NM_007801	cathepsin H	proteolysis and peptidolysis	extracellular space;lysosome	cathepsin H activity	-0,09	-0,06	-0,07	-0,06	0,29	0,51	0,08	0,01
9	AK028745	clone:4732452C17				-0,25	-0,36	-0,26	-0,35	0,58	0,58	-0,63	-0,39
9	NM_009287	stromal interaction molecule 1	cell adhesion;positive regulation of c	extracellular space;integral to plasma	cell adhesion molecule activity;nucle	0,12	-0,36	-0,13	-0,38	0,67	0,51	-0,27	-0,36
9	NM_008800	phosphodiesterase 1B, Ca2+-calmodulin dep	apoptosis;signal transduction	insoluble fraction	calmodulin binding;calmodulin-deper	-0,10	-0,37	-0,33	-0,58	0,80	0,18	-0,28	-0,51
9	NM_010929	Notch gene homolog 4	cell differentiation;cell growth and/or	extracellular space;integral to membr	ATP binding;calcium ion binding;rece	0,41	0,14	1,27	0,99	-1,16	-0,75	0,38	1,05
9	NM_013758	adducin 3 (gamma)	cytoskeleton organization and bioger	cytoskeleton;membrane	calmodulin binding;structural constitu	0,41	0,73	0,08	0,43	-1,00	-0,47	0,08	0,35
9	AK034610	Hedgehog-interacting protein	carbohydrate metabolism;lung develo	extracellular space;integral to plasma	protein binding;scavenger receptor a	0,13	0,75	0,42	0,94	-1,41	-0,62	0,60	0,43
9	NM_010732	leucine rich repeat protein 2, neuronal				-0,85	-0,19	-0,74	-0,65	-1,78	-1,49	-1,13	-0,40
9	NM_009328	transcription factor 15	development;regulation of transcripti	transcription factor complex	transcription factor activity	-0,46	-0,62	0,14	0,10	-1,75	-1,33	-0,48	0,21
9	AK021193	clone:C330008K14				-0,64	-1,11	0,31	0,15	-2,00	-1,83	-0,61	-0,01
9	NM_011461	Spi-C transcription factor	regulation of transcription\, DNA-dep	transcription factor complex	transcription factor activity	0,01	-0,96	-0,12	-0,42	-2,29	-1,25	0,05	-0,16
9	NM_138956	Ras association (RalGDS/AF-6) domain famil	biological_process unknown;neurope	cellular_component unknown;cytopla	molecular_function unknown;zinc ion	-0,13	-0,60	0,30	0,06	-1,32	-1,10	0,65	0,08
9	XM_130308	low density lipoprotein-related protein 2	receptor mediated endocytosis;vitam	endosome;membrane	DNA binding;calcium ion binding;pro	-0,05	-0,15	-0,29	-0,38	-1,02	-0,98	0,27	-0,30
9	NM_175140	carbohydrate (N-acetylgalactosamine 4-0) su	peptide hormone processing;proteog	cellular_component unknown;extrace	N-acetylgalactosamine-4-O-sulfotran	-0,56	-0,83	-0,30	-0,22	-1,29	-1,06	-0,44	-0,13
9	NM_007631	cyclin D1	G1/S transition of mitotic cell cycle;a	cytosol;nucleus	cyclin-dependent protein kinase\, inti	0,01	-0,57	0,07	-0,14	-1,19	-1,27	-0,54	-0,40
9	NM_010063	dynein, cytoplasmic, intermediate chain 1	microtubule-based movement	cytoplasmic dynein complex	microtubule motor activity	-0,43	-0,22	-0,32	-0,25	-0,67	-0,81	-0,39	-0,19
9	NM_197990	RIKEN cDNA 1700025G04				-0,33	-0,20	-0,14	0,01	-0,89	-1,04	-0,44	-0,18
9	NM_016866	serine/threonine kinase 39, STE20/SPS1 hon	protein amino acid phosphorylation;r	cytoplasm	ATP binding;protein tyrosine kinase a	-0,51	-0,15	-0,28	0,11	-1,05	-0,91	-0,41	-0,10
9	NM_008057	frizzled homolog 7	G-protein coupled receptor protein si	extracellular space;integral to membr	G-protein coupled receptor activity;fr	-0,66	-0,43	-0,28	-0,22	-0,91	-1,04	-0,66	-0,43
9	NM_145833	lin-28 homolog	regulation of transcription\, DNA-dependent		DNA binding	-0,44	-0,47	-0,34	-0,22	-1,04	-0,90	-0,64	-0,07
9	NM_027285	RIKEN cDNA 1700029I01				-0,47	0,34	0,06	-0,03	-1,61	-0,71	-0,26	-0,05
9	NM_023894	placenta specific homeobox 2	regulation of transcription\, DNA-dep	transcription factor complex	transcription factor activity	-0,13	-0,14	0,15	0,12	-1,67	-0,59	-0,15	0,17
9	NM_173419	cDNA sequence BC038059				-0,32	-0,16	0,52	0,66	-0,70	-0,65	0,41	0,23
9	AK007352	clone:1810006K23				-0,25	-0,29	0,78	0,84	-0,71	-0,82	0,07	0,44
9	NM_013627	paired box gene 6	anterior/posterior pattern formation;b	transcription factor complex	transcription factor activity	-0,26	-0,48	0,63	0,49	-1,08	-0,93	-0,19	0,37
9	AJ428068	leucine-rich repeat-containing 2 protein				-0,44	-0,29	0,62	0,60	-1,01	-0,69	-0,15	0,38
9	AK003999	Rattus norvegicus general transcription factor	regulation of transcription\, DNA-dep	transcription factor TFIIF complex	ATP binding;DNA binding;RNA polyr	-0,32	-0,22	0,36	0,35	-0,68	-0,64	-0,13	0,35
9	NM_026555	reticulocalbin 3, EF-hand calcium binding domain		endoplasmic reticulum	calcium ion binding	-0,56	-0,33	0,33	0,54	-0,55	-0,62	0,13	0,21
9	NM_016709	AU RNA binding protein/enoyl-coenzyme A h	mRNA catabolism\, deadenylation-de	mitochondrion	RNA binding;enoyl-CoA hydratase a	-0,31	-0,45	0,19	0,25	-0,53	-0,79	0,19	0,23
9	NM_033571	FK506 binding protein 6	peptidyl-proline modification;protein f	cytosol;membrane fraction	FK506 binding;peptidyl-prolyl cis-tran	-0,26	-0,46	0,59	0,34	-0,66	-0,69	0,06	0,05
9	NM_011987	phospholipase A2, group X	lipid catabolism	extracellular space	calcium ion binding;calcium-depende	-0,67	-0,92	0,75	0,43	-0,85	-1,16	0,09	0,42
9	NM_011912	ventral anterior homeobox containing gene 2	regulation of transcription\, DNA-dep	transcription factor complex	transcription factor activity	-0,42	-0,49	0,15	0,11	-1,05	-1,27	0,18	0,32
9	NM_011943	mitogen activated protein kinase kinase 6				-0,11	-0,59	0,36	0,23	-1,11	-1,24	-0,29	0,19
9	NM_023063	DNA segment, Chr 15, ERATO Doi 366	biological_process unknown	actin cytoskeleton	molecular_function unknown	-0,16	0,10	0,10	0,25	-0,55	-1,10	-0,09	-0,19
9	AK008856	clone:2210408F11				-0,05	0,20	-0,28	0,31	-0,85	-0,78	-0,34	-0,01
9	X82786	M.musculus mRNA for Ki-67	meiosis	chromosome\, pericentric region;con	densed chromosome;cytoplasm;nucle	-0,01	0,01	-0,06	0,04	-0,47	-0,62	-0,34	-0,02
9	AK037065	clone:9930106P14				0,12	0,19	-0,12	0,01	-0,62	-0,58	-0,38	0,04
9	AK030046	clone:4932417I16				0,16	0,03	0,43	0,47	-0,45	-0,66	0,25	0,11
9	NAP107478-1	Unknown				0,08	0,30	0,12	0,27	-0,51	-0,35	-0,12	0,44
9	NM_023142	actin related protein 2/3 complex, subunit 1B	cell motility	Arp2/3 protein complex	structural constituent of cytoskeleton	0,12	-0,14	0,31	0,13	-0,35	-0,49	-0,12	0,10
9	NM_015829	solute carrier family 25 , member 13	transport	integral to plasma membrane;mitoch	calcium ion binding;carrier activity	-0,08	-0,03	0,13	0,28	-0,64	-0,53	-0,19	-0,04